What do we know so far?

$$\Delta\mu=\mu^{+}-\mu^{-} \sim \Delta(\underline{P}\cdot\underline{M})$$

- XMCD is element specific
  - Good for complex compounds like $Nd_2Fe_{14}B$
- Separates Spin S and Orbital L magnetizations in real "Bohr-Magnetons"
  - Very important to understand coercive fields and magnetic anisotropy

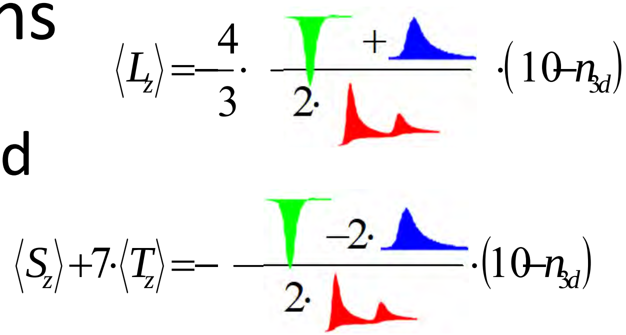

- Any X-ray related technique could be transferred into it's magnetic counterpart, by tuning the X-ray energy to a corresponding XMCD sensitive edge !

- Now we start with XRMR= X-ray Resonant Magnetic Reflectivity

XRMR

- Short introduction with optical analogue
- Thickness = Chemical Profile
- What happens with roughness?
- Real Example: Pt/Co ➔ magnetic profile
- How to quantify this? ➔ Simulation
- Another example showing XRMR capabilities!

Further details Review: S. Macke and E. Goering, J. Phys. Cond. Mat. **26** (2014) 363201

Modern functional magnetic material

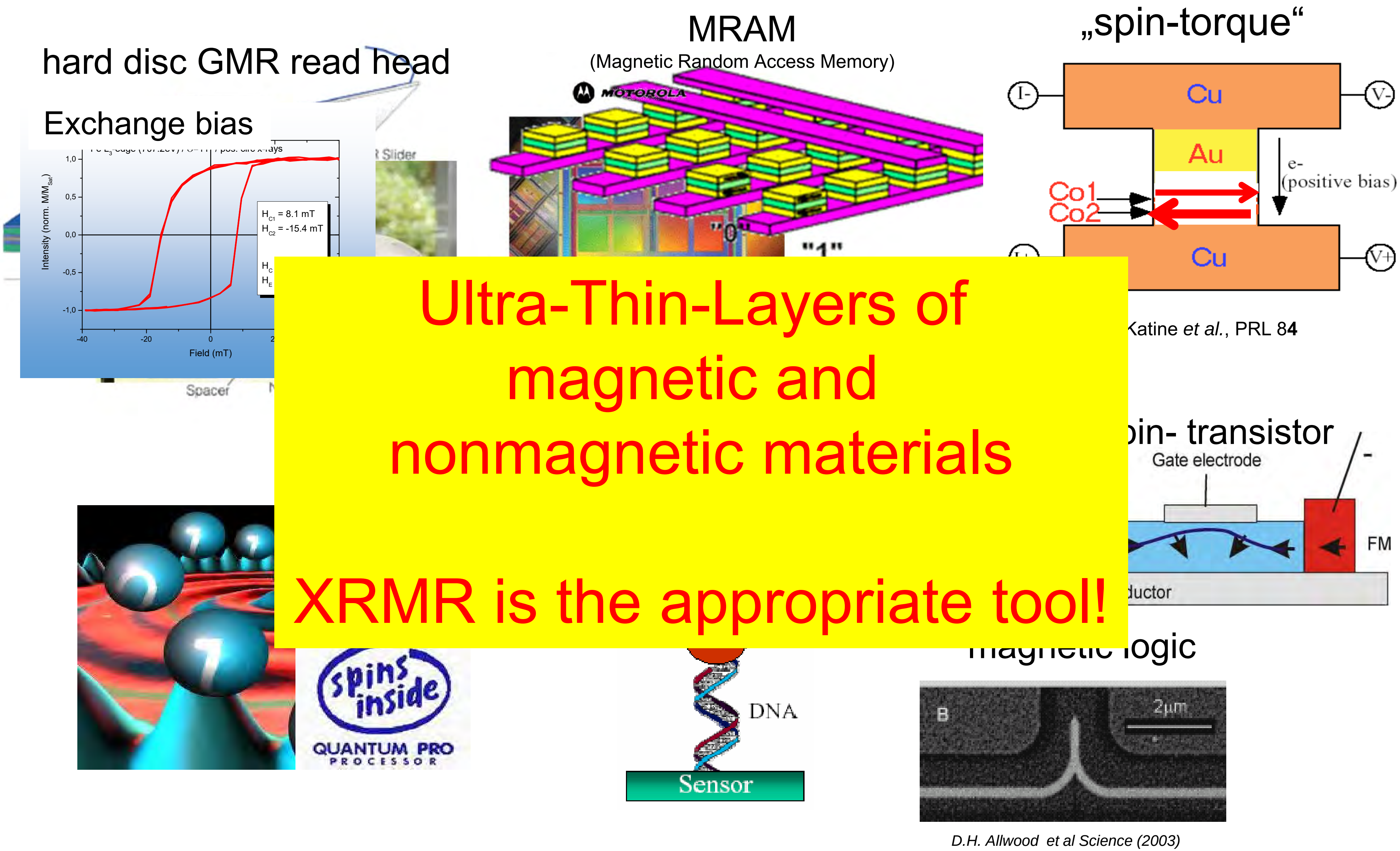

Ultra-Thin-Layers of magnetic and nonmagnetic materials

XRMR is the appropriate tool!

Interference at thin layers? That's what we know!

Thickness variable!
Reflection increases with the change
In the optical constants ➔Fresnel-law

Reflection is proportional to the weighted difference of the index of refraction Δn_{eff}

Fresnel-law:

$$t_s = \frac{E_t}{E_e} = \frac{2n_1 \cos\alpha}{n_1 \cos\alpha + n_2 \cos\beta}; \quad r_s = \frac{E_r}{E_e} = \frac{\overbrace{n_1 \cos\alpha - n_2 \cos\beta}^{\Delta n_{eff}}}{n_1 \cos\alpha + n_2 \cos\beta}$$

$$t_p = \frac{E_t}{E_e} = \frac{2n_1 \cos\alpha}{n_2 \cos\alpha + n_1 \cos\beta}; \quad r_p = \frac{E_r}{E_e} = \frac{n_1 \cos\beta - n_2 \cos\alpha}{n_2 \cos\alpha + n_1 \cos\beta}$$

We start with a simplified oil film!

- oil film is colored

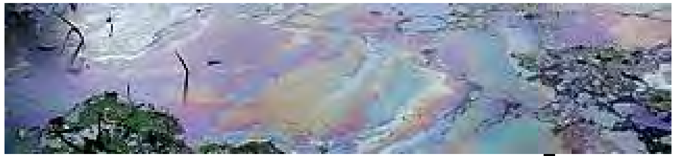

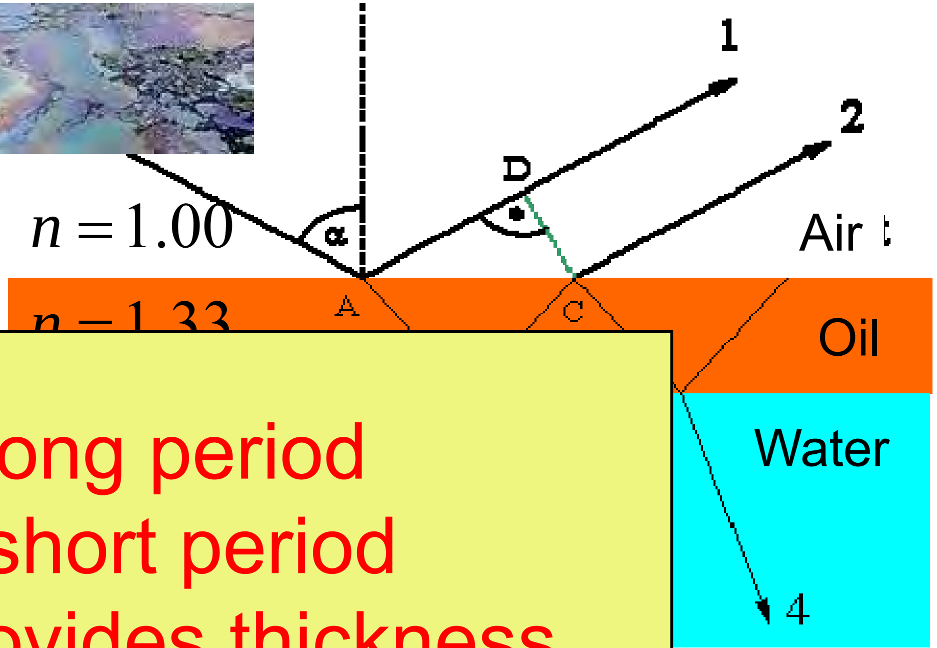

$$\Delta s = 2 \cdot d \cdot \sqrt{n^2 - \sin^2 \alpha} = N \cdot \lambda$$

Exam

$n = 1.$

thin layers ➔ long period
thick layers ➔ short period
oscillation period provides thickness

very thin layers (nm) require
very short wavelength ➔ X-rays

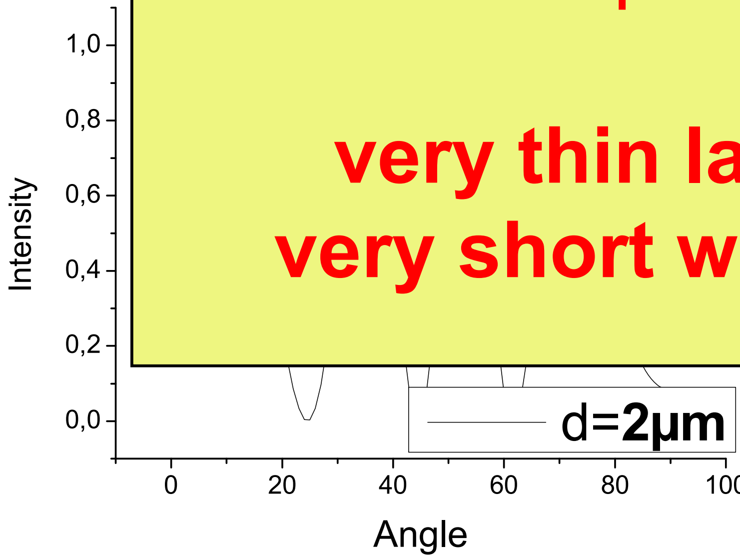

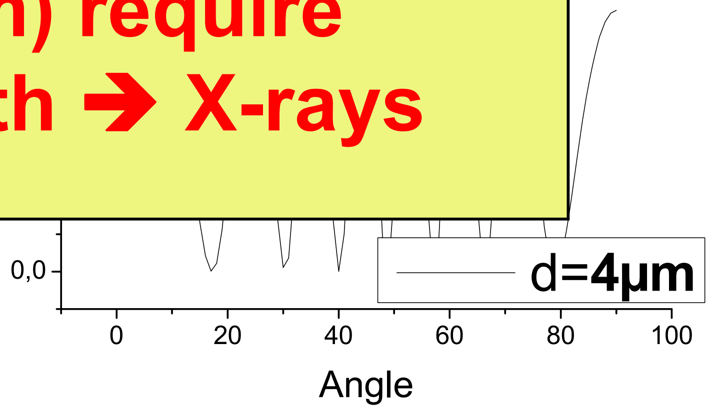

The previous example was very simple:

- Both interfering partial waves had the same intensity
- No intensity change by the angle of incidence
- Just a single layer with two partial waves
- Perfect interfaces

➔ Next level: Co on Si

Now nanoscale and more realistic!

- Ultrathin Co layers on Si substrate

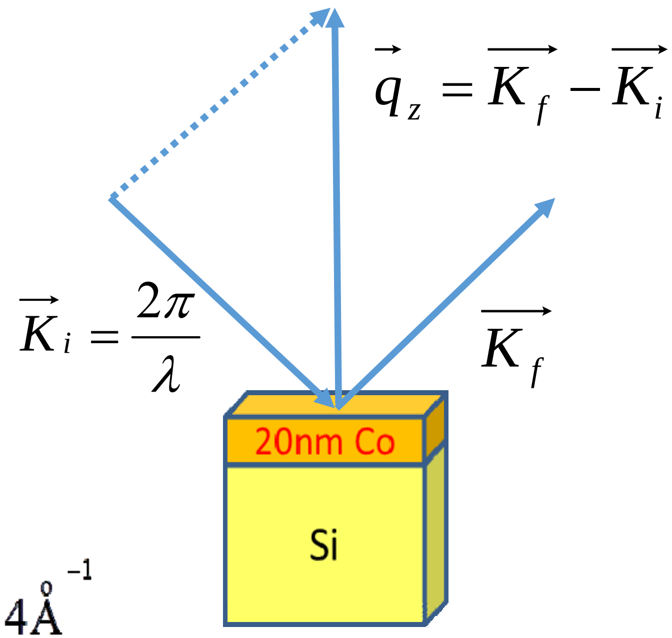

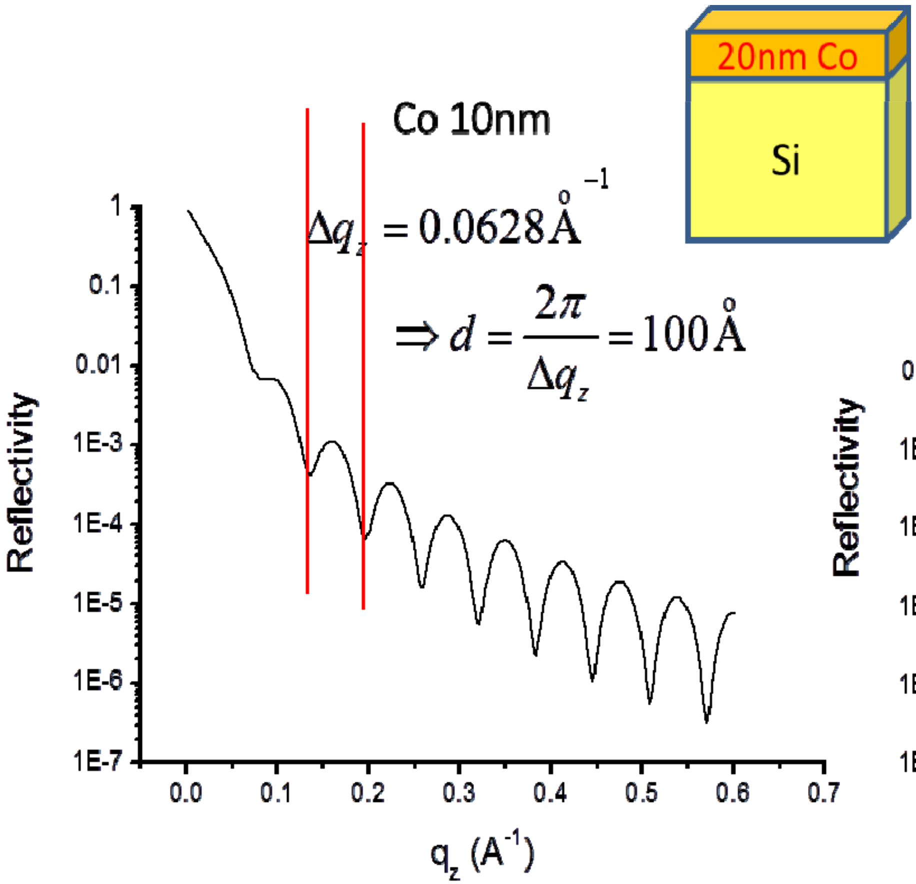

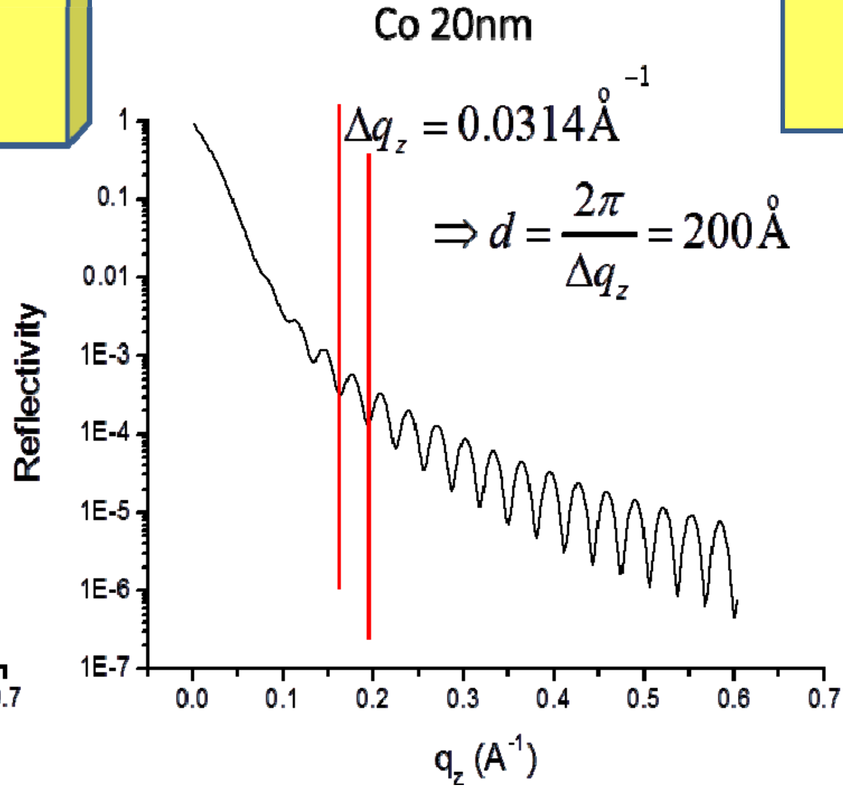

E_{phot}= 800eV ➔ λ=1.55nm K_i = 0.4 1/A

Review: S. Macke and E. Goering, J. Phys. Cond. Mat. **26** (2014) 363201

Waves at hard interfaces?

hard wall!

Reflection is strong at hard walls!

➔ i.e. steep change in index of refraction

What happens at rough (smooth) interfaces?

No reflection at the beach!

➔ Continuous change in index of refraction

Well known optical phenomenon!

- Reflectivity reduction
  - A „beach“ for light does not reflect! ➔ moth-eyes

Quelle: http://www.hitechnatur.ch/bauen/4/motten.html

„Invisible Eyes“

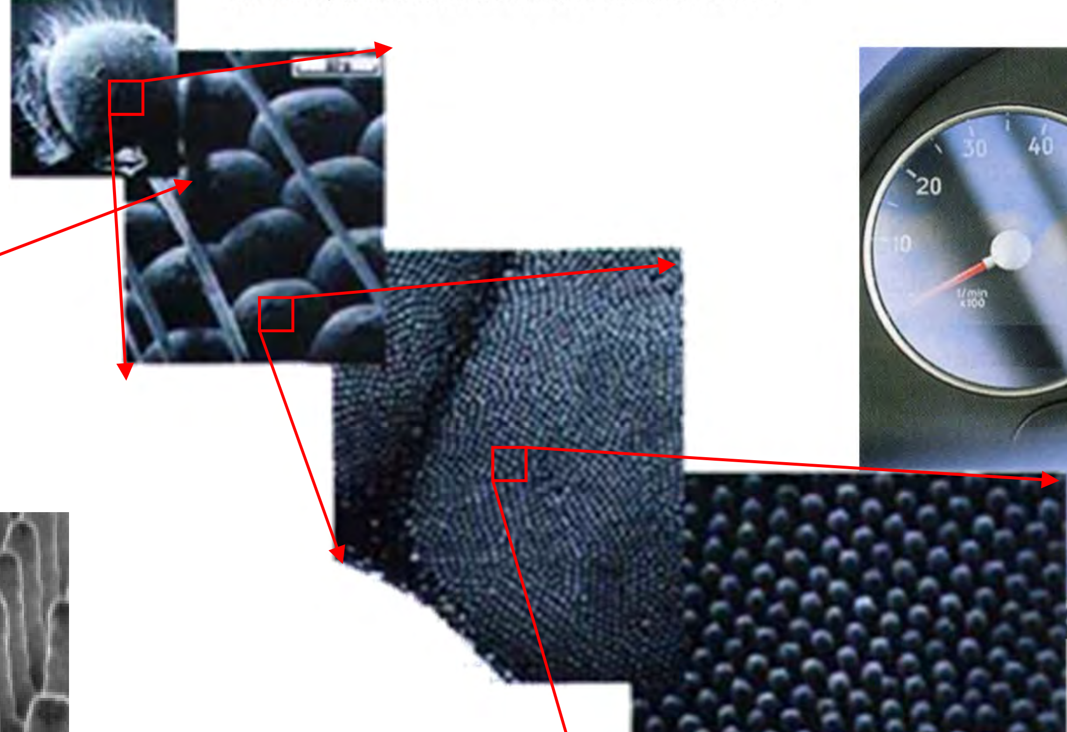

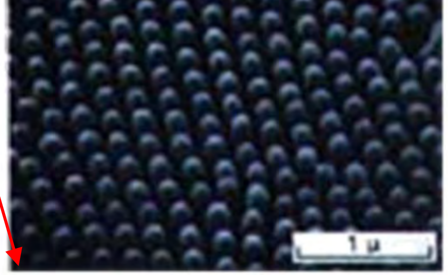

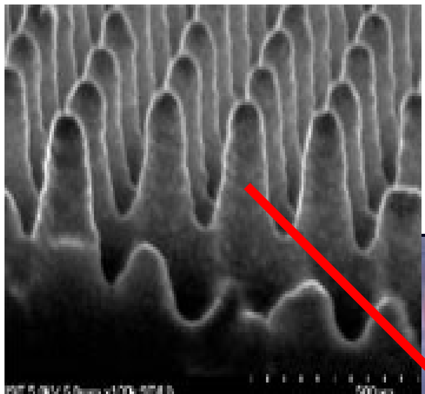

Pimples must be smaller than the wavelength!

Physik Journal Mai 2006

First real X-ray example: Non resonant

experimental setup

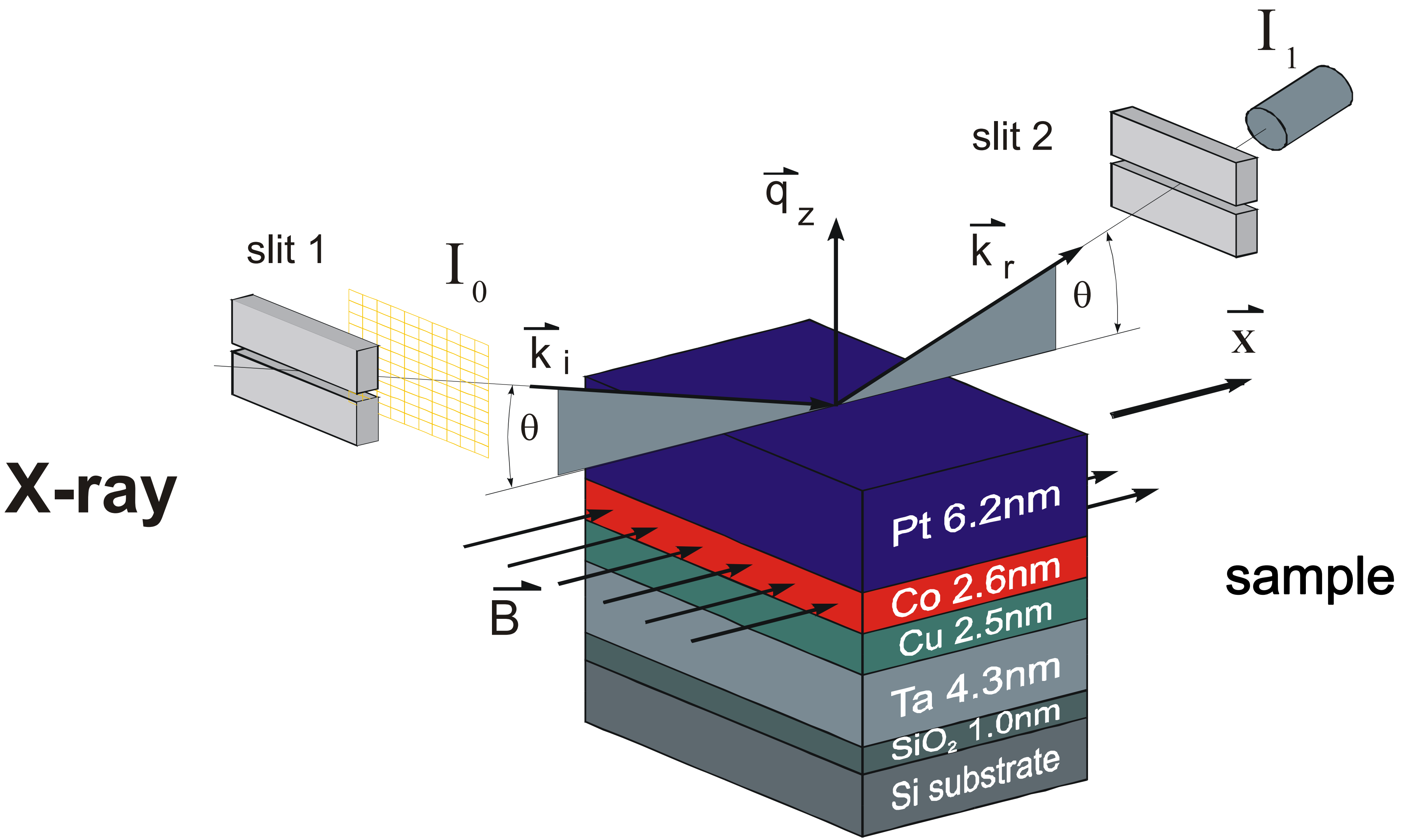

CoPt- System as a “real-world” example!

Cu K_α: Conventional “hard X-ray” non-resonant reflectivity

layered system

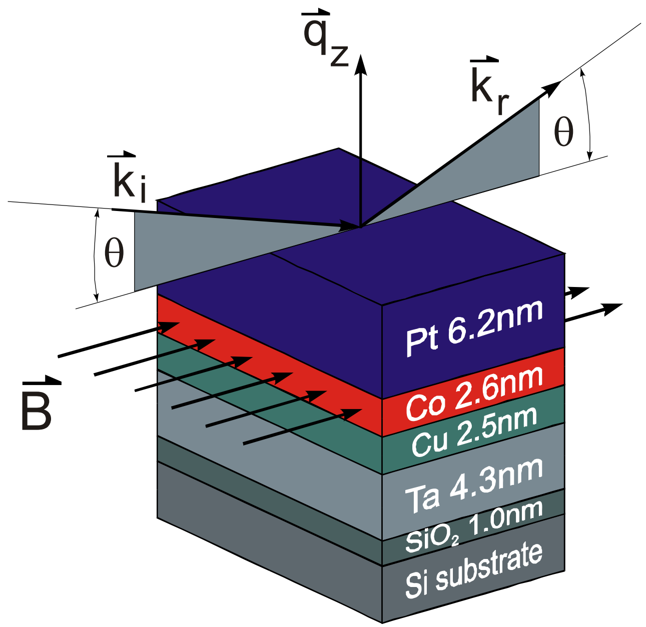

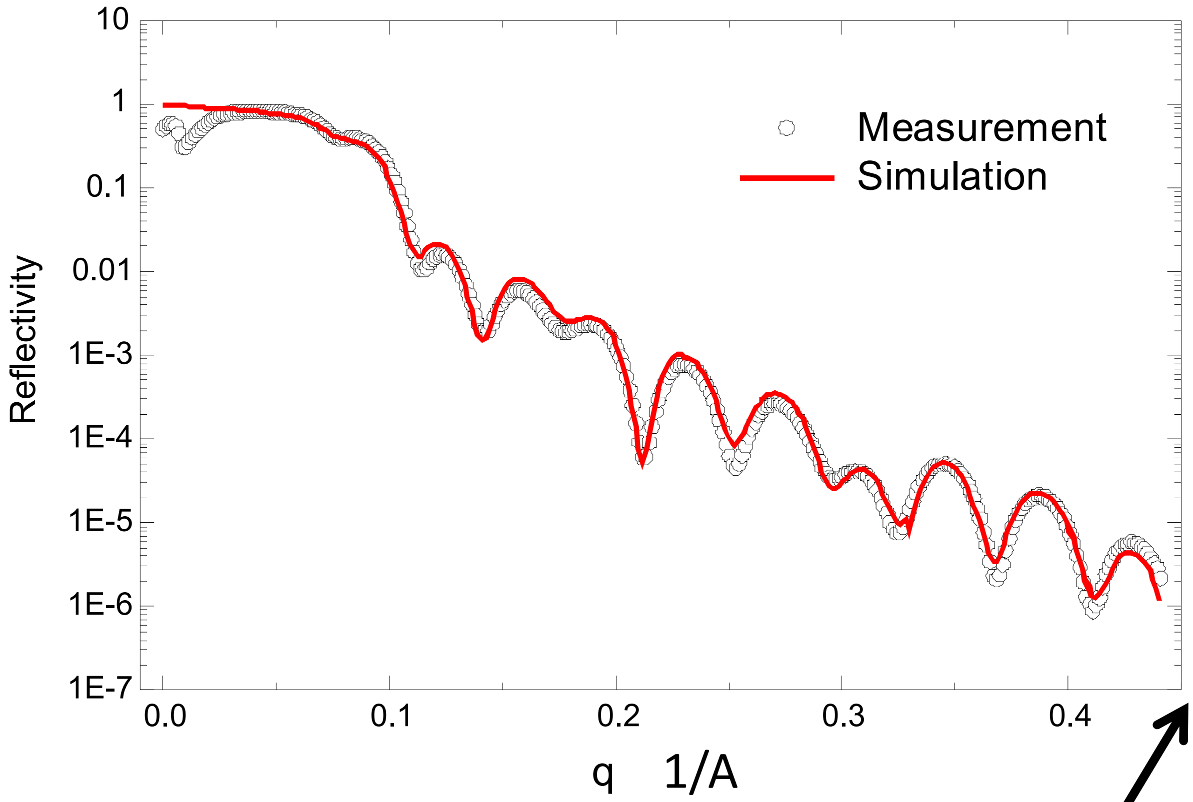

- Complex Reflectivity
- Parratt- Algorithm solves the problem (conventional reflectometry)!
- Layer thickness and roughness can be extracted
- Non resonant ➔ simple estimates for the index of refraction

1.1°

Pt induced Ferromagnetism :
X-ray Resonant Magnetic Reflectometry

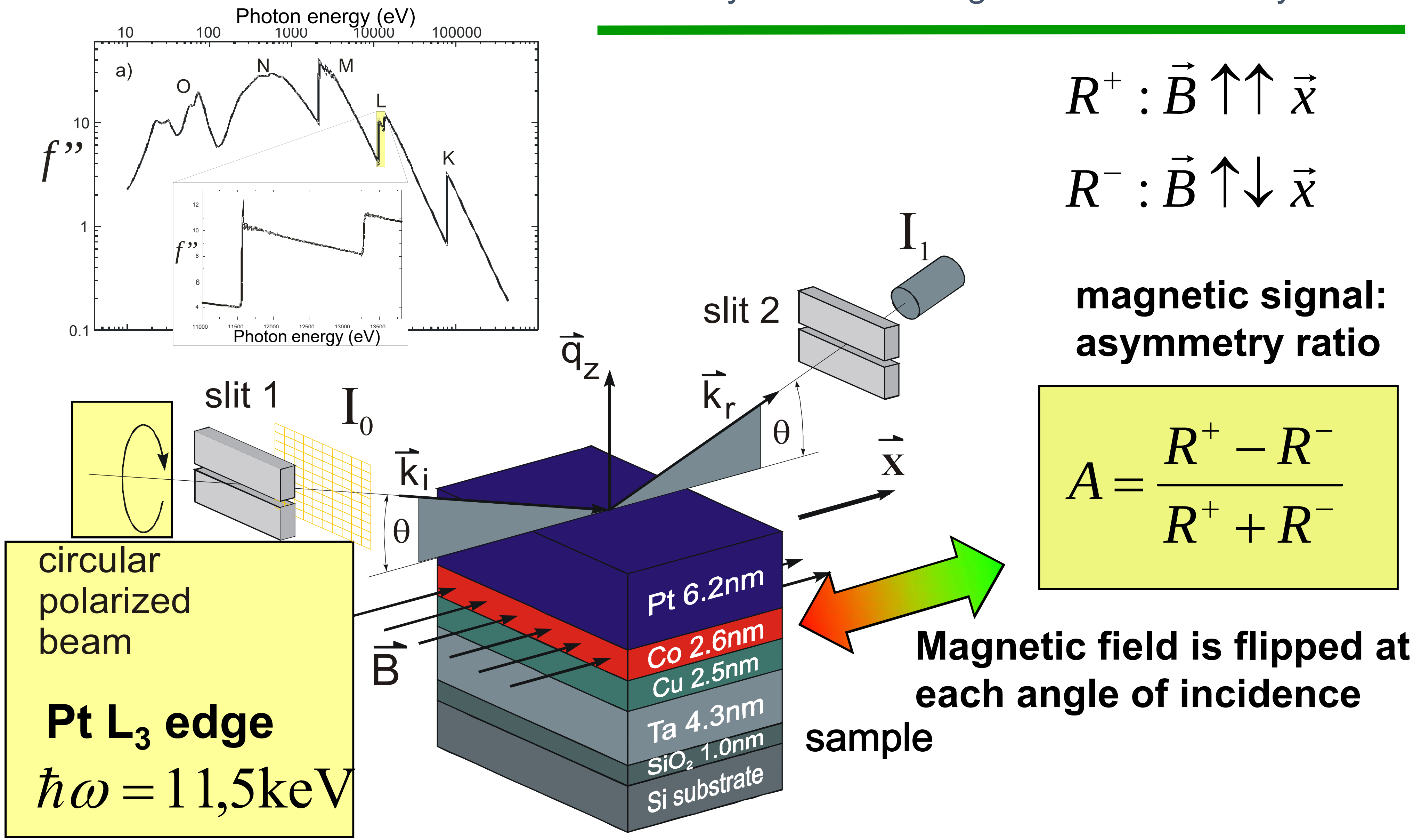

experimental setup

Magnetic response: asymmetry-ratio

Extraction of magnetization depth profiles

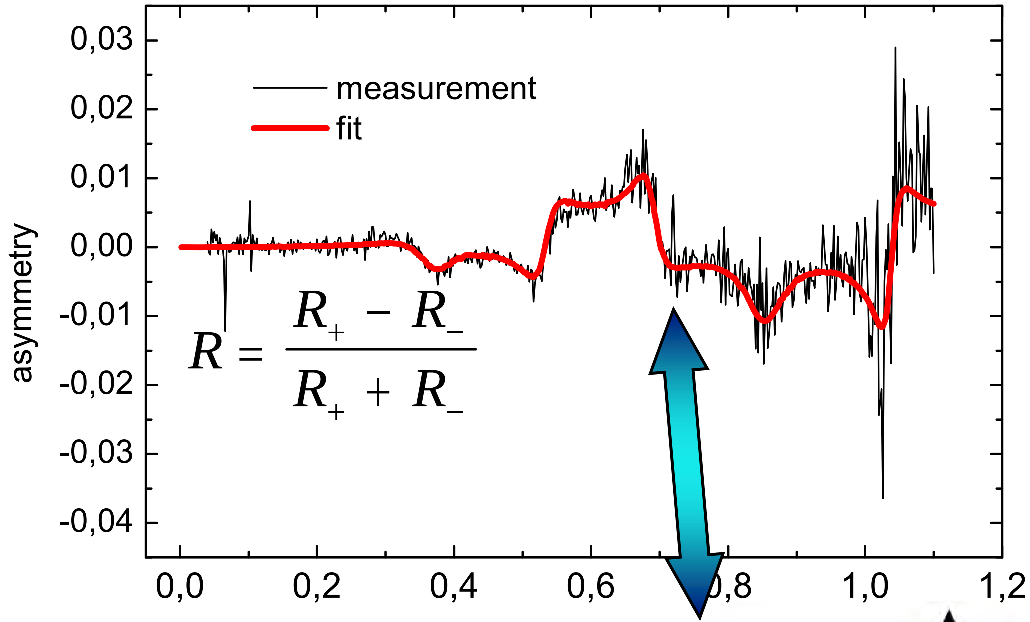

0.21μ_B
at the interface

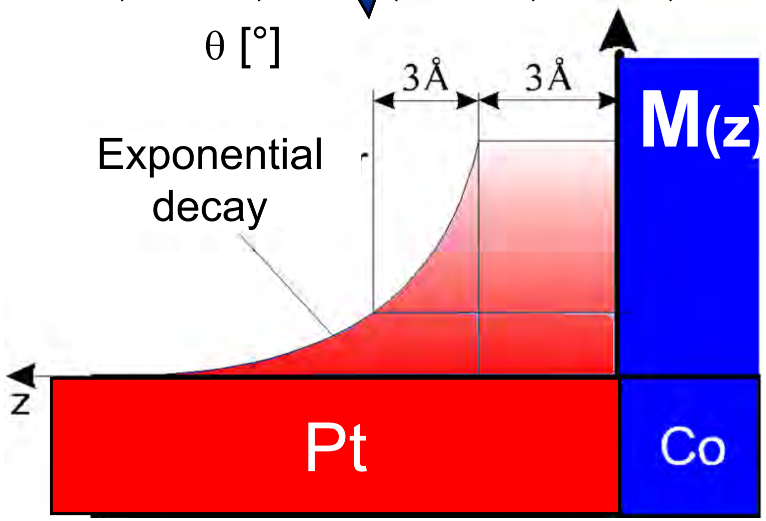

- Magnetic Simulation
  - **Nearly perfect** representation of the data
  - Quantitative magnetization profiles
  - Magnetic roughness (domains)
  - Measurement at the Pt L_3-edge (hard X-rays)
  - Element specific (just Pt!)
- Ideal tool to analyze interface properties of magnetic coupled thin layer systems (GMR,TMR,MRAM etc.)

J. Geissler, E. Goering *et al.*, PRB **65** (2001) 020405(R)

Resonance provides even more improvements

- Contrast at „hidden“ interfaces
- Co and Cu have nearly the same number of electrons ➔ nearly equal non resonant scattering length

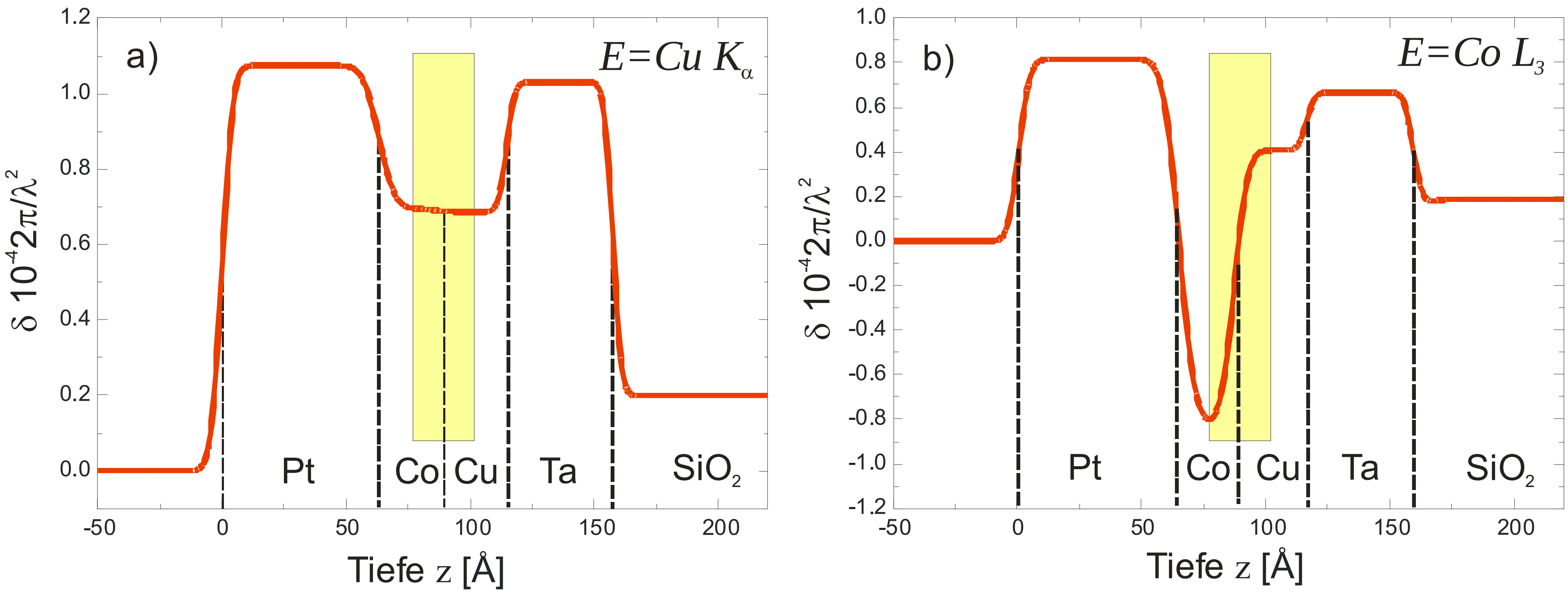

Questions:

1: Determine the Fe thickness

2: Explain the difference between left and right ➔ can we use this as an advantage?

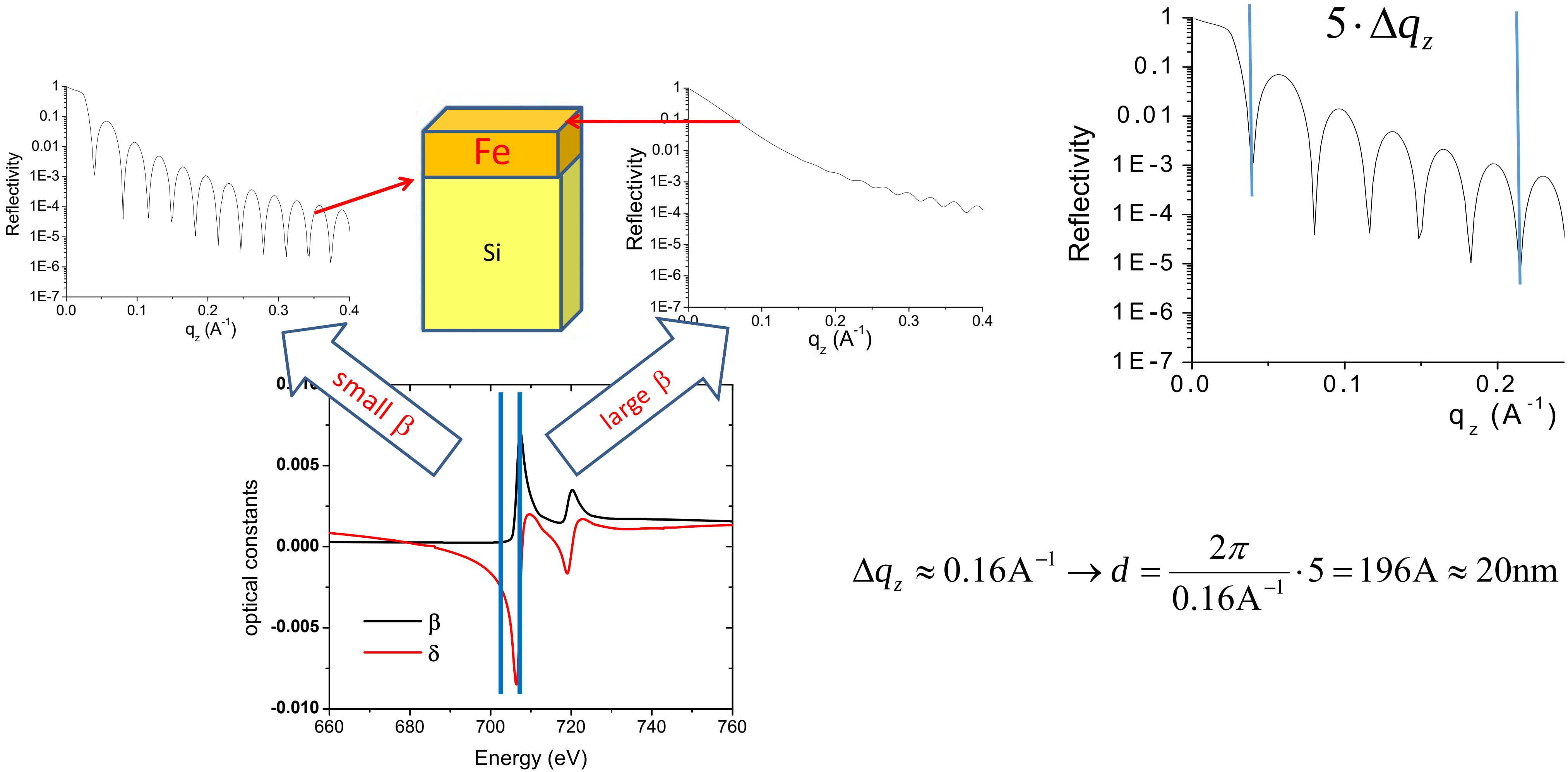

$$\Delta q_z \approx 0.16\text{A}^{-1} \rightarrow d = \frac{2\pi}{0.16\text{A}^{-1}} \cdot 5 = 196\text{A} \approx 20\text{nm}$$

How does this (XRMR) works?

1) Magnetic scattering in dipole approximation

2) Resonant optical properties: from $\mu(E)$ to $n(E,\theta)$

3) Simulation of resonant optical profile: chemical and magnetic

4) Example: Pt roughness variation in Pt/Co

1) Absorption ➔ Scattering amplitude ➔ Dispersive part ➔ complex index of refraction

Optical theorem **Absorption Experiment**

$$f''(E,\theta=0)=\frac{1}{2r_0\lambda\cdot n}\left(\mu_{\downarrow\uparrow}(E)+\mu_{\uparrow\uparrow}(E)\right)/2$$

$$m''(E,\theta=0)=\frac{1}{2r_0\lambda\cdot n}\left(\mu_{\downarrow\uparrow}(E)-\mu_{\uparrow\uparrow}(E)\right)/2$$

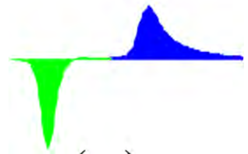

Kramers-Kronig-Relation

$$f'(E_0)=\frac{2}{\pi}P\int_0^\infty \frac{E_0 f''(E)}{E_0^2-E^2}dE$$

$$m'(E_0)=\frac{2E_0}{\pi}P\int_0^\infty \frac{m''(E)}{E_0^2-E^2}dE$$

Dipoleapproximation

J. P. Hannon, PRL 61, 1988, 1245

$$f_{res}^{E1}=-r_0\left\{\left(\varepsilon'^{*}\cdot\varepsilon\right)\left[f_0+f'+if''\right]+i\left(\varepsilon'^{*}\times\varepsilon\right)\cdot\mathbf{z}\cdot\left[m'+im''\right]\right\}$$

$$n=1-\delta(E)-\Delta\delta(E)+i\left[\beta(E)+\Delta\beta(E)\right]=1-\frac{r_0}{2\pi}\lambda^2\sum_i n_i f_i(E)$$

non magnetic part magnetic part

Jackson, J. D., **2nd Edition**, 281 (1975)

Review: S. Macke and E. Goering, J. Phys. Cond. Mat. **26** (2014) 363201

2) From $\mu(E)$ to $n(E,\theta)$: Pt L_3 optical constants

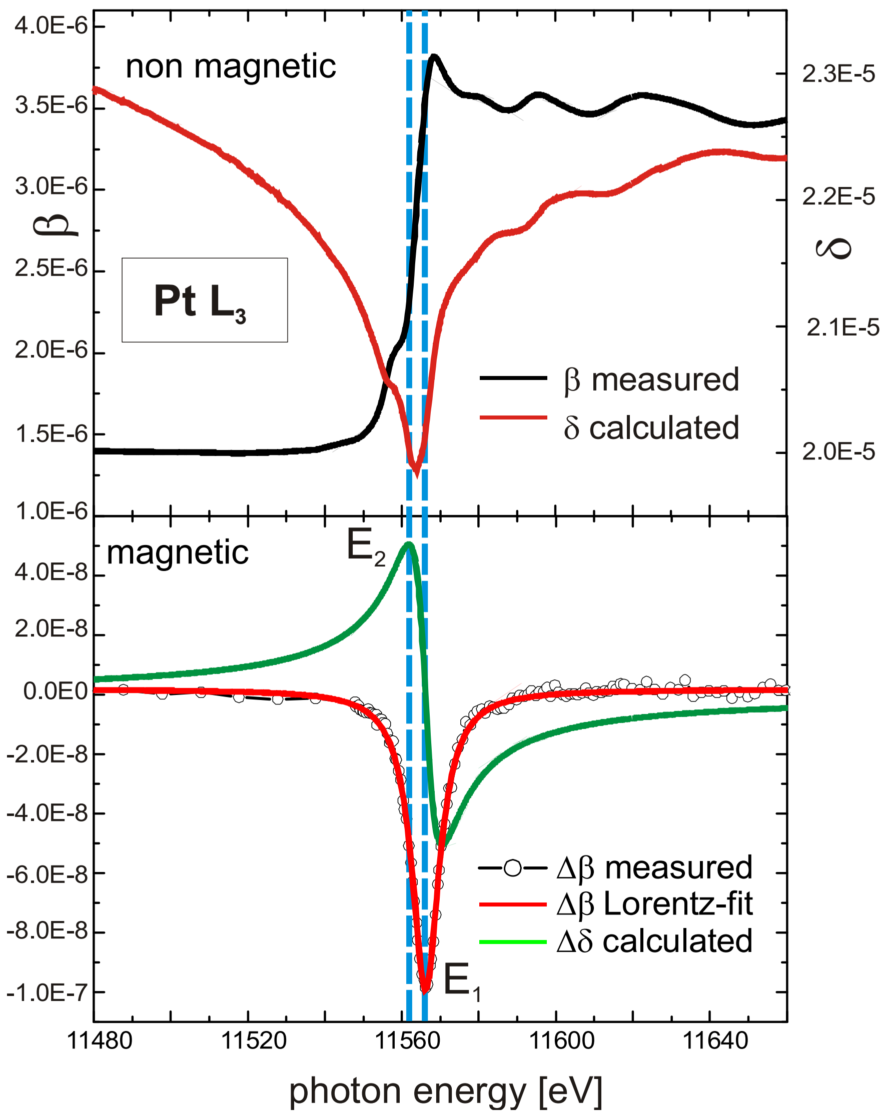

- Absorptive part
  - Non magnetic β
  - Magnetic $\Delta\beta$
- Dispersive part via Kramers-Kronig-Relation
  - Non magnetic δ
  - Magnetic $\Delta\delta$
- Requires simultaneous measurement of the nonmagnetic (XAS) and magnetic (XMCD) absorption coefficients

$$n = 1 - \delta + i\beta - \Delta\delta + i\Delta\beta$$

Reflectivity of multilayer systems

interference

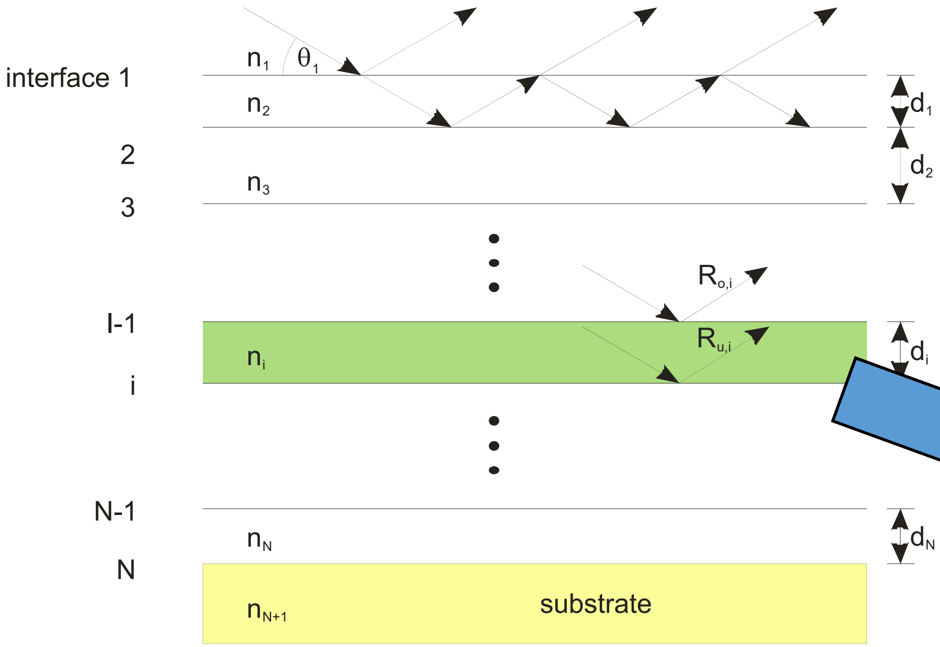

roughness

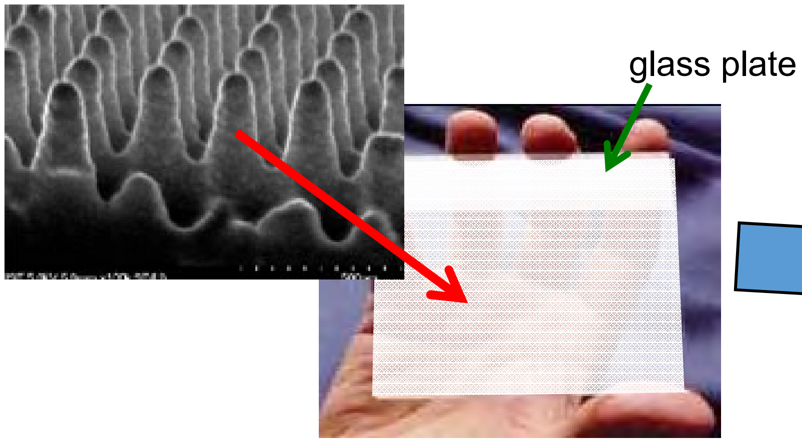

Optical approach

$$n = 1 - \delta + i\beta$$

reflection at each interface described by Fresnel-law

multilayer → L.G. Parratt formalism Phys. Rev 95, 1954, 359

$$R_{F,i} = \frac{R_{o,i} + R_{u,i}\, exp(2i\varphi_i)}{1 + R_{o,i} \cdot R_{u,i}\, exp(2i\varphi_i)}$$

interface roughness described by modified Fresnel coefficients

→ vertical rms-roughness σ

L. Nevot, P. Croce, Rev. Phys. Appl.15, 1980, 761

$$R_{rough} = R_0 \cdot e^{-2\Delta k \sigma^2}$$

Parratt

Simulation of reflectivity...

Parratt algorithm = iteratively calculate R from bottom up (by L.G. Parratt 1954)

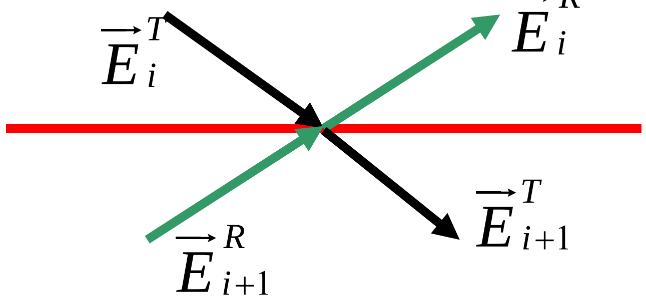

$$r_i = \frac{R^{\pi}_{i,i+1} + r_{i+1} e^{-2ik_{i+1}\Delta z}}{1 + R^{\pi}_{i,i+1} r_{i+1} e^{-2ik_{i+1}\Delta z}}$$ π-light

$$r_i = \frac{R^{\sigma}_{i,i+1} + r_{i+1} e^{-2ik_{i+1}\Delta z}}{1 + R^{\sigma}_{i,i+1} r_{i+1} e^{-2ik_{i+1}\Delta z}}$$ σ-light

Advantages: Easy & fast calculation
Roughness can be treated

Problem: σ and π-light are treated separately,
... not exact with magnetism!!

L.G. Parratt: Phys. Rev 95, 1954, 359

Matrix Formalism

$$A = \begin{pmatrix} 1 & 0 & 1 & 0 \\ -\frac{i}{2}\alpha_y^2 \, Q\left(\frac{g_i}{\alpha_z} - 2\cos\varphi + 2\frac{\alpha_z}{\alpha_y}\sin\gamma \, \sin\varphi\right) & \alpha_z + i\alpha_y \cos\gamma \, \sin\varphi \, Q & \frac{i}{2}\alpha_y^2 \, Q\left(\frac{g_r}{\alpha_z} + 2\cos\varphi + 2\frac{\alpha_z}{\alpha_y}\sin\gamma \sin\varphi\right) & -\alpha_z + i\alpha_y \cos\gamma \sin\varphi \, Q \\ \frac{i}{2} g_i \, Q N & -N & \frac{i}{2} g_r \, Q N & -N \\ \alpha_z \, N & \frac{i}{2} g_i \, Q \frac{N}{\alpha_z} & -\alpha_z \, N & -\frac{i}{2} g_r \, Q \frac{N}{\alpha_z} \end{pmatrix} \quad (3.30)$$

Magneto-optical approach

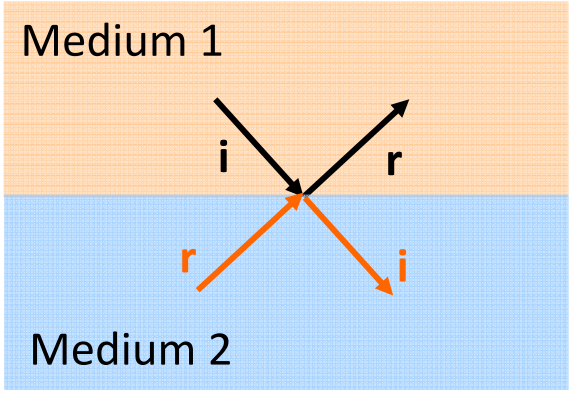

$$\vec{P} = \begin{pmatrix} E_\sigma^i \\ E_\pi^i \\ E_\sigma^r \\ E_\pi^r \end{pmatrix}$$

... + Interface

continuity requires...

$$A_1 \overrightarrow{P_1} = A_2 \overrightarrow{P_2}$$

Medium Boundary Matrix
(from the dielectric tensor)

... + Propagation

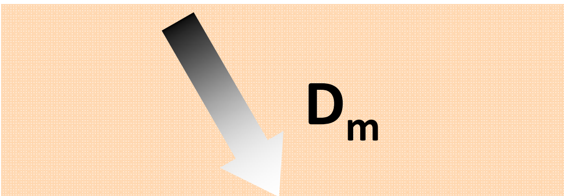

accounts for damping
and changes in phase and polarization
propagation

$$A_{vac} \overrightarrow{P_{vac}} = \prod_{m=1}^{l} (A_m D_m A_m^{-1}) A_{Subs} \vec{P}_{Subs}$$

Benefit: describes magnetism completely

Drawback: complex calculation roughness difficult to include

Review: S. Macke and E. Goering, J. Phys. Cond. Mat. **26** (2014) 363201

NOW: XRMR- Software

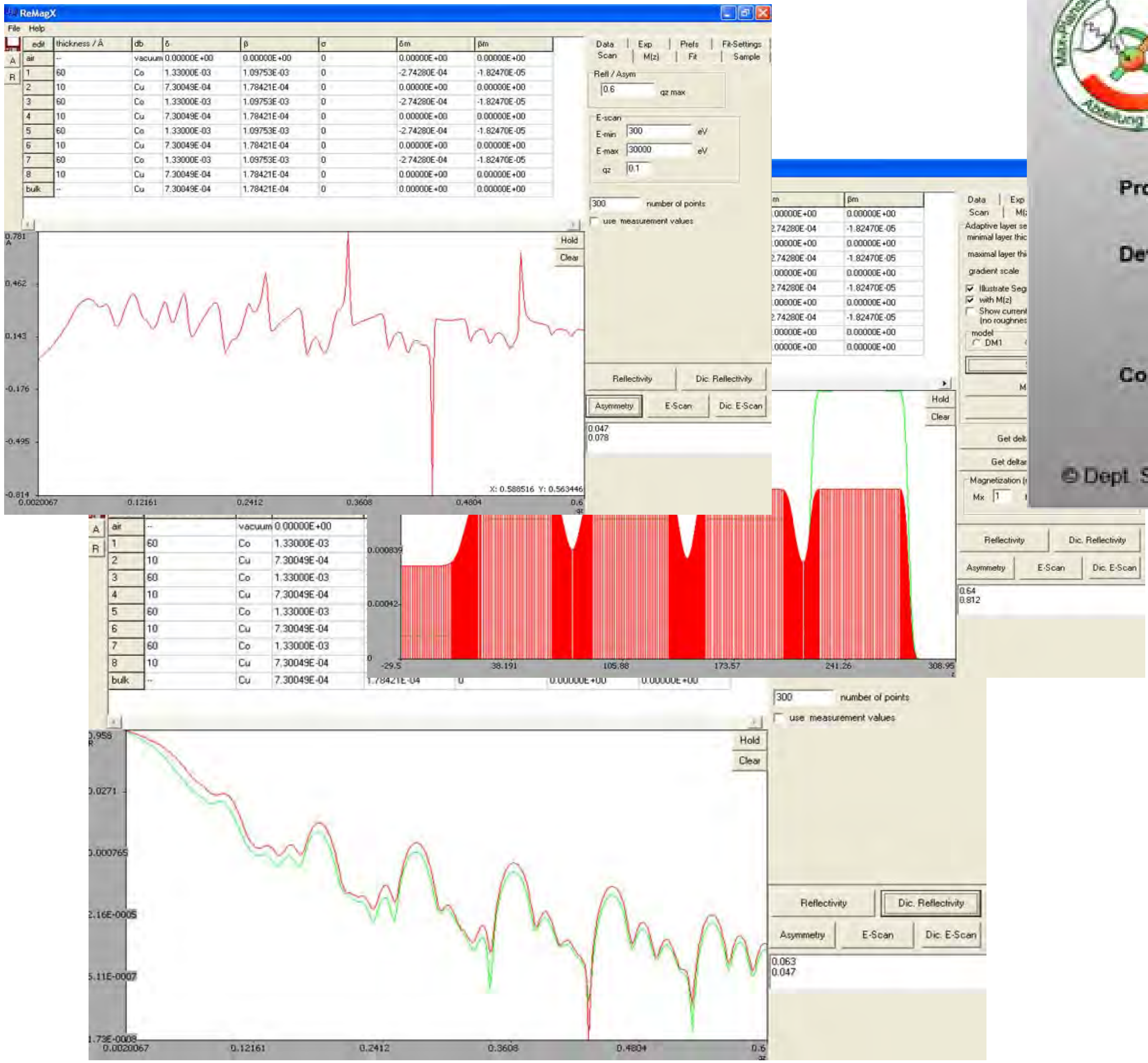

- Two different algorithms for reflectivity calculation (Matrix/Parratt)
- Adaptive slicing/layer segmentation module
- Three different methods for optical density calculation
- Processes optical-constant database files for maximum flexibility
- Variable x-ray polarization
- Magnetism on a per-layer base or by introducing artificial moment
- Four different fit routines (Genetic Algorithm, Levenberg-Marquardt, Simplex, Simulated Annealing)
- Data import modul

For details: https://www.remagx.org/wiki/doku.php

XRMR – from Θ-2Θ to a magnetic depth profile

Step 1: A layered sample

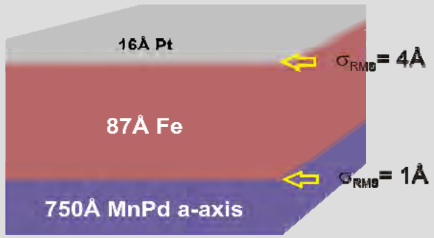

Step 2: Θ-2Θ measurements with N-S

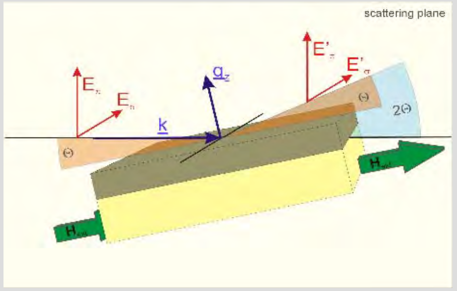

Intermediate result: dichroic Θ-2Θ spectra

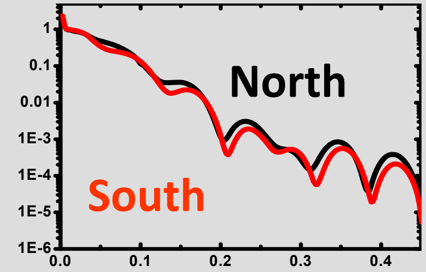

Step 3: Simulate spectra

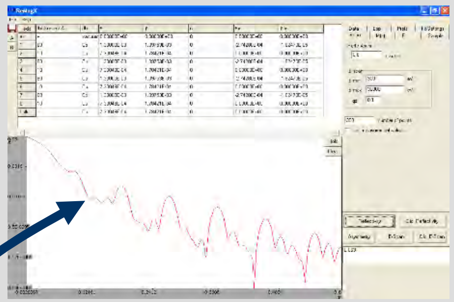

Step 4: Compare with measured spectra

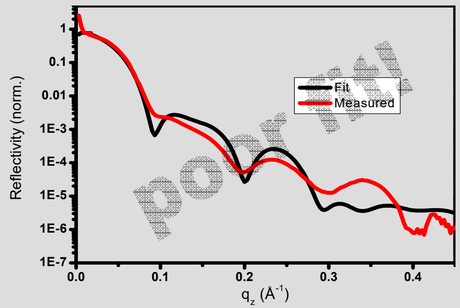

Step 5: Refine parameters

- **d_1, d_2, d_3,...thickness**
- **δ_1, δ_2, δ_3,...roughness**
- **magnetism**

Repeat

Ultimate goal:
Set of parameters reproducing the measurement perfectly.

Realistic goal:
Good fit.

Schematics of the measurement

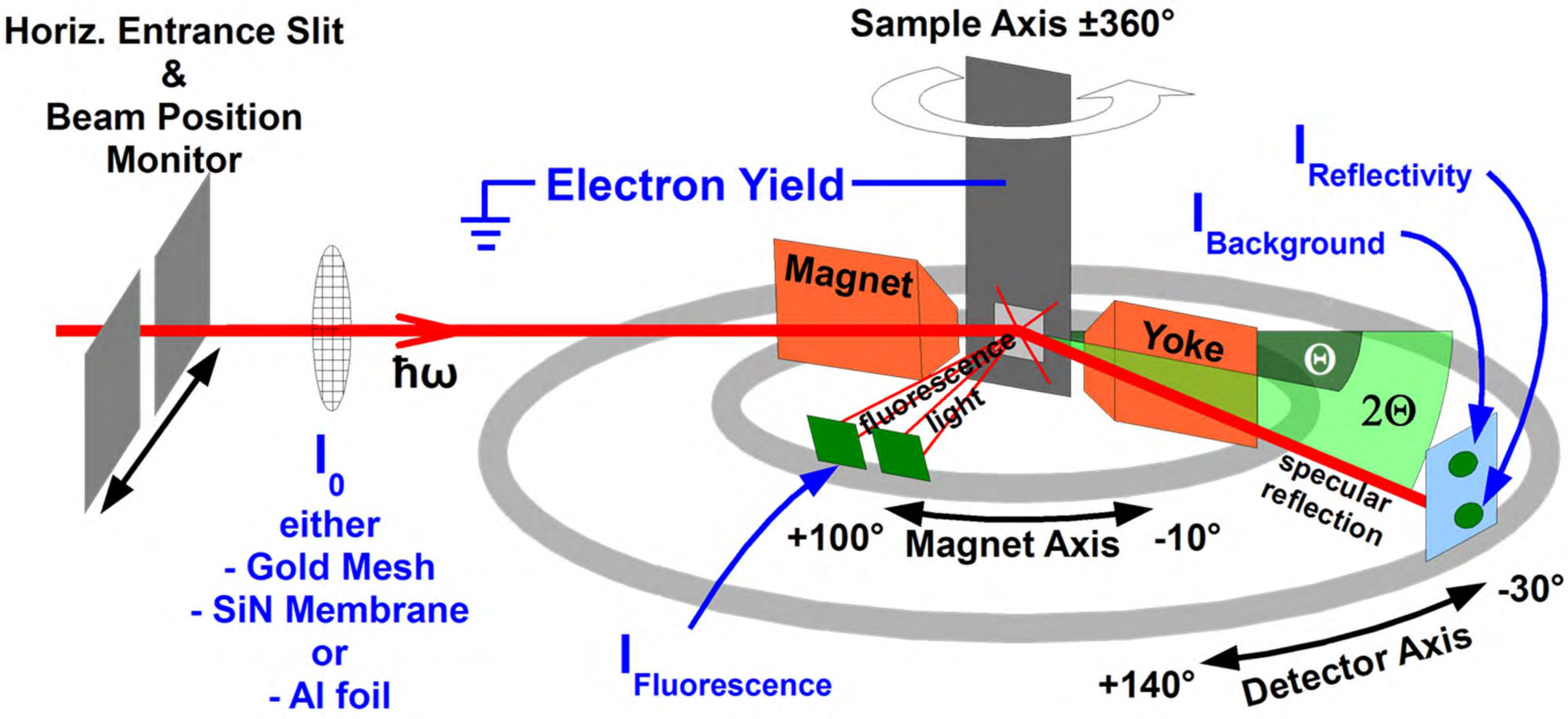

And in reality…

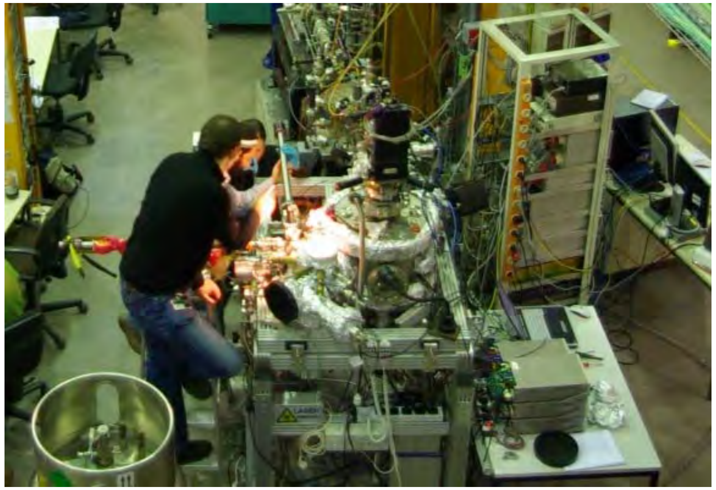

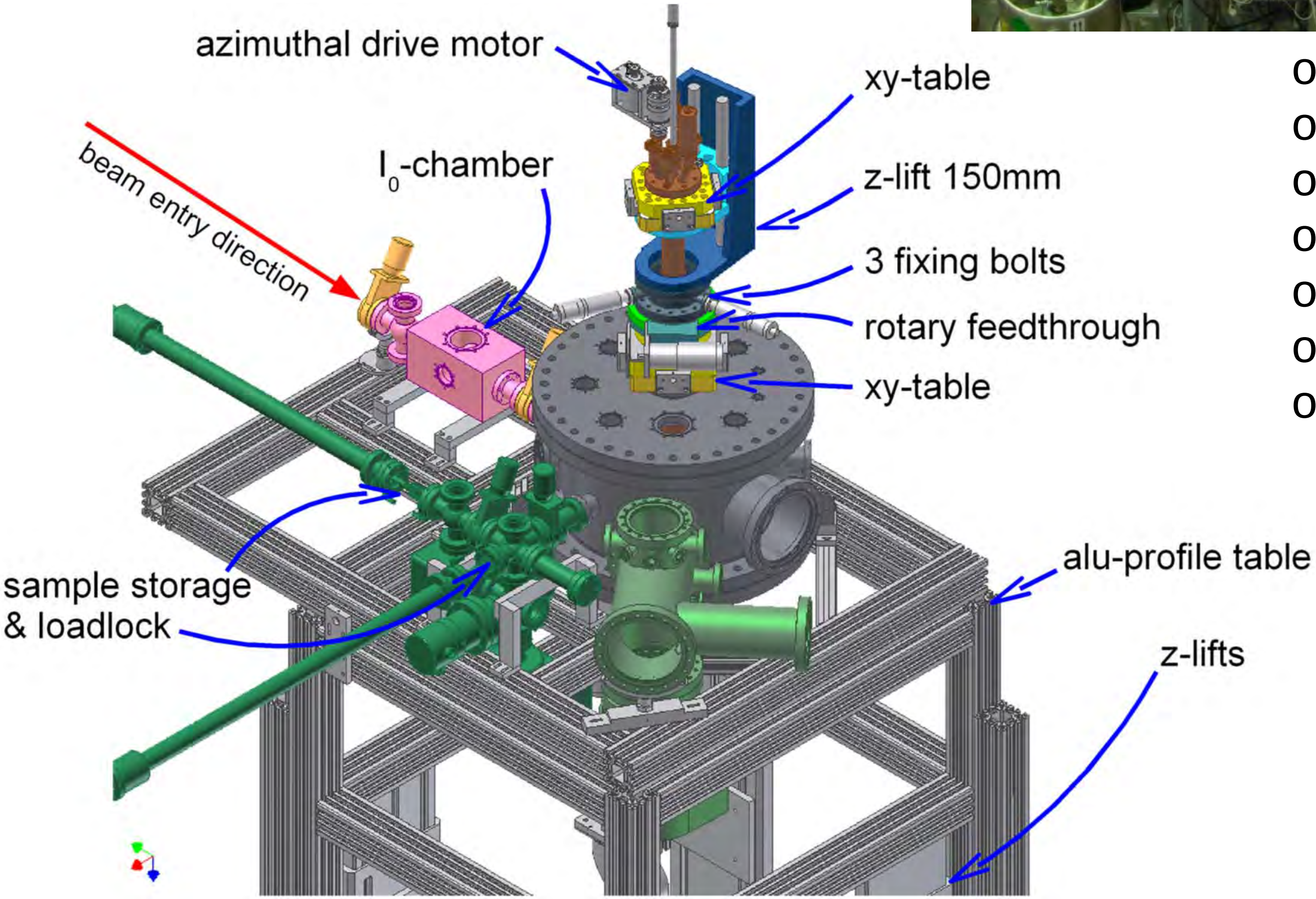

- full UHV
- fast load lock
- 20 - 450 K
- up to 1.2 T
- azimuthal rotation
- high precision
- encoder stage

XRMR² from top-down

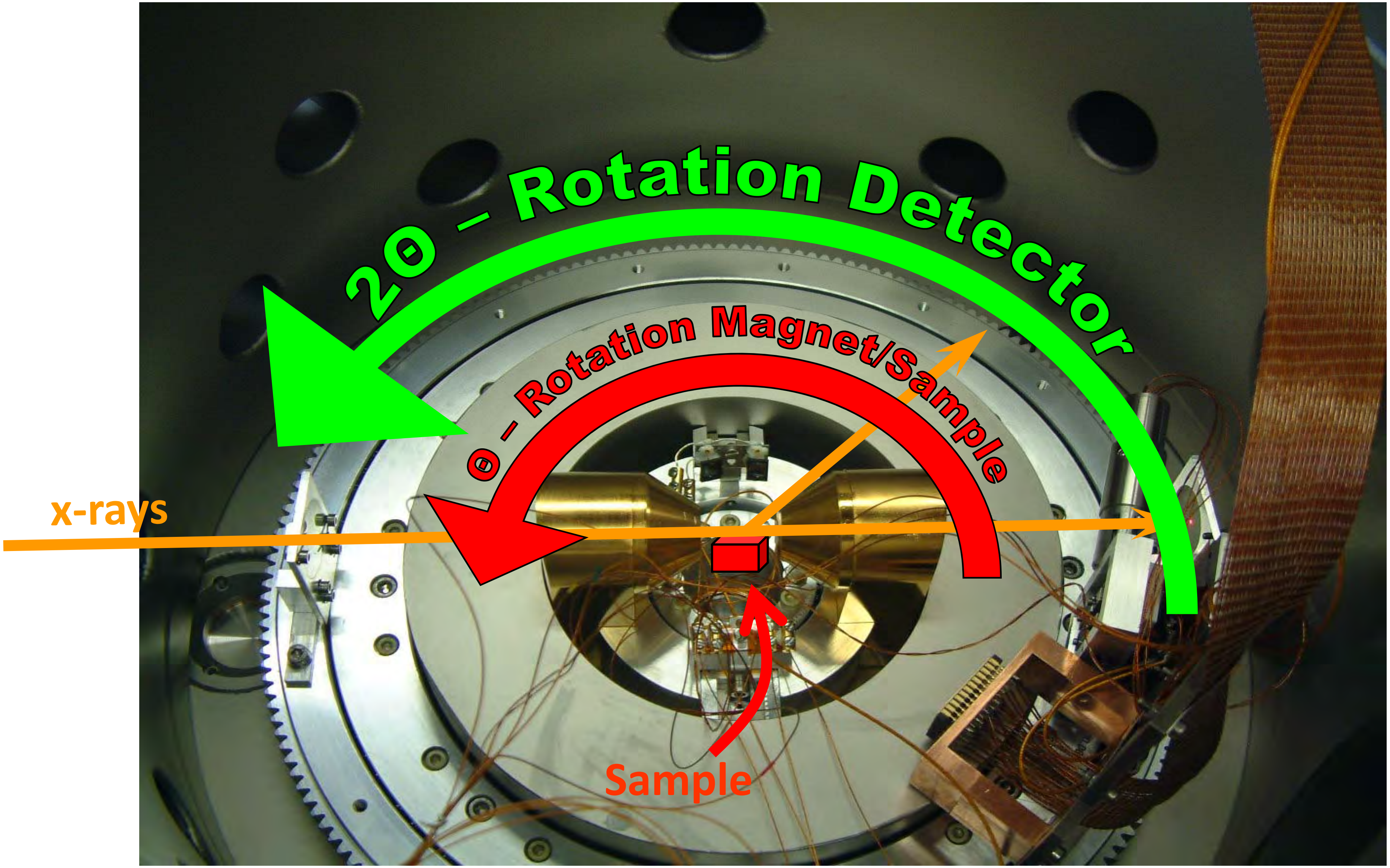

Simulation of X-ray (Neutron) reflectivity:
A brief historical overview

• L.G. Parrat	Dynamic Theory (lin pol.; intensity)	1954
• L. Nevot et al.	Roughness	1980
• J.P. Hannon et al.	Magnetic resonant scattering	1988
• S.K. Sinha et al.	Diffuse scattering (DWBA)	1988
• J. Zak et al.	Magneto optics (Matrix formalism)	1990
• L. Seve et al.	Ce/Fe and La/Fe (MF; no rough.)	1999
• S.A. Stepanov et al.	Magnetic Multilayers (MF; no rough.)	2000
• J. Geisler et al.	Pt/Co (Parratt, full magn. profiles)	2001
• D.R. Lee et al.	Magn. Matrix form. with transition layers	2003

Review: S. Macke and E. Goering,
J. Phys. Cond. Mat. **26** (2014) 363201

Exchange Bias in MnPd/Fe

MgO(001)/MnPd(750Å)/Fe(70Å)/Pt(15Å)

MnPd with a- axis growth

➔ grown at 85°C and annealed at 250 degree °C for 1 hour

element selective hysteresis – Fe

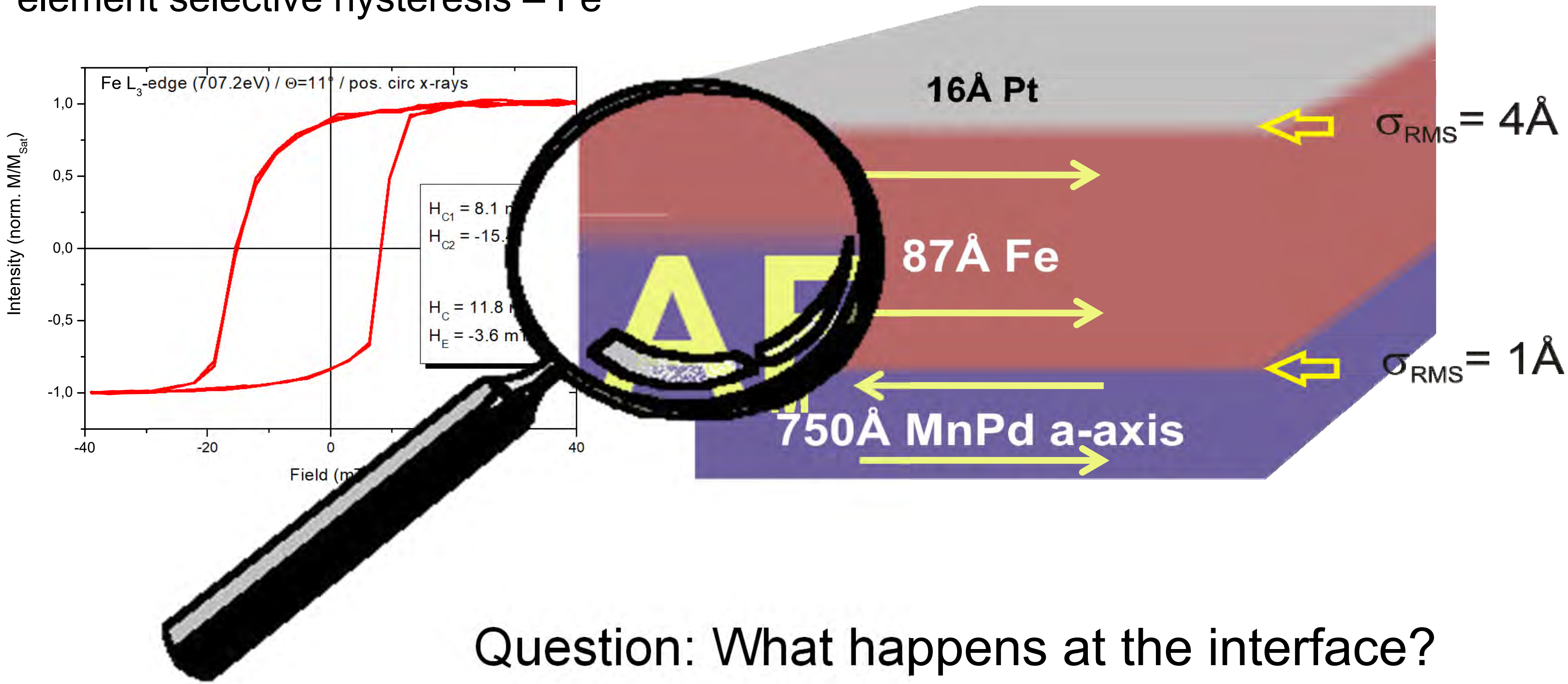

Question: What happens at the interface?

Sample provided by K. Krishnan et al. University of Washington Seattle

Determination of optical constants

optical constants for MnPd around the Mn L-edges

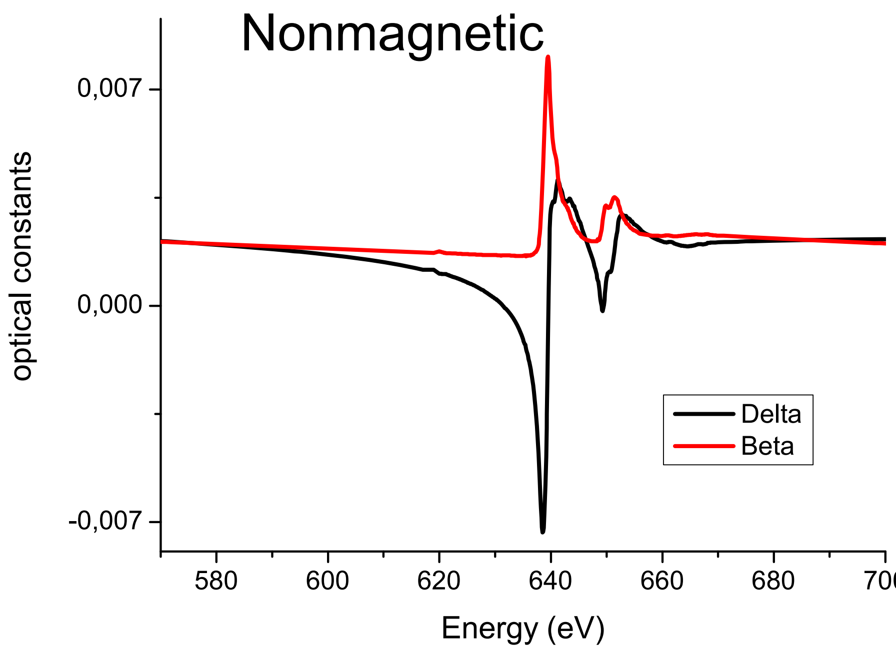

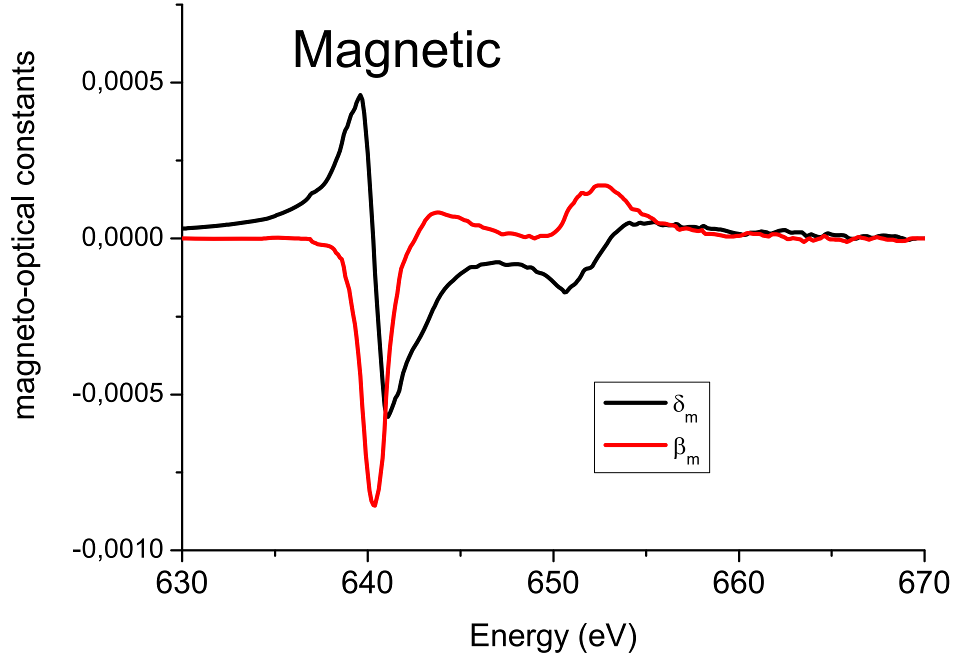

$$n = 1 - \delta(E_{phot}) - \beta(E_{phot})$$

$$\delta' = \delta(E_{phot}) + \Delta\delta_{mag}(M, E_{phot})$$

$$\beta' = \beta(E_{phot}) + \Delta\beta_{mag}(M, E_{phot})$$

XAS and XMCD experiment at
Mn $L_{2,3}$-edge normalized to Henke tables

→ Determination of charge and magnetic absorptive parts

→ Dispersive parts via Kramers-Kronig-relation

→ Absolute values from Henke tables for non resonant elements

B. L. Henke, Atomic data and nuclear data tables 54, 1993, 181
See http://cindy.lbl.gov/optical_constants

XRMR at the Mn L_3 edge

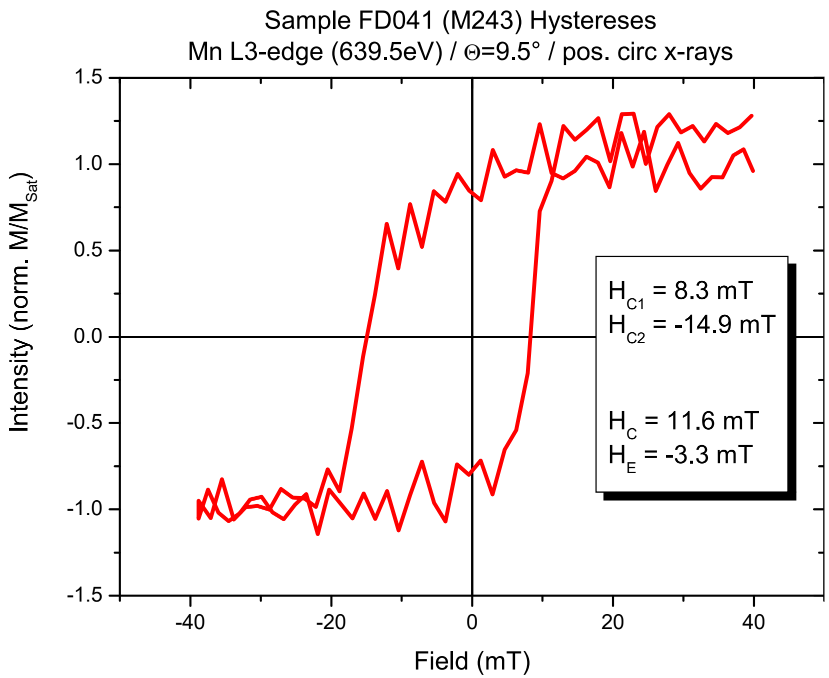

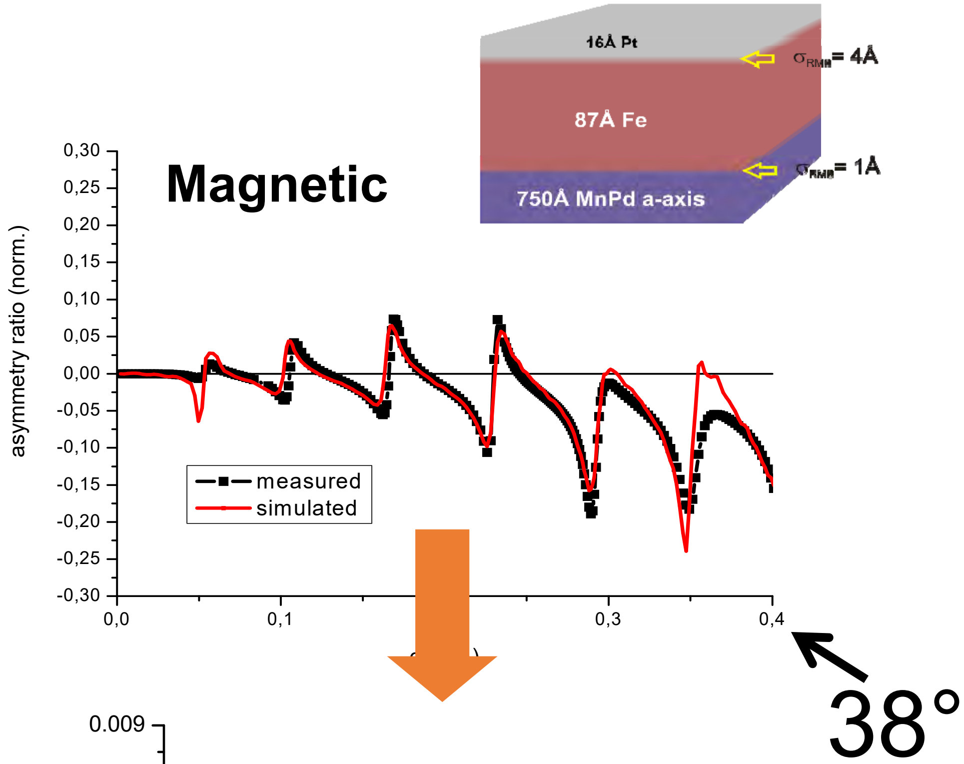

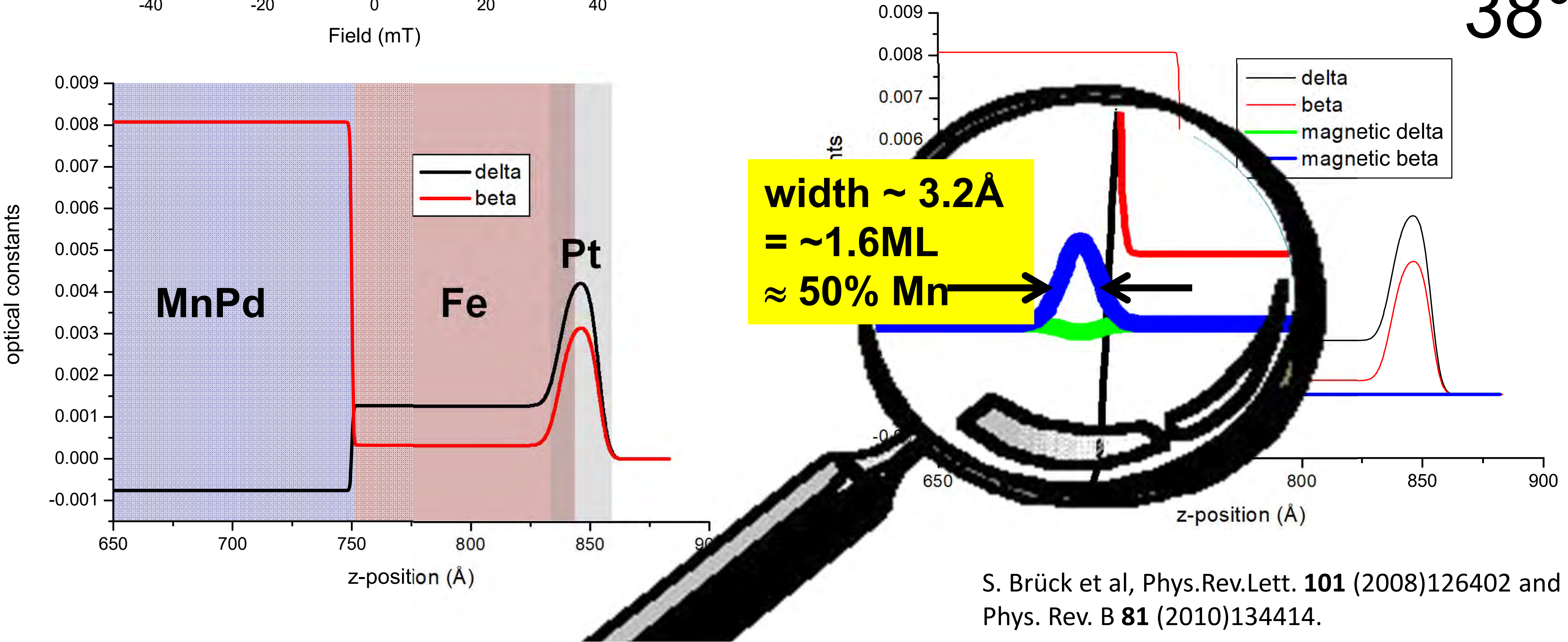

S. Brück et al, Phys.Rev.Lett. **101** (2008)126402 and Phys. Rev. B **81** (2010)134414.

„Pinned“ asymmetry

XMCD → Asymmetry →

$$\Delta I \propto \Delta(\vec{M} \cdot \vec{P})$$

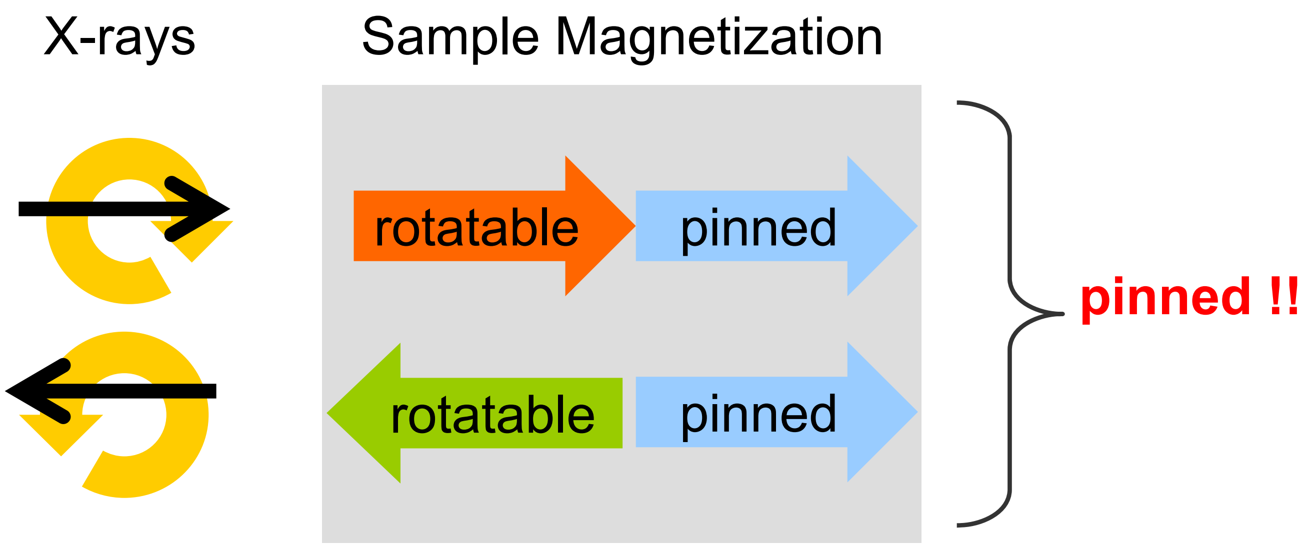

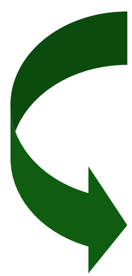

$$A = \frac{R^{++} - R^{--}}{R^{++} + R^{--}}$$

„pinned asymmetry“

XRMR at the Mn L_3 edge

We rotate helicity and the field to separate pinned from rotatable magnetic moments!

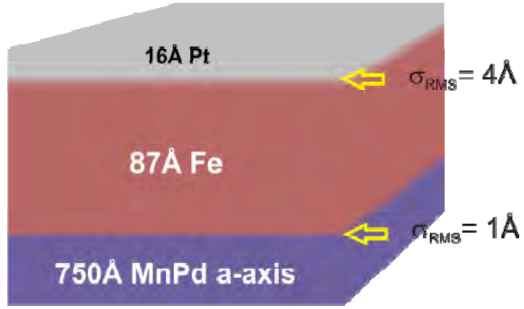

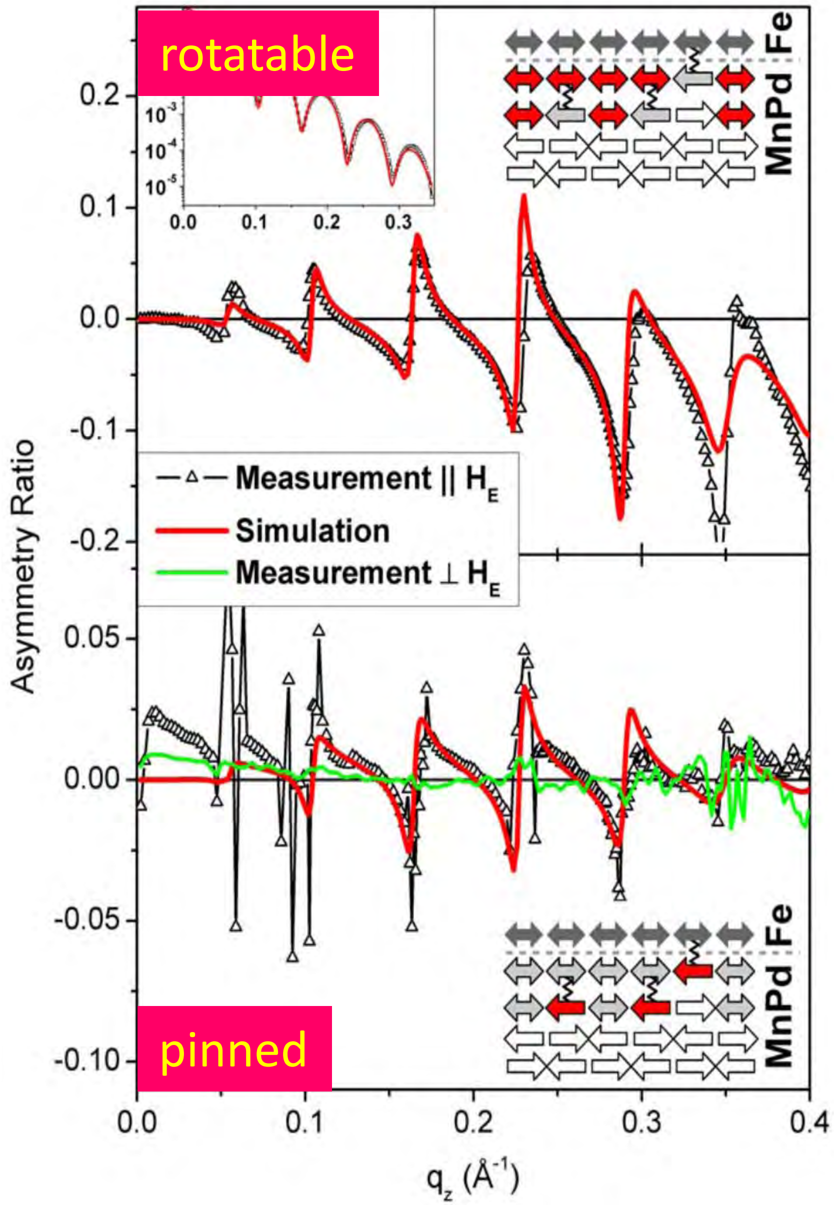

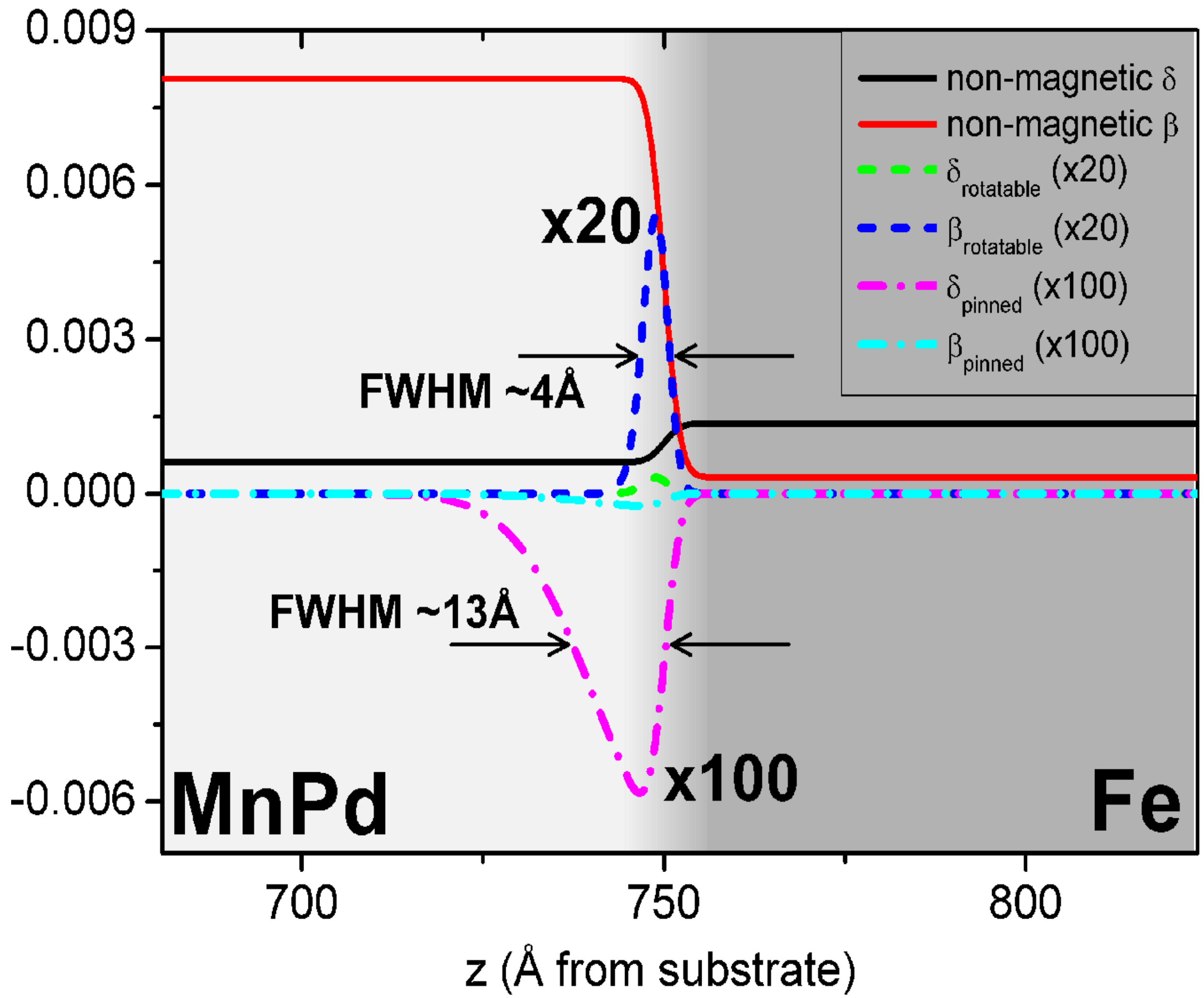

S. Brück et al. PRL **101** (2008) 126402 und Phys.Rev.B. **81** (2010) 134414.

Some „own“ examples

Induced magnetism in Pt

Hard x-rays: Pt L_3

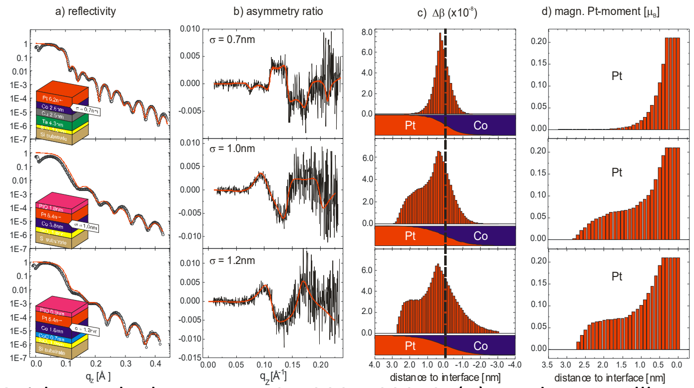

Geisler et al. Phys. Rev. B 65, 2001, 020405(R), und Z. Metallk. 93, 2002,946

Magnetite/ZnO

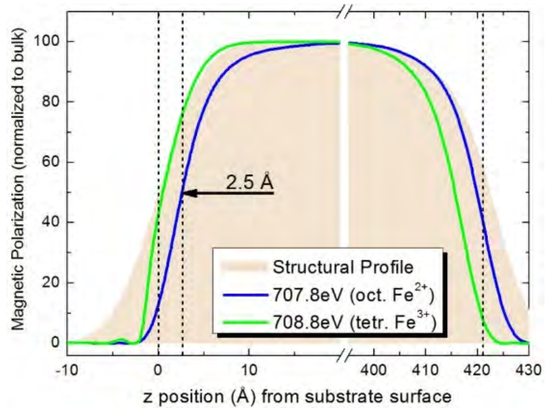

S. Brück et al. *Applied Physics Letters* **100**, 081603 (2012)

Exchange Bias in Fe/MnPd

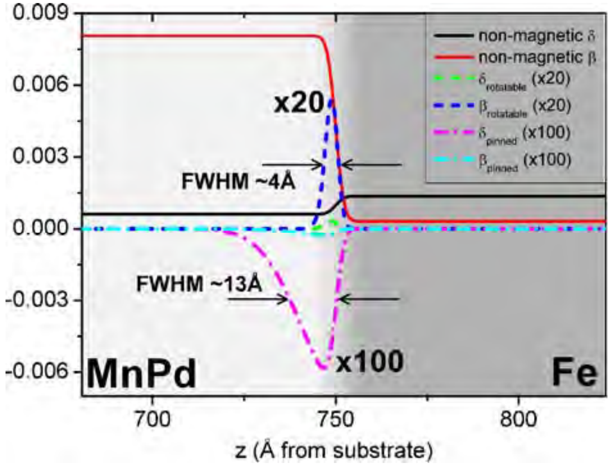

orbital reflectometry

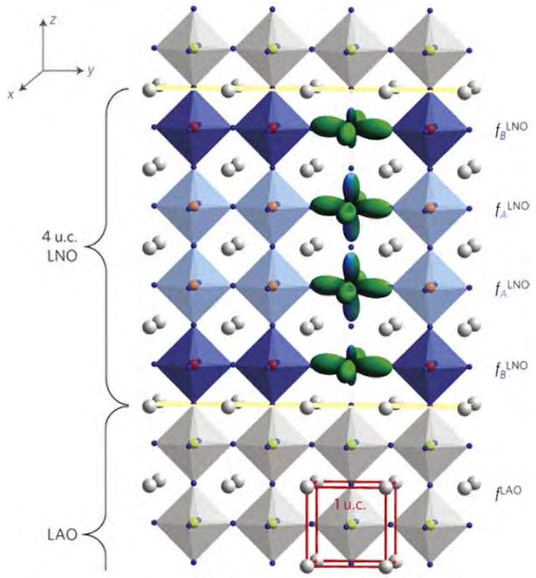

E. Benckiser et al., Nature Materials **10** (2011) 189-193.

GMR at $CrO_2/RuO_2/CrO_2$

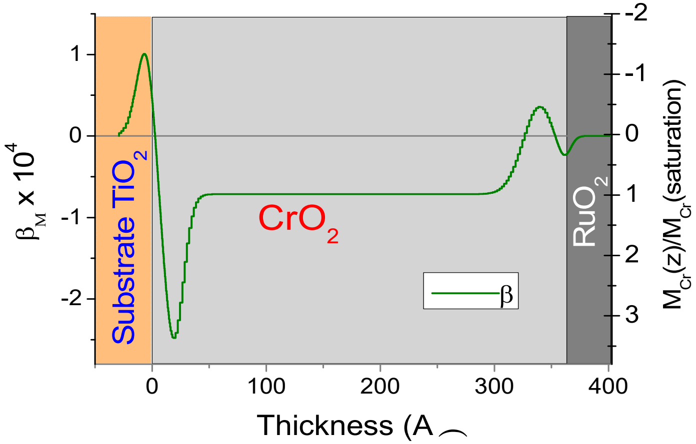

Zafar et al. Phys. Rev. B **84** (2011) 134412

supercond. vs. magnetism

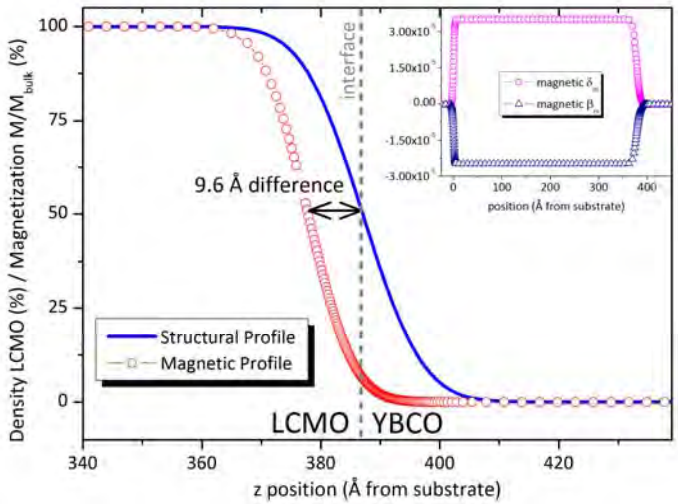

Brück et al. New Journal of Physics **13** (2011) 33023.
D.K. Satapathy et al.; Phys. Rev.Lett. 108 (2012) 197201

Summary of possibilities

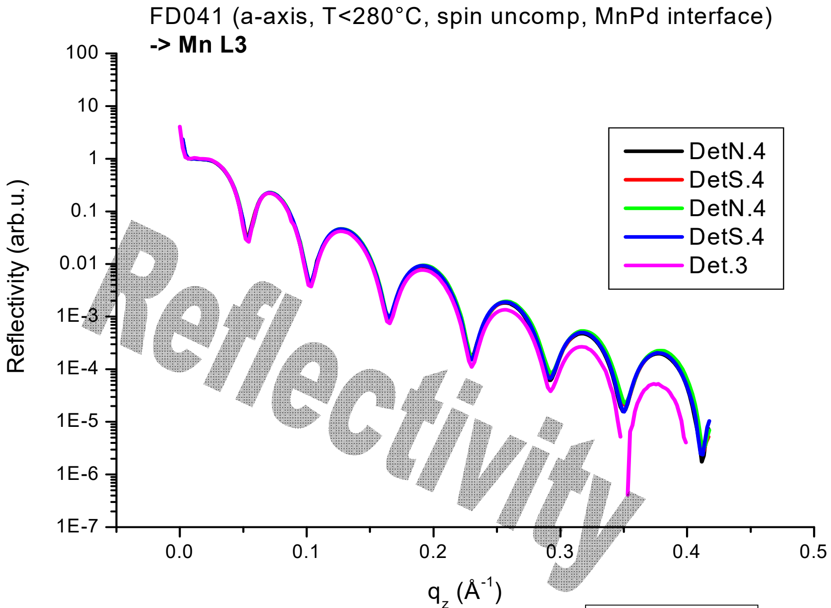

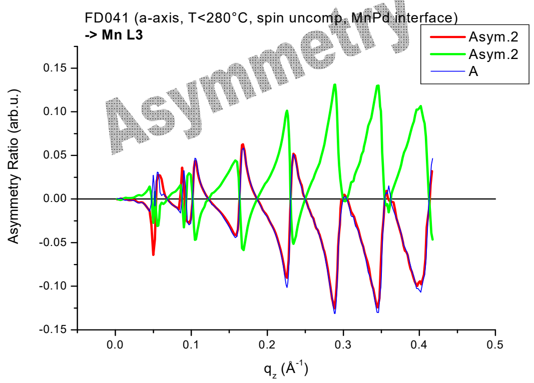

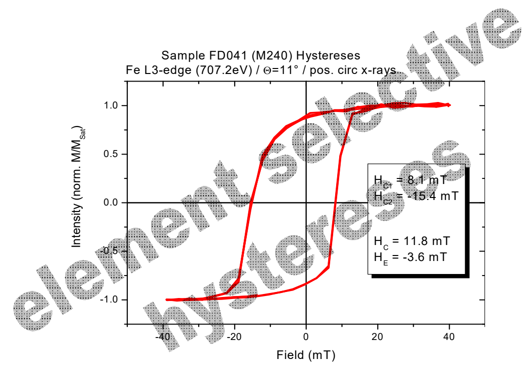

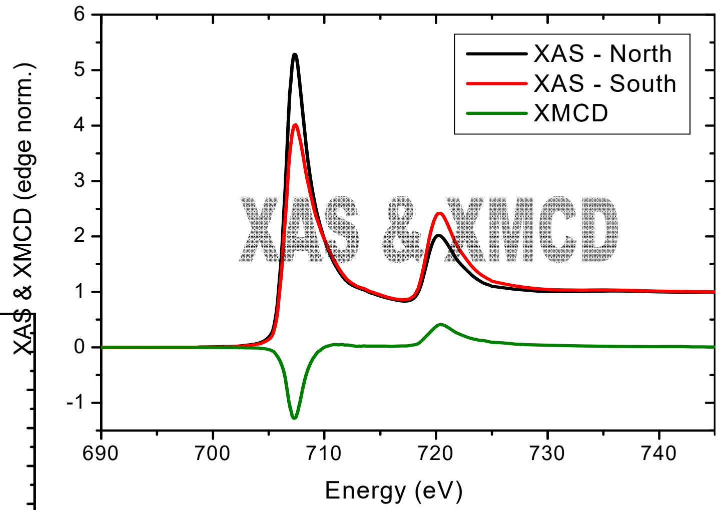

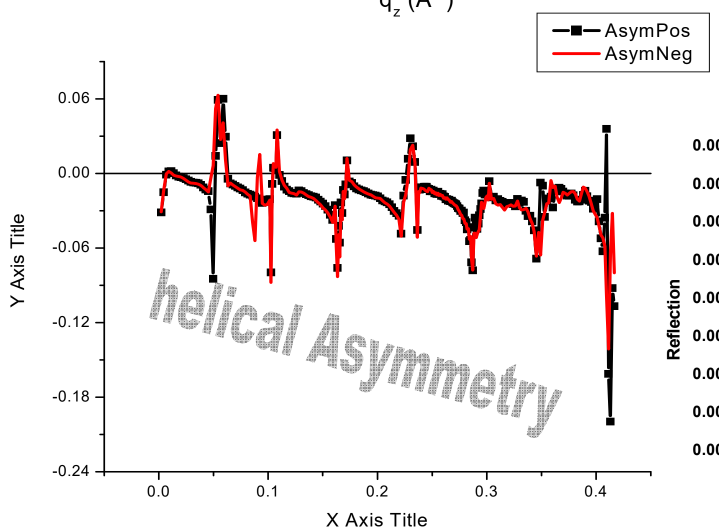

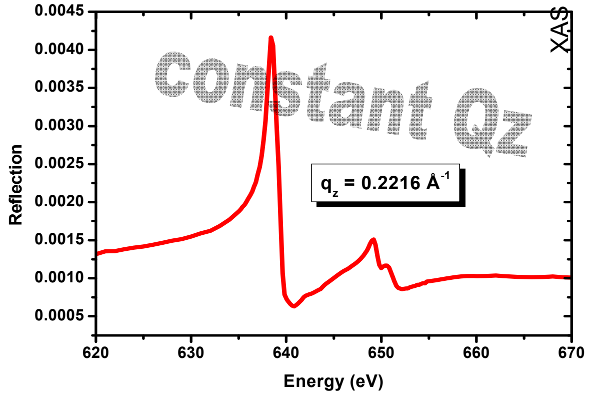

Another X-ray technique used for magnetism

- Full field X-ray Microscopy
- Scanning X-ray Microscopy (STXM)

    STXM Examples

Magnetic transmission microscopy: MTXM

The full field experimental setup

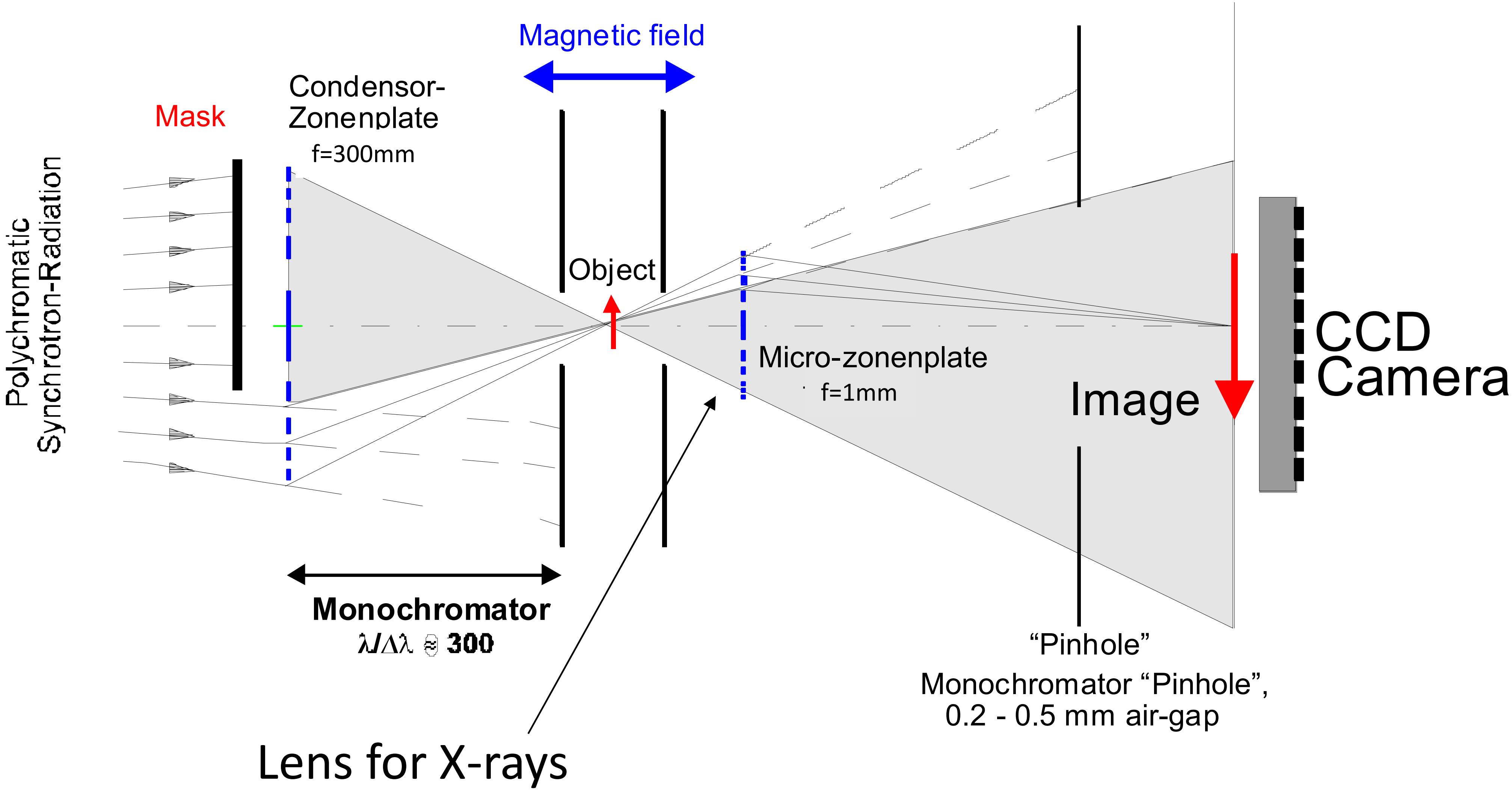

Fresnel Zonenplates

Optical element in a X-ray microscope

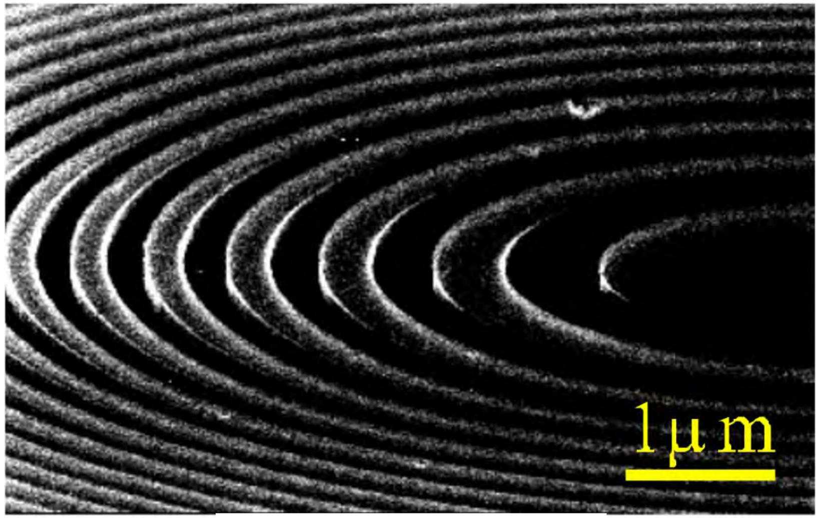

SEM image
of a zoneplate

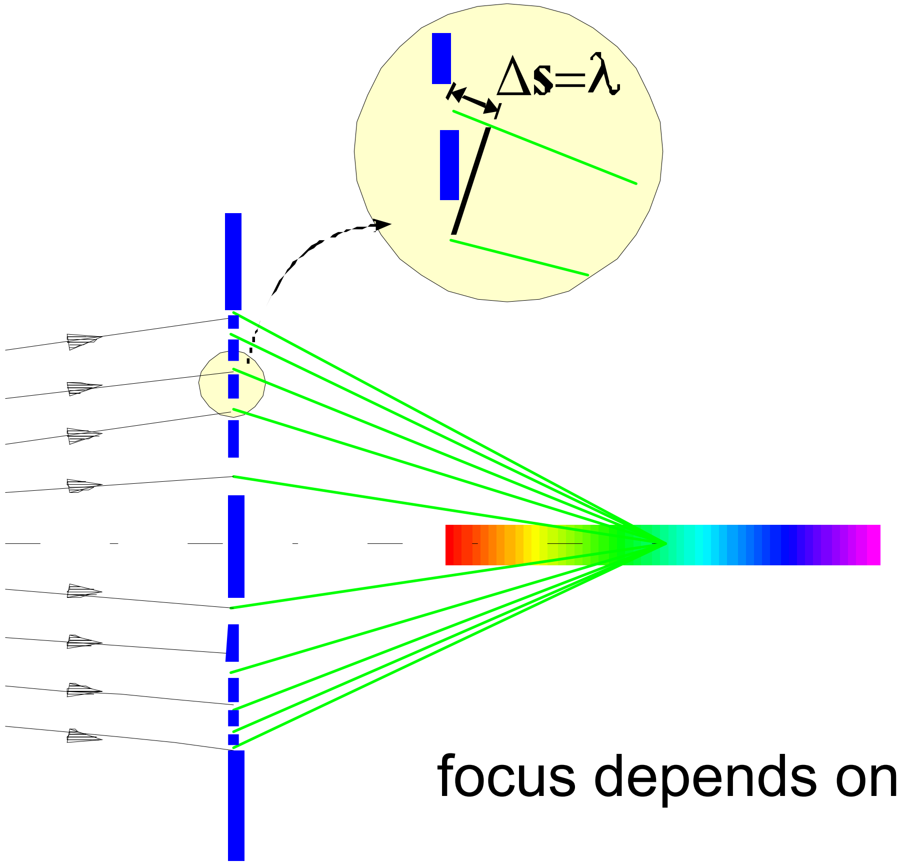

focus depends on energy

It is more or less a grating, where the distance is varied to get constructive interference only at one point. Not a parallel beam!
For details see any optics book!

Magnetic Contrast

Simple modulation of the intensity behind the sample

- XMCD changes dramatic the intensity of the transmitted light

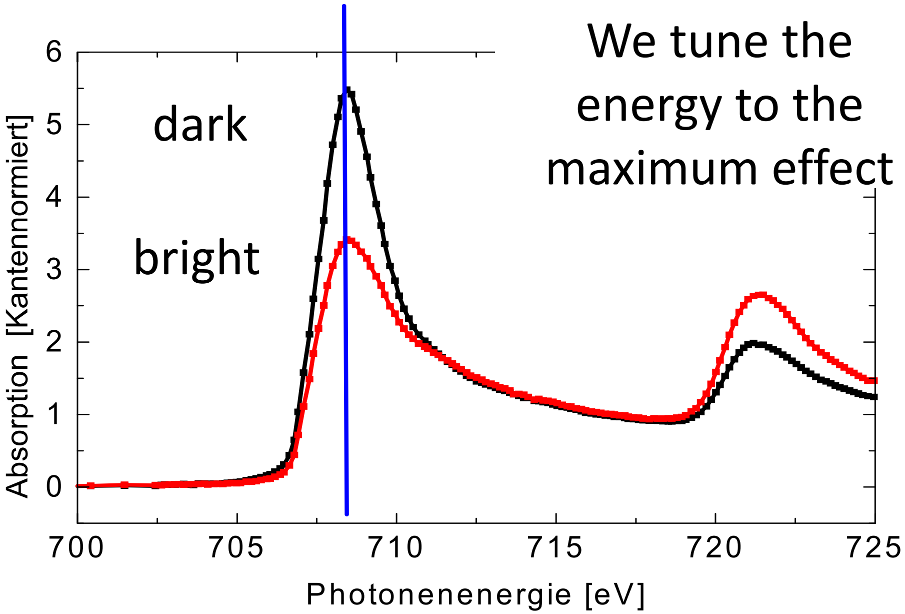

We tune the energy to the maximum effect

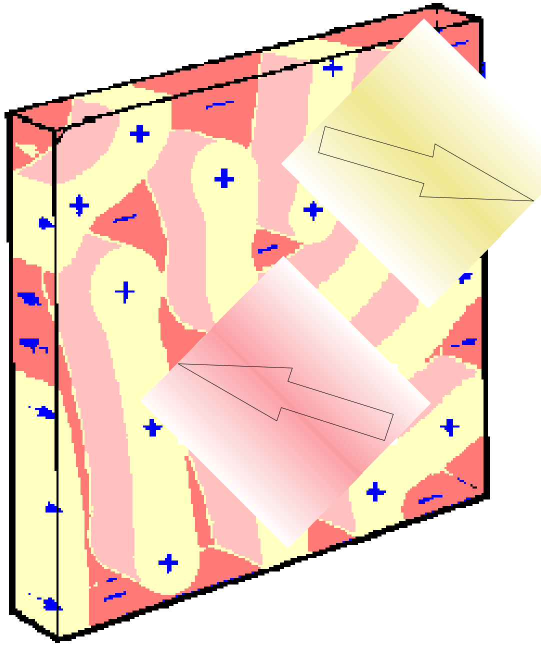

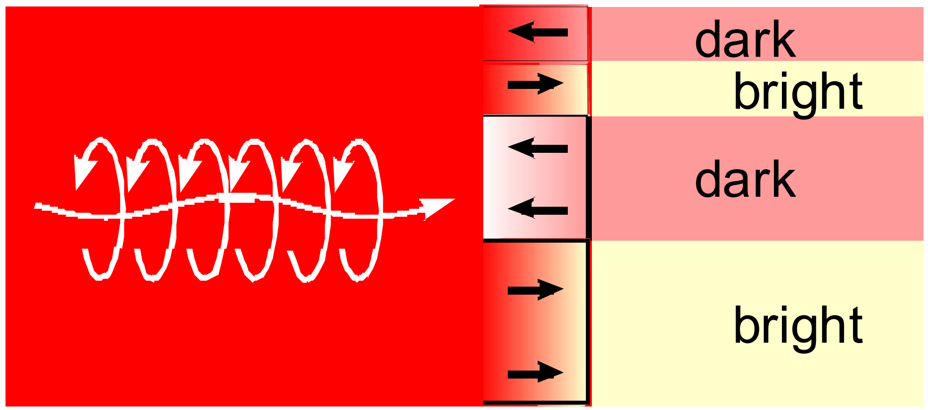

How to measure magnetism? An example: Co/NiO

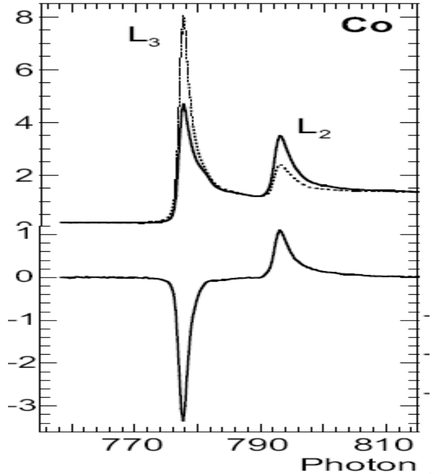

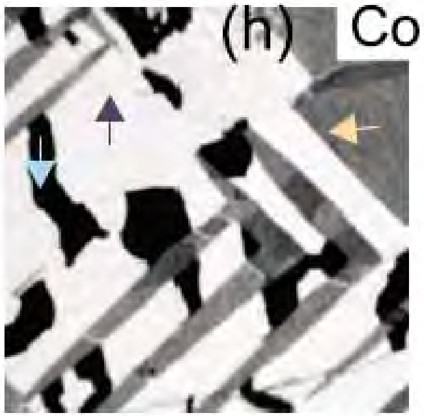

XMCD Co L-edge

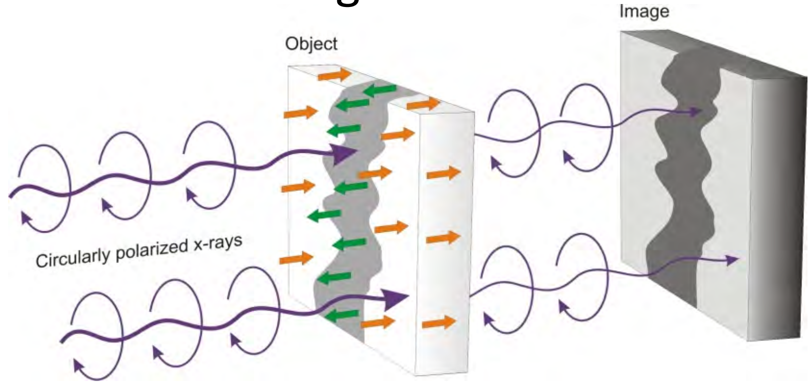

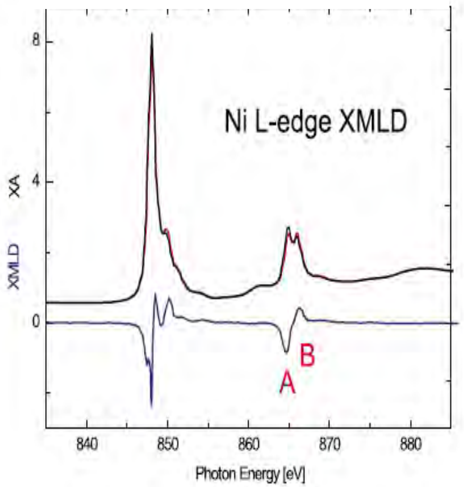

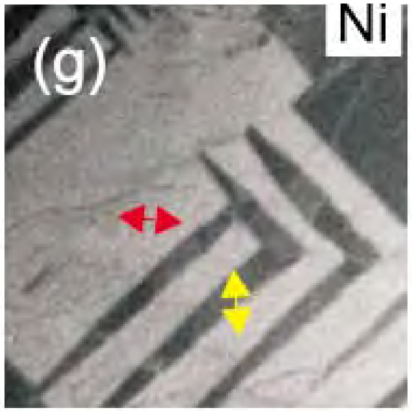

Linear dichroism due to antiferromagnetic domains Ni L edge

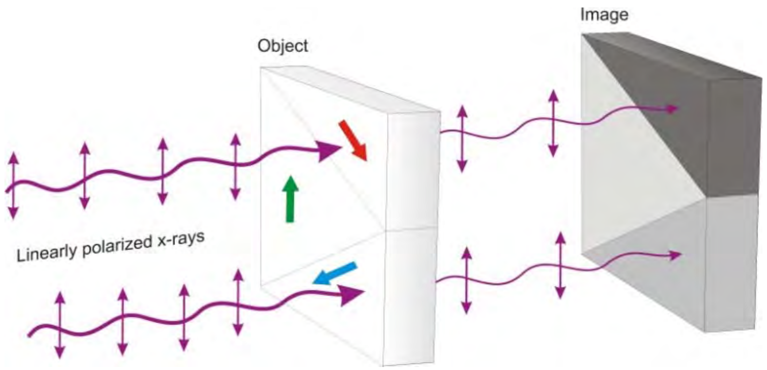

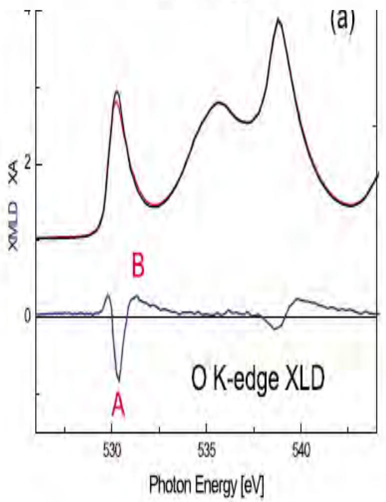

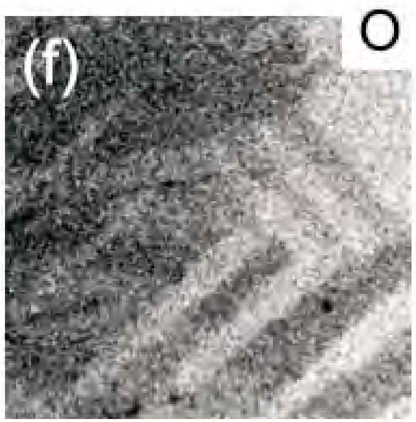

Linear dichroism due to crystal Orientation: O-K edge

H. Ohldag et al. PR B **79**, 052403 (2009)

MTXM – hysteresis of „nanodots“

magnetization of a single 1µm x 1 µm Fe/Gd dot

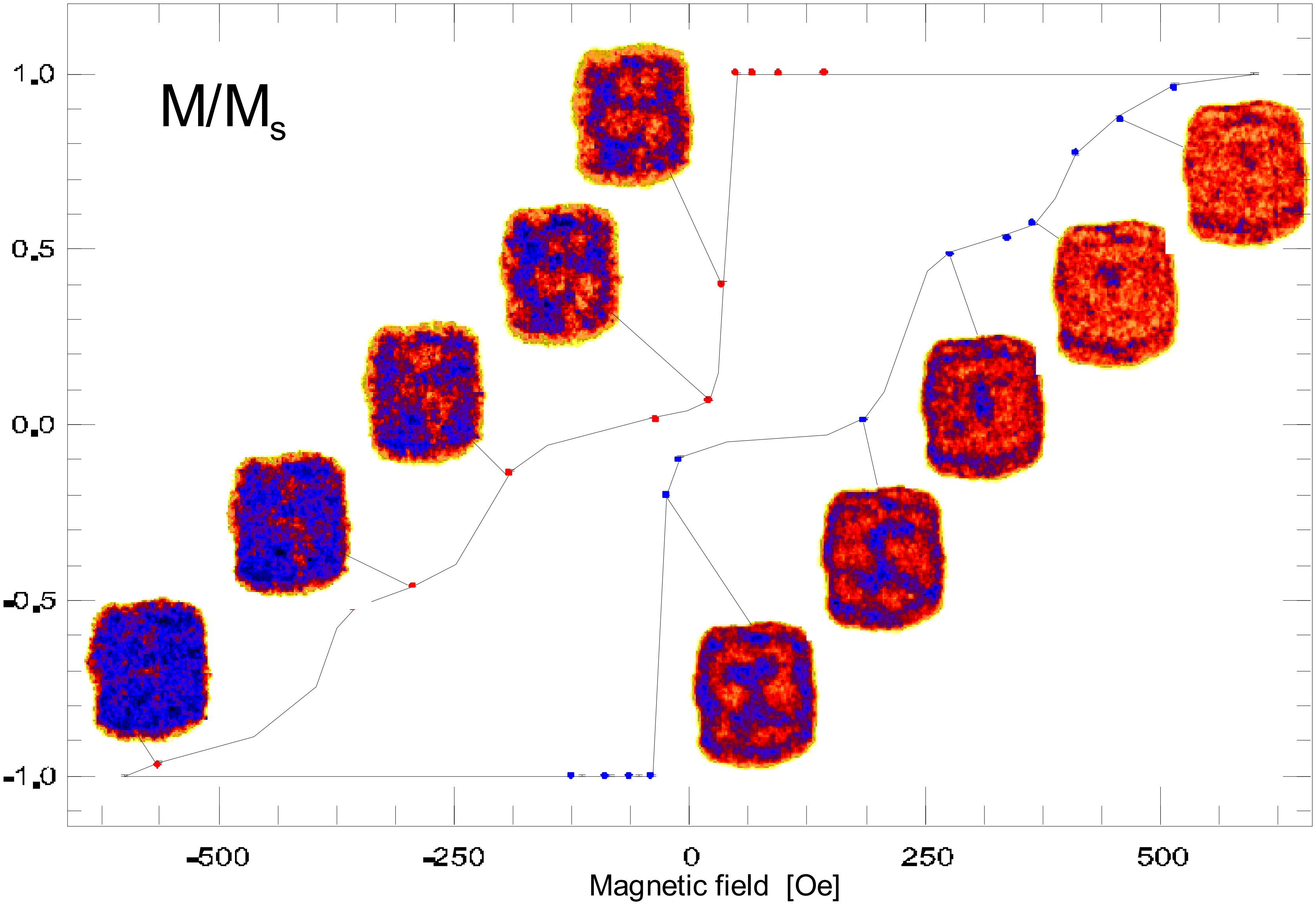

Blue: Magnetization down **Orange**: Magnetization up

STXM: Our soft X-ray UHV microscope at HZB-BESSY-Berlin

circular polarized undulator beamline UE46

BESSY - Berlin

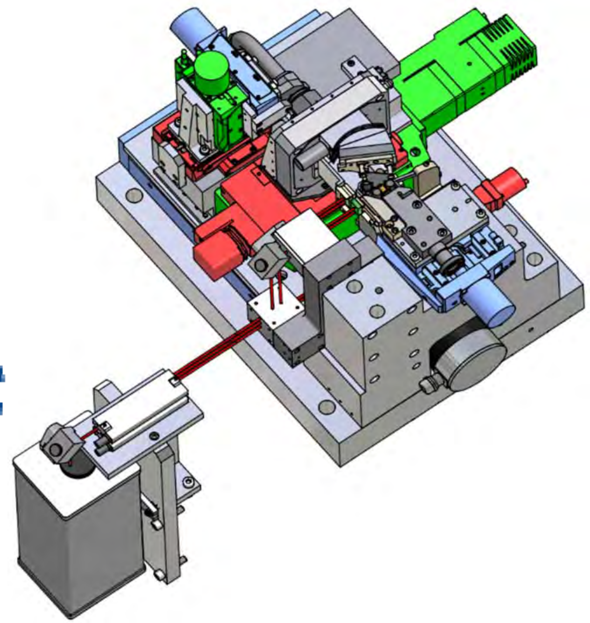

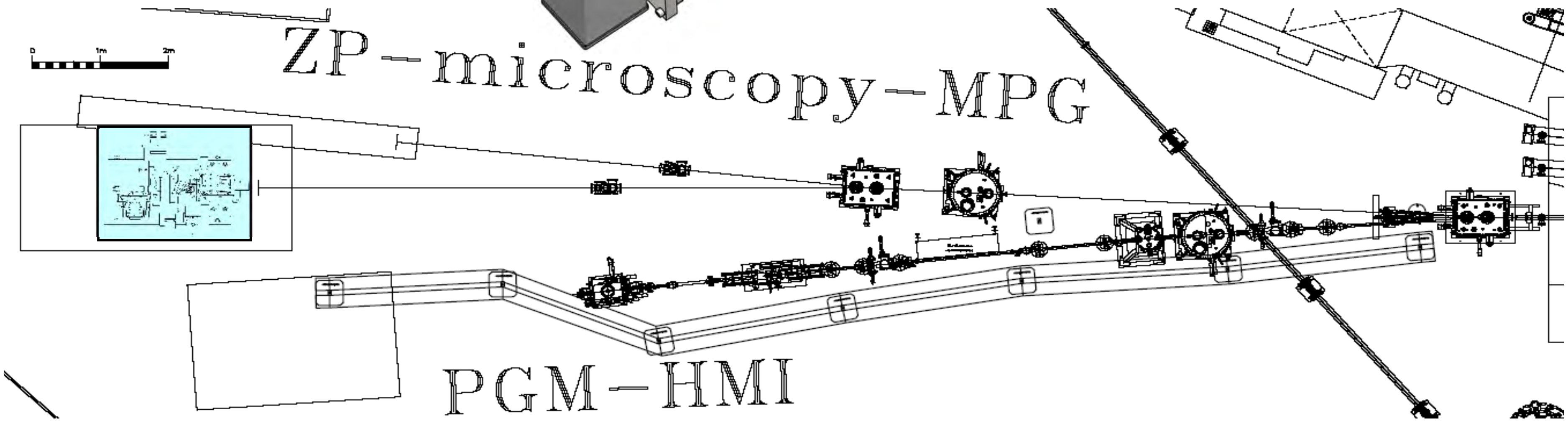

Concept of Scanning Transmission X-Ray microscopy

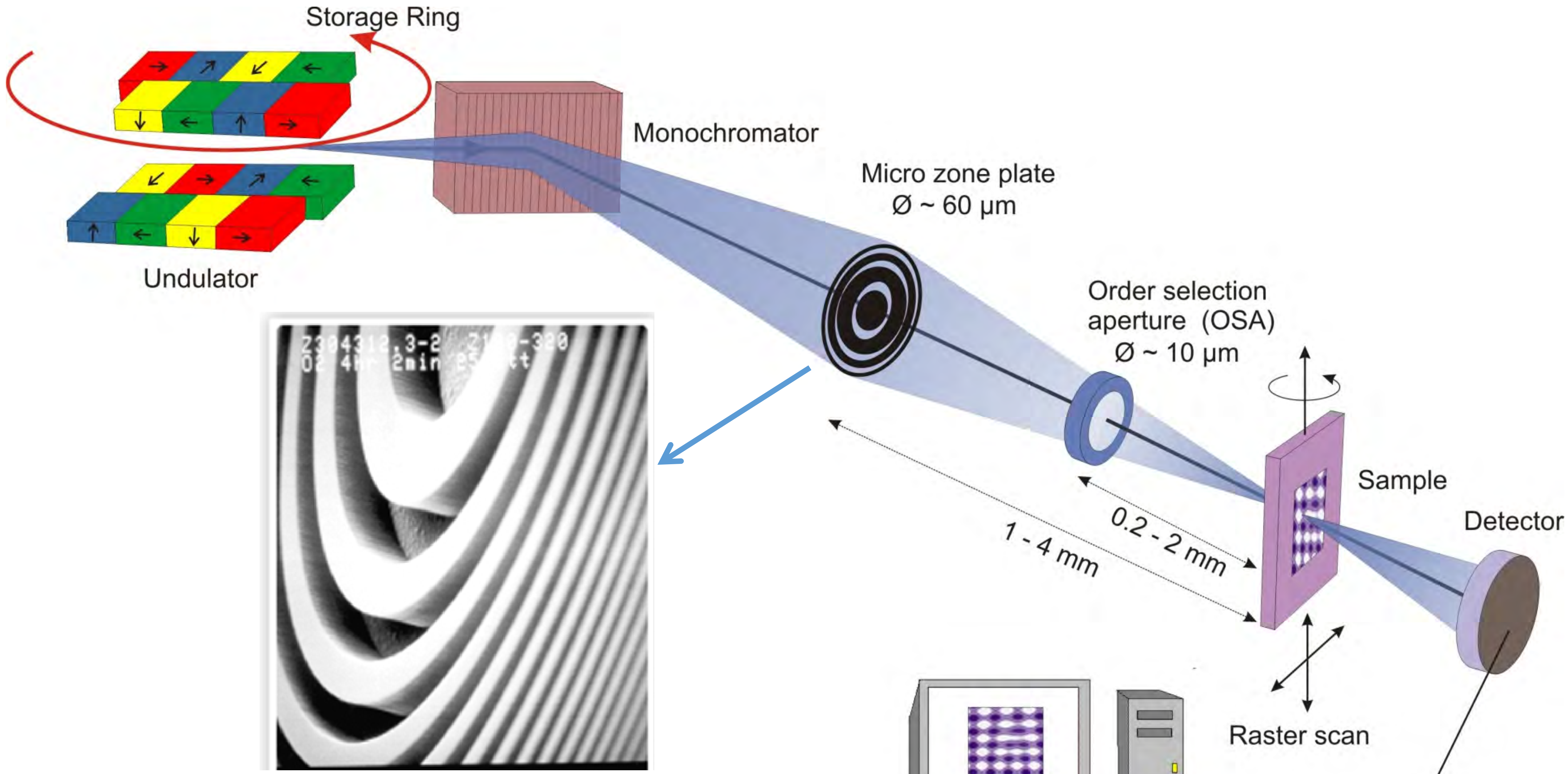

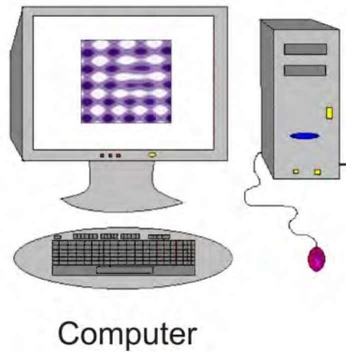

Fresnel zone plate
Resolution is given by the thickness of the outermost zone:
Todays world record 9 nm

Field of view
10µm x 10µm

Further reasons for an STXM

Oper

Combines the advantages of
PEEM, SXM and TXM
a) High B-fields
b) Full intensity for local spectroscopy
c) Rough and bulg samples

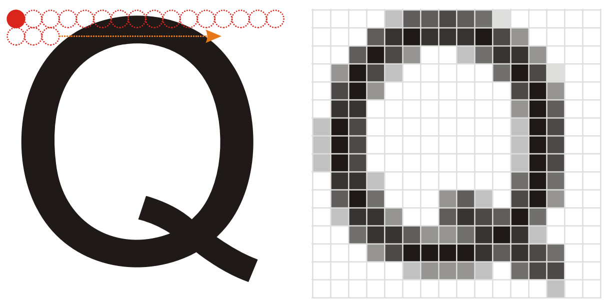

Why STXM?

- High spatial resolution
- Microspectroscopy (many contrast mechanisms)
- Flexibility in detector (photon, electrons , TEY,…)
- Time –resolved imaging

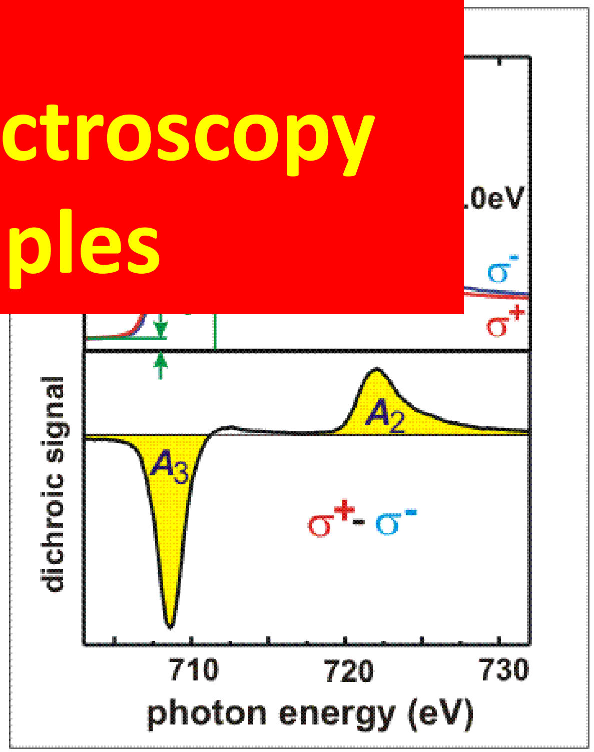

Something exceptional (worldwide)

- 2nd Magnet System

„Dynamic (25GHz) sample holder

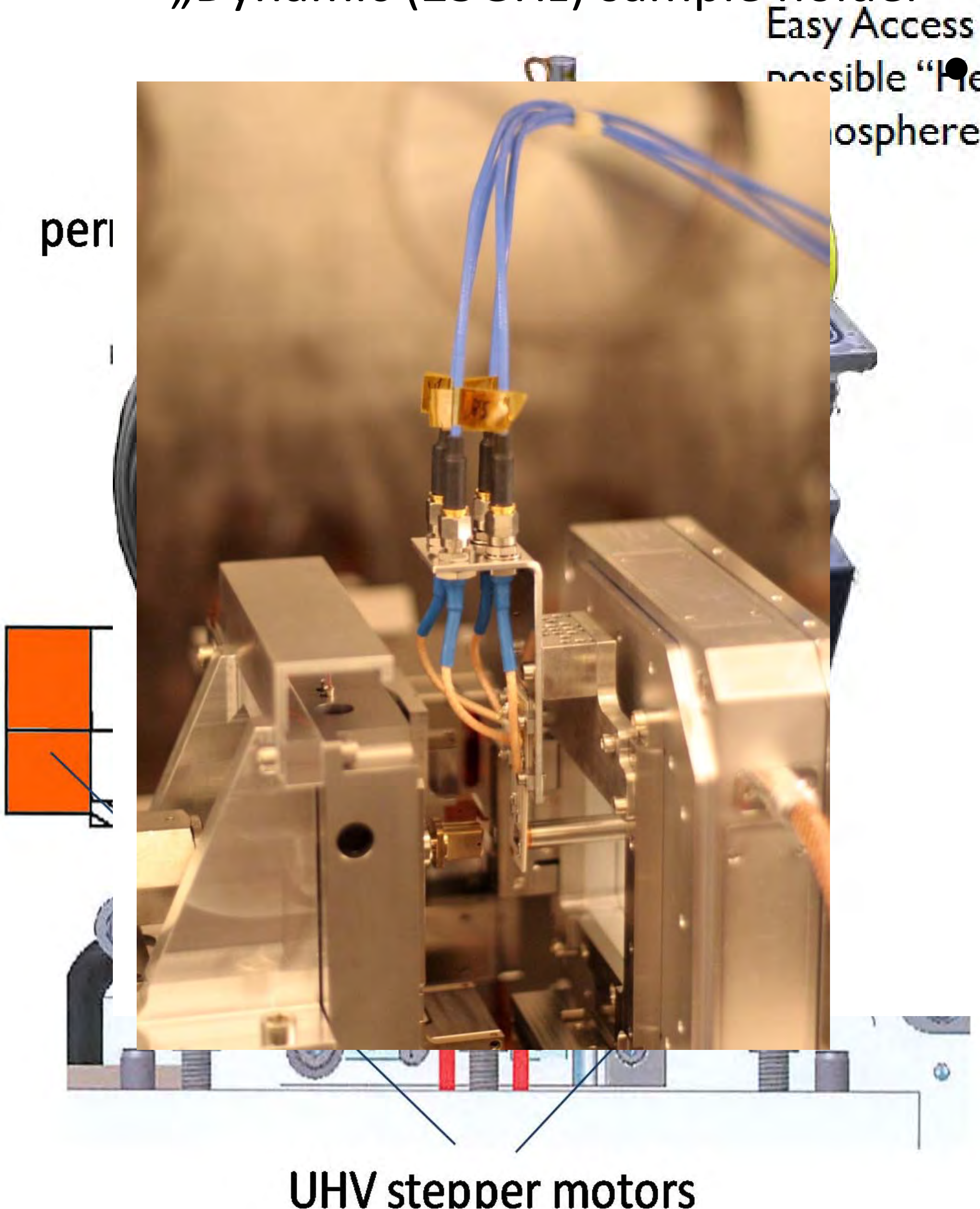

- Magnet system
- any direction and strength
  - 1st: 40mT

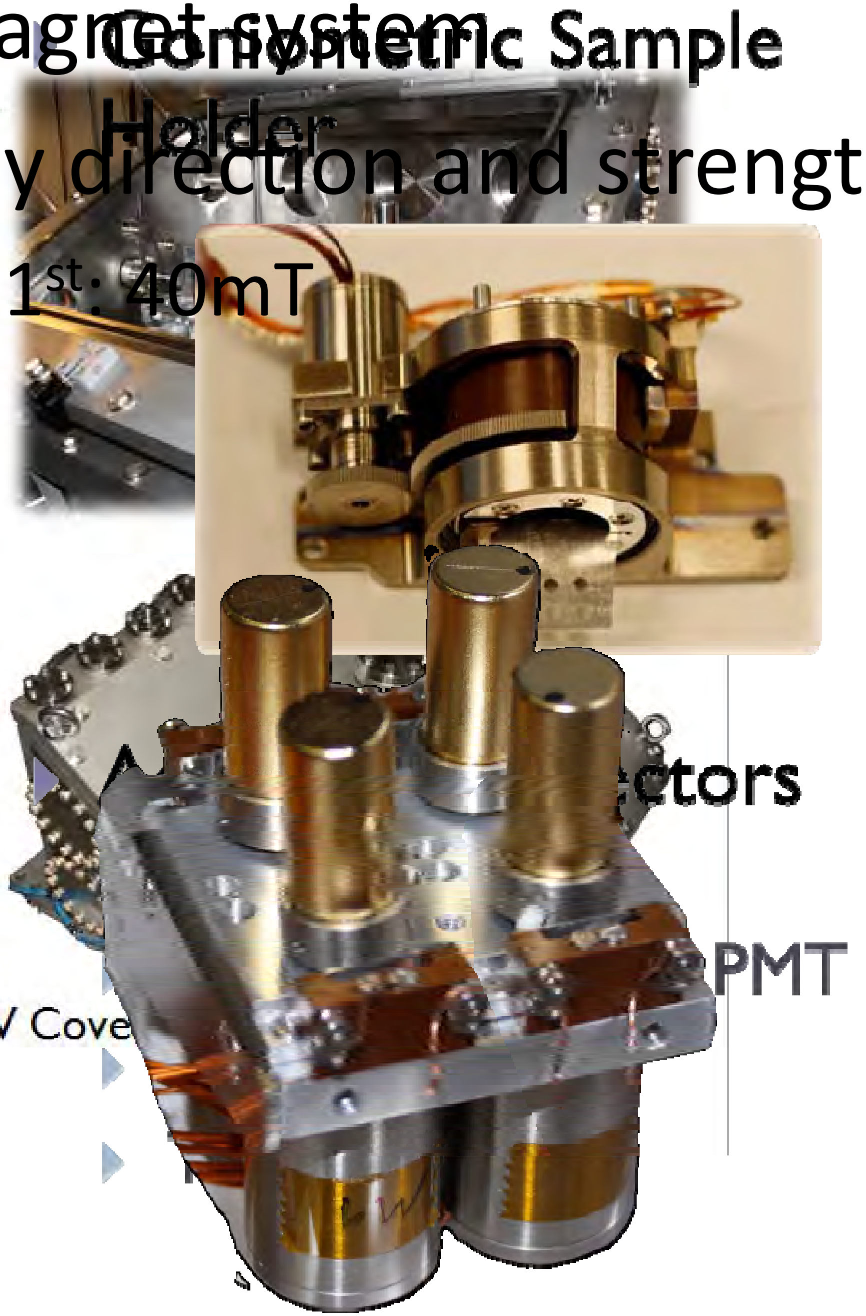

Zone Plate Scanning

- Works very fine
- 24µm usable field of view
- Interferometer-limited performance
- Becomes more and more standard

Noise less than 0.2nm

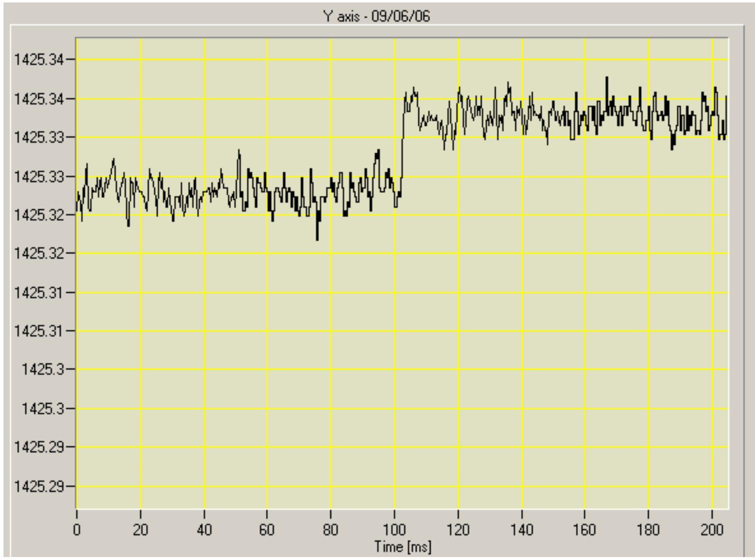

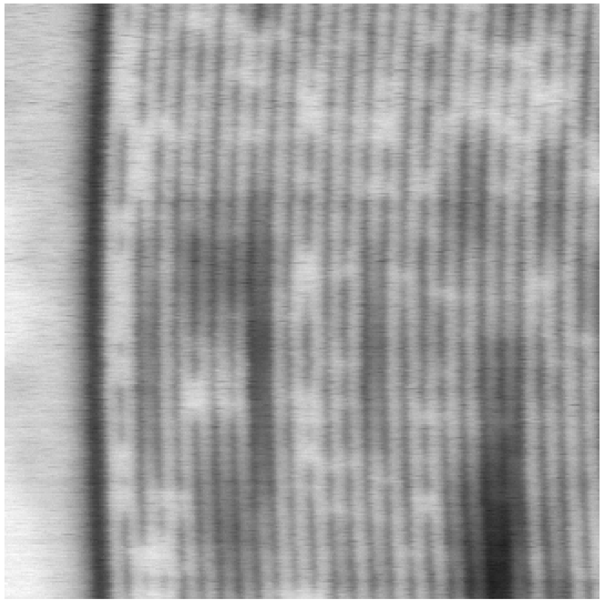

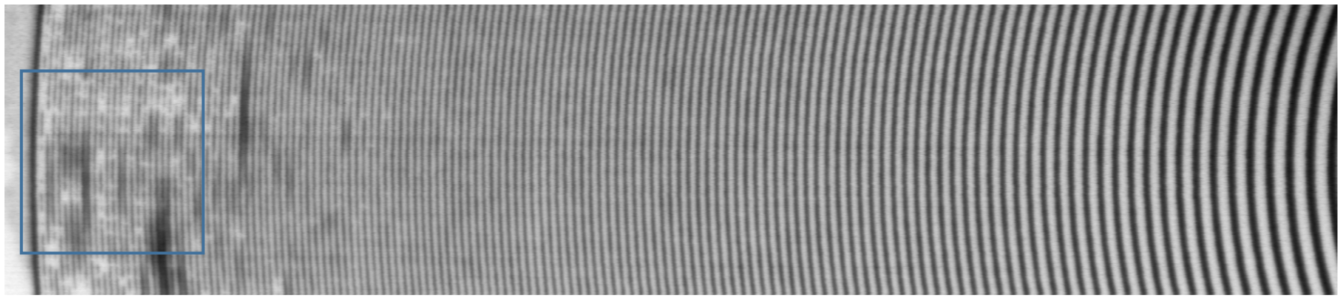

Real UHV microscope ➔ electron yield possible

- UHV mode
  - Microscope fully bakeable at 110C

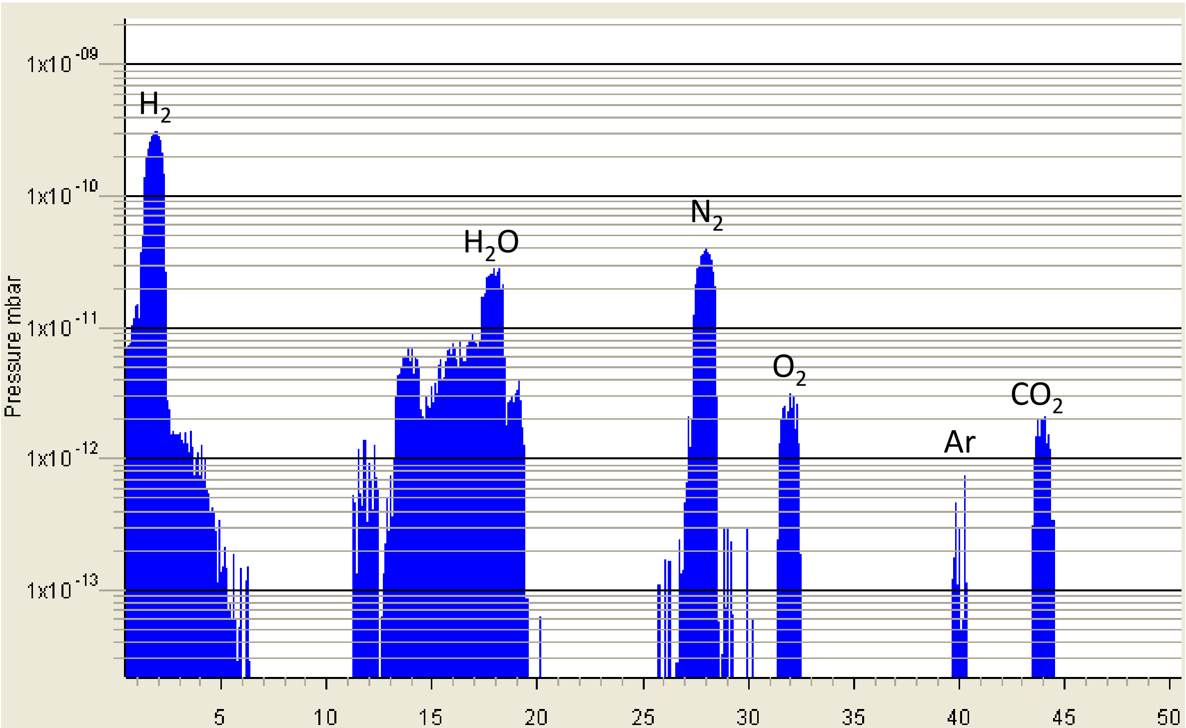

- "Helium" mode incl. cryo pump: 12h after pumping down better than 10^{-7} mBar

Combined TEY (surface) and Transmission (bulk)

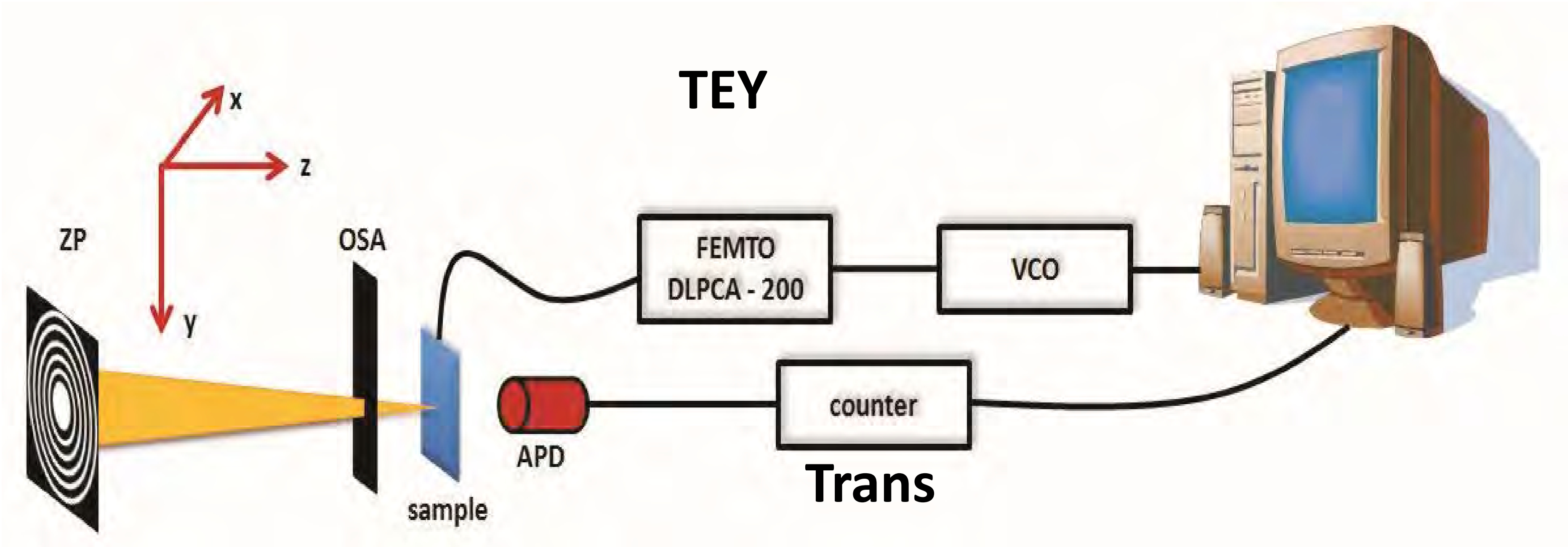

D. Nolle et al. , microscopy and microanalysis (2011)
D. Nolle et al. , Rev. Sci. Inst (2012)

Aglumerated FeO_x/FePt hybrid Nanoparticles at the Fe- L_3 edge

Field of view **7x7µm**

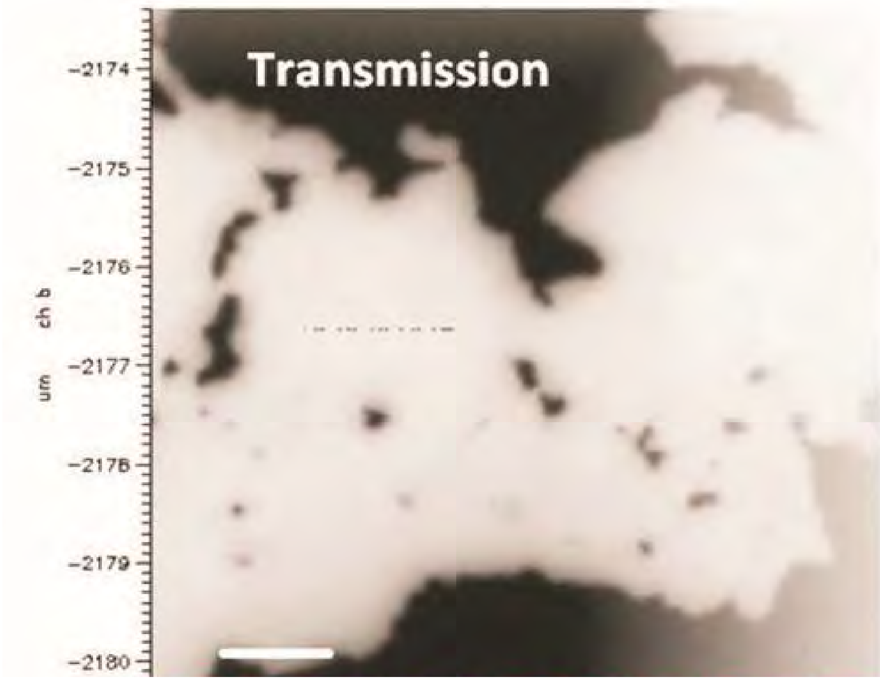

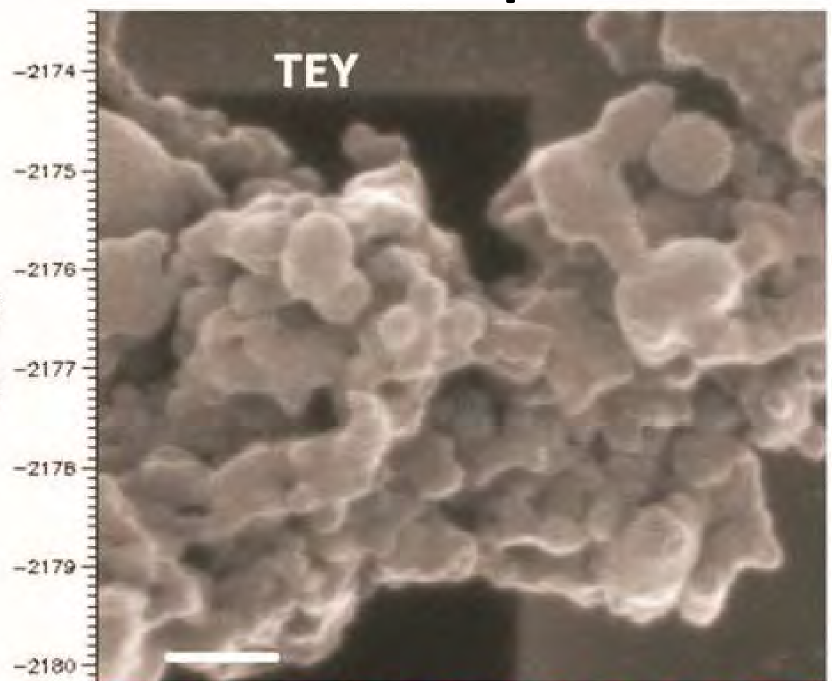

SiN membrane

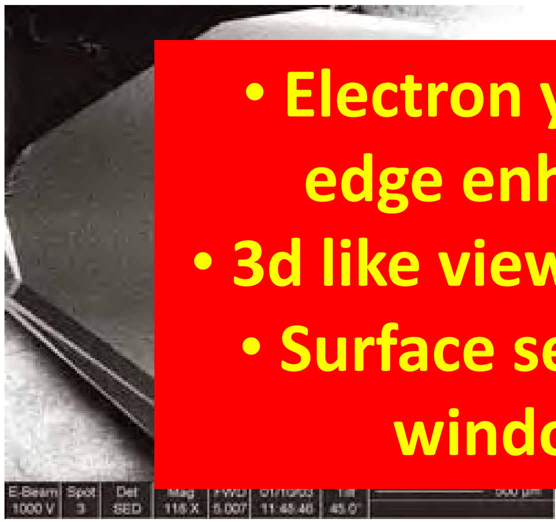

- **Electron yield provides edge enhancement!**
- **3d like view as in the SEM**
- **Surface sensitive → no window prep.**

Origin for the “3d-like” TEY edge enhancement

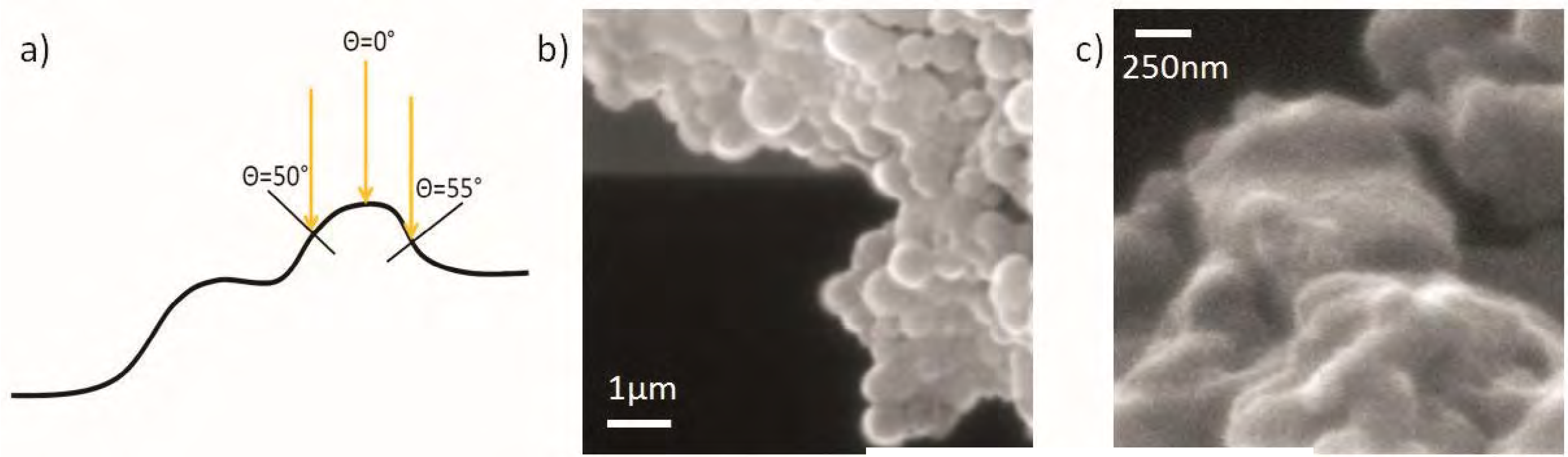

PHYSICAL REVIEW B VOLUME 59 1 MARCH 1999-I

Electron-yield saturation effects in *L*-e … ıroism
spectra of Fe

Reiko N
Department of Materials Science and Engineering … 305
J. S
IBM Research Division, Almaden Research Cent … 20
Y. U. I
Naval Research Laboratory

(Received 2 September 1998)

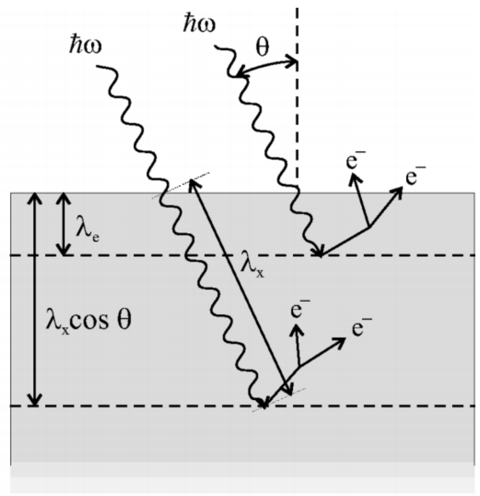

(b) Electron yield

$$dY_{e,0}(z) = I_0 e^{-\mu z/\cos\theta} \frac{\mu\, dz}{\cos\theta} \quad (4)$$

D. Nolle et al. , microscopy and microanalysis (2011)
D. Nolle et al. , Rev. Sci. Inst (2012)

Spectroscopy for TEY and Transmission

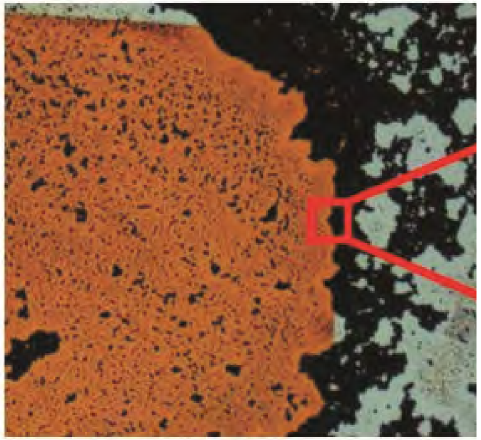

optical microscope

TRANSMISSION-SXM

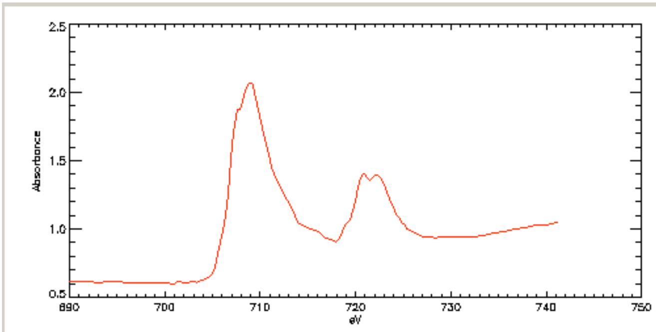

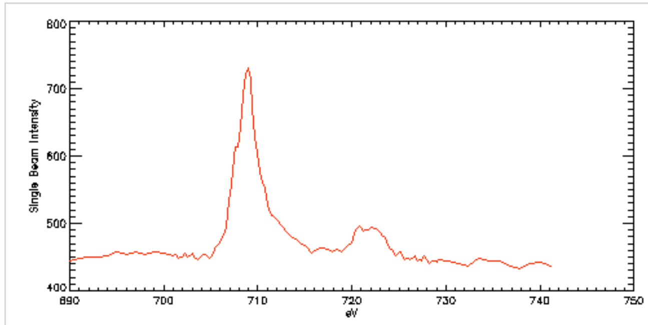

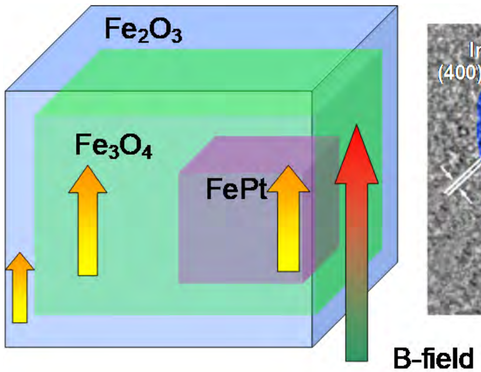

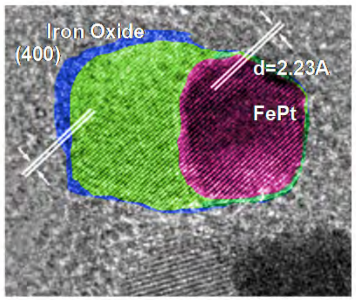

Transmission:
More FePt signal visible

TEY:
Dominated by Fe_2O_3 like spectra

Similar to conventional XAS as in
D. Nolle et al. , New J. Phys. **11** (2009).

Magnetic SXM ➔ in and out off plane

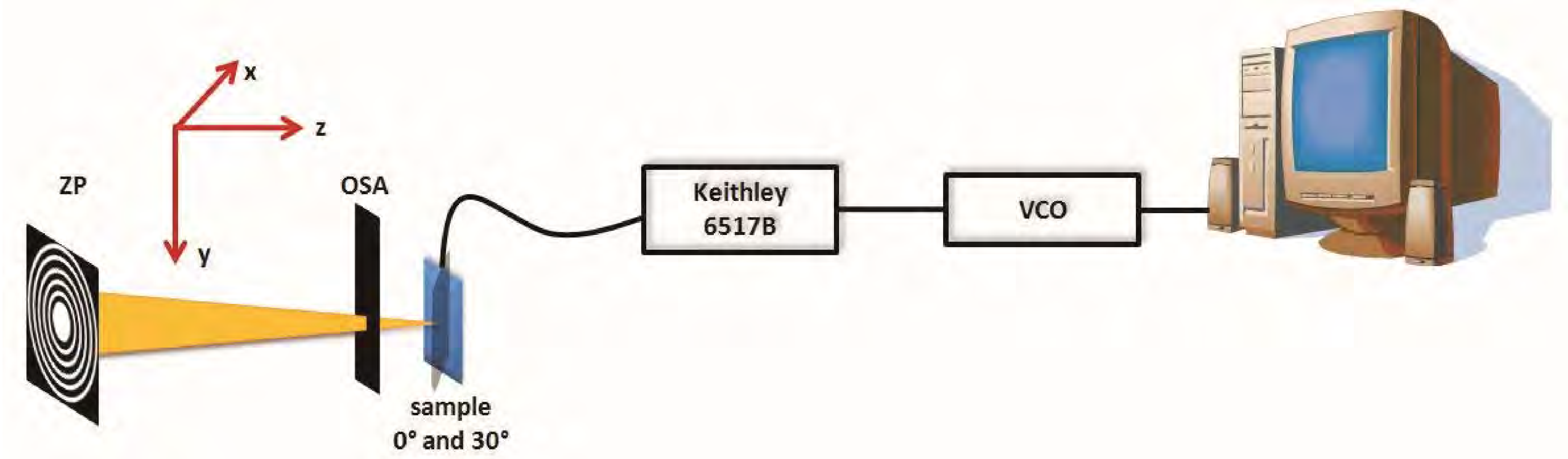

- 0° angle (NI) for out of plane sensitivity
- 30° angle for in plane sensitivity
- Using circular polarized X-rays for XMCD effect

Magnetic SXM ➔ in- and out-off-plane

- out of plane:
  - FePt @NI
  - 40ms/Pixel
  - Out off plane Domains

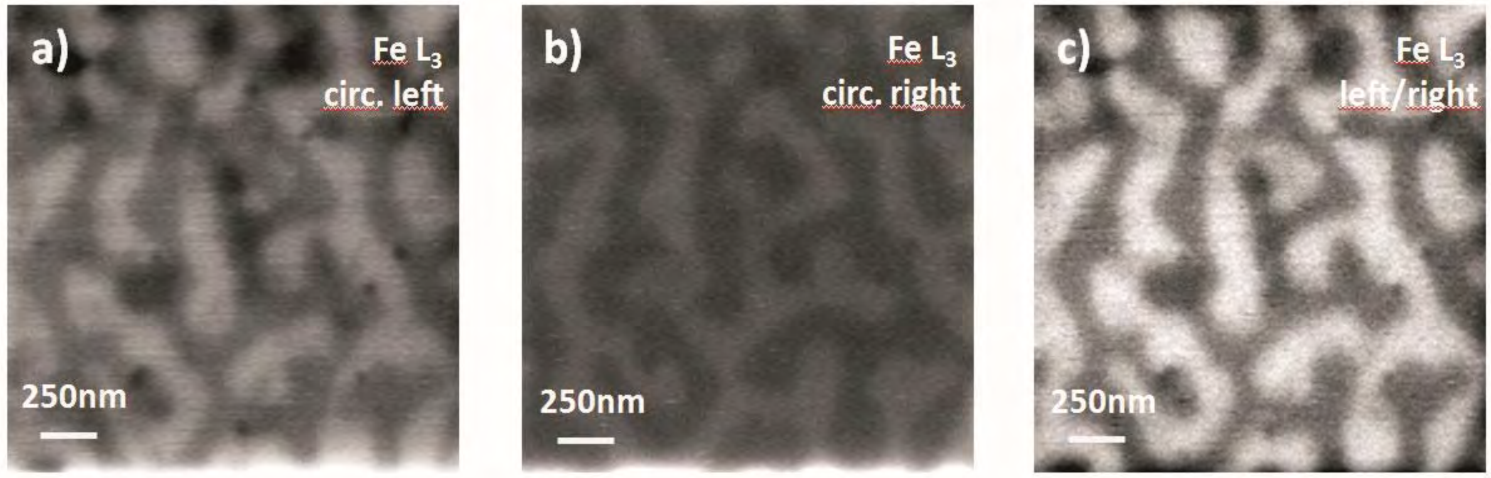

- In plane
  - CoTb @30°
  - 40ms/Pixel
  - In plane Domains

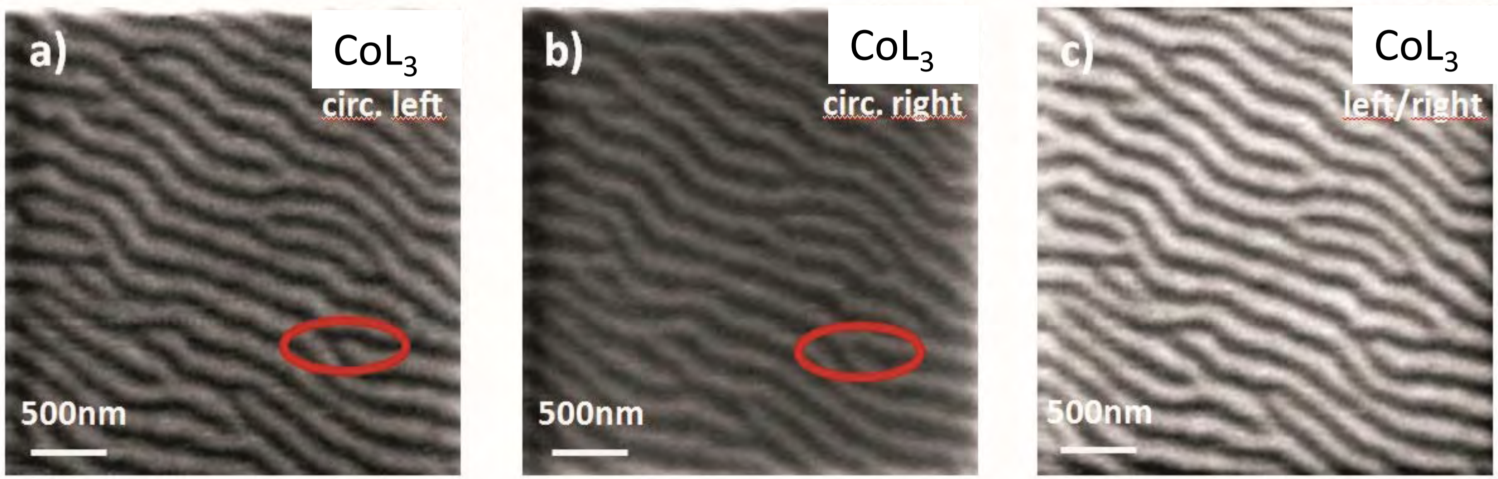

magnetic hysteresis curves

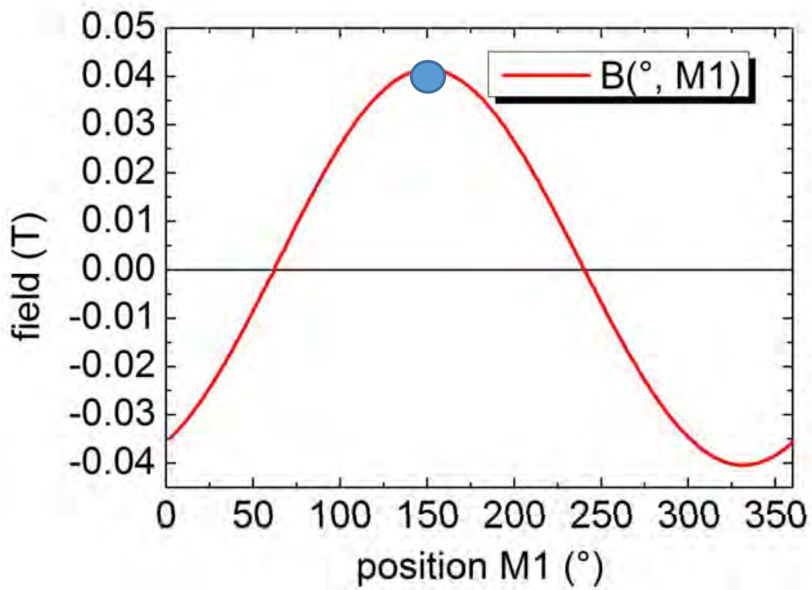

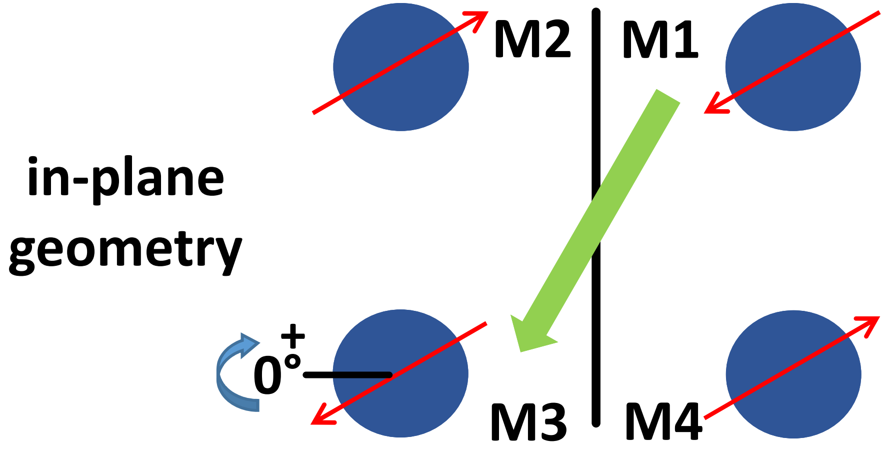

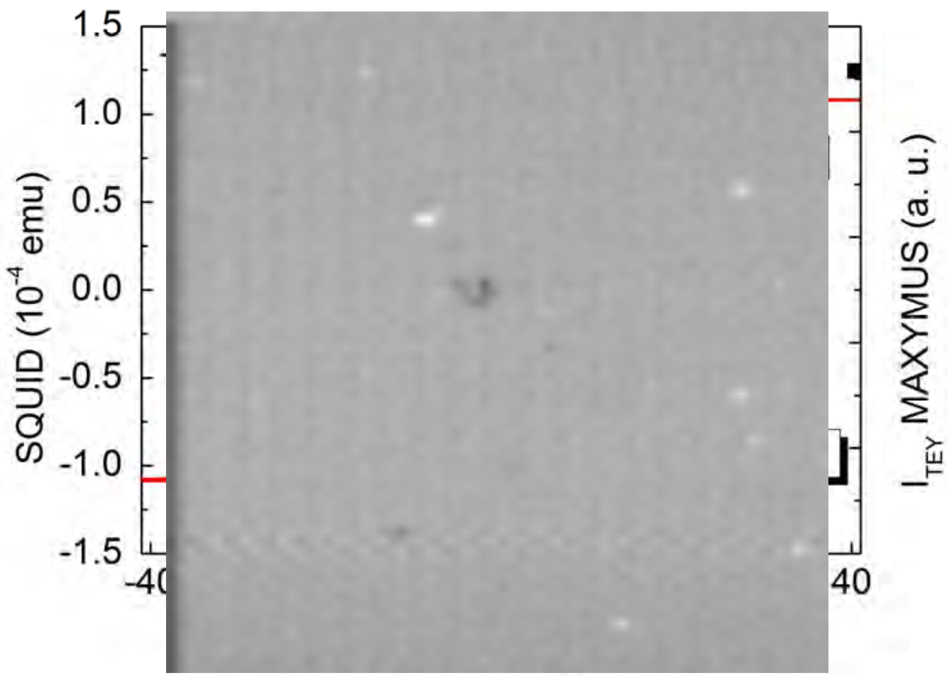

-exemplarily shown for TEY
-no further corrections to values of magnetic field
-different behavior in both branches

Recent developments

- 5GHz dynamics ➔ operational since July. 2010
- Total electron yield (TEY) mode ➔ since July. 2010
- New blazed grating ➔ 3-5x flux ➔ since Oct. 2010
- 0.5T ➔ since November 2011
- Variable Temperature 80-400k ➔ 2nd quarter 2012
- 360° Tomography Sample Holder ➔ 3rd quarter 2012
- L-He Temperature 15K ➔ 2016
- Ultrafast CCD camera for Ptychography➔ 2016

- 25GHz dynamics ➔ in development

Using the time structure: Pump – probe experiments

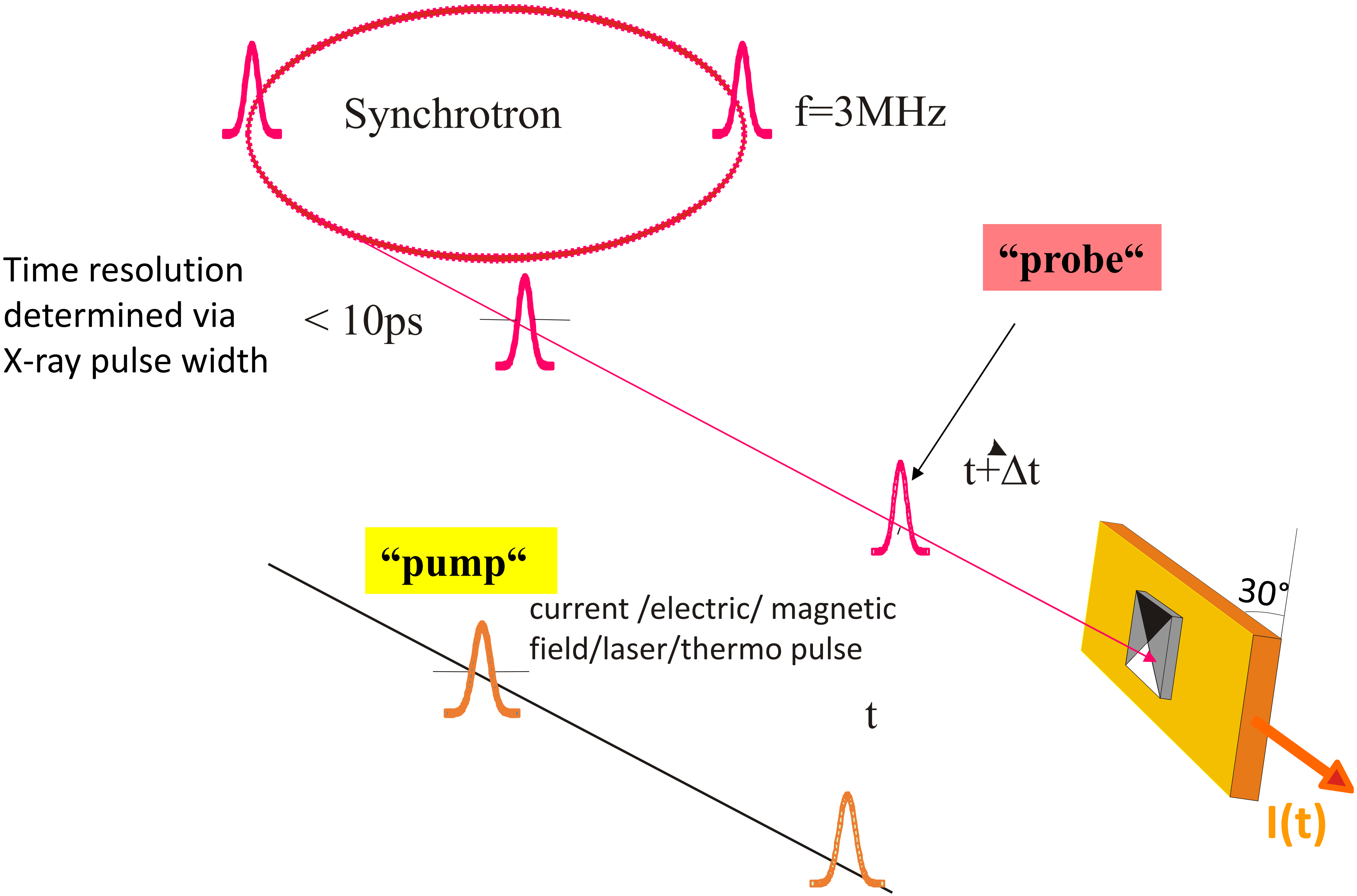

STXM: Sine Excitation in Multi-Bunch Mode

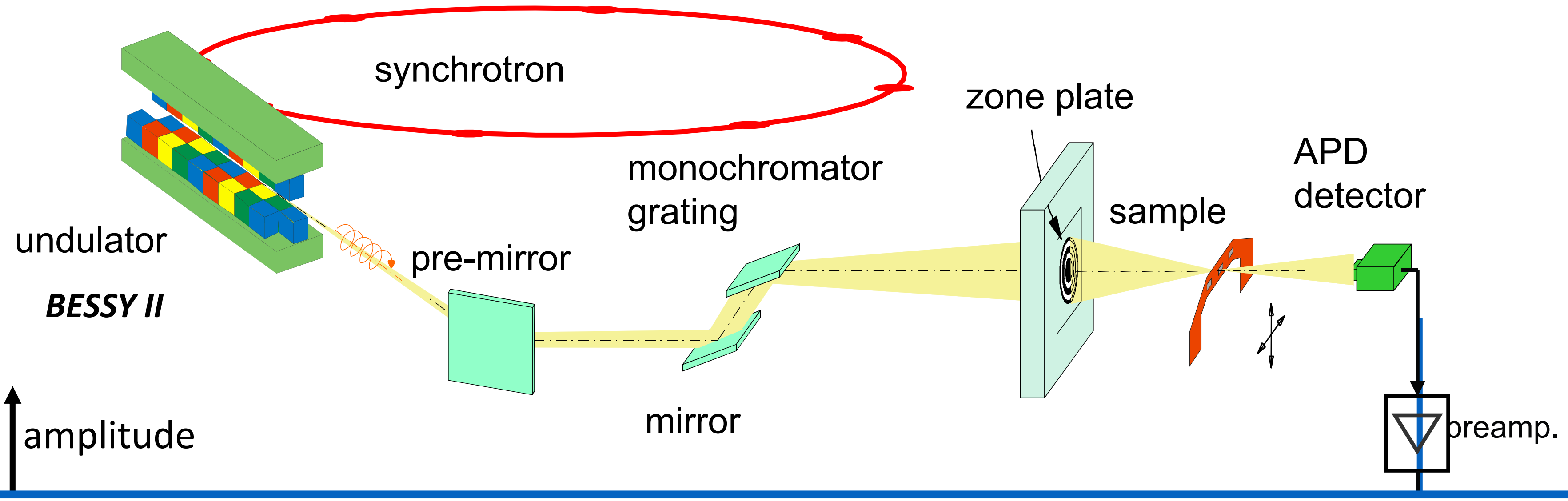

Multi-bunch-mode operation *(STXM equipped with a fast APD detector):*

→ speeding up measurements by a factor of ≈ 10

Fast cyclic switching between different phases (`sophisticated lock-in´)

→ elimination of low frequency fluctuations, e.g. beam instabilities

Can be implemented at **Scanning** Transm. X-ray Microscopes (STXM) **only**

Magnetic dynamic imaging of vortices

- Magnetic Vortex Core imaging
- Out of plane XMCD Contrast <1%

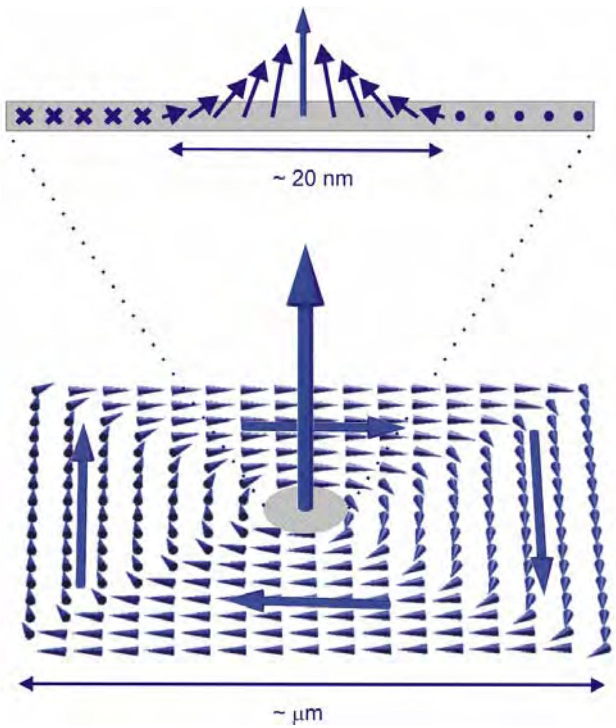

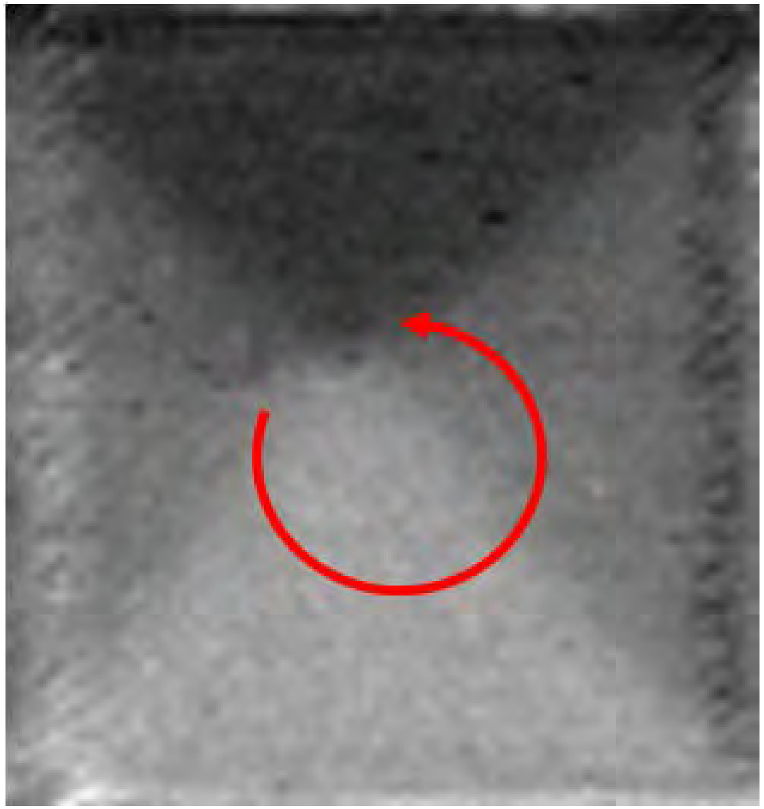

„Rotation“ (gyromode) depends on the Vortex orientation → here CCW

One can excite magnons and „see them" directly!

- This is a thin platelett of permalloy (Fe20% Ni80% ➔ soft magnetic) excited by a rotating high frequency field (5.9 Ghz)!

micromagnetic simulation

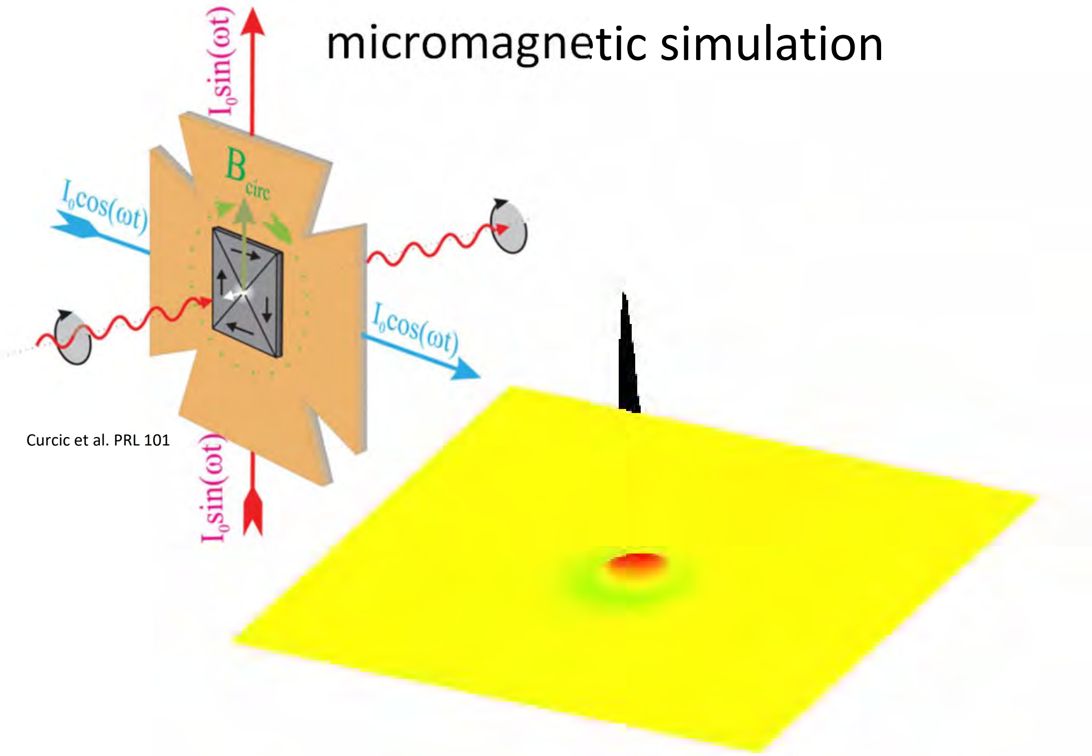

magnetic x-ray microscopy movie

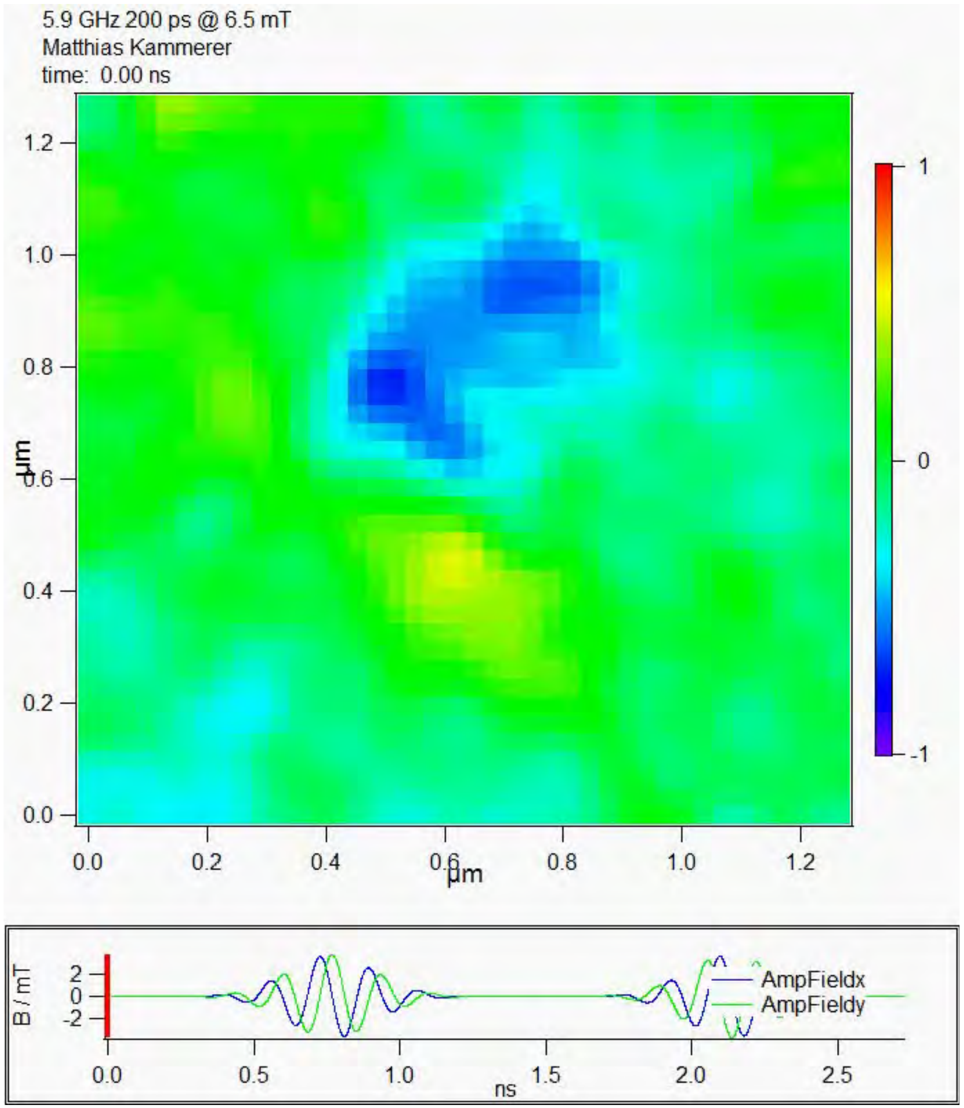

10ps frame distance and 20nm spatial resolution
Source: M. Kammerer et al. Nature Com. **2** (2011) 279
Abt. Sc MPI-IS at „Maxymus STXM Berlin"

Magnon Propagation in a “Magnonic Lattice”

a=500nm d=50nm
propagation could be switched on an off by external field

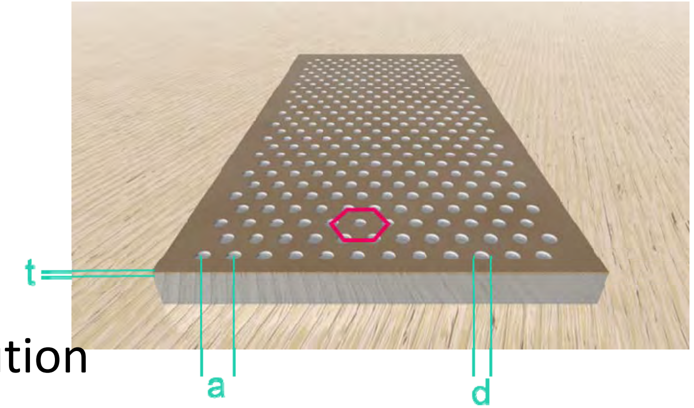

GHz excitations ➔ 50ps time and less than 20nm spatial resolution

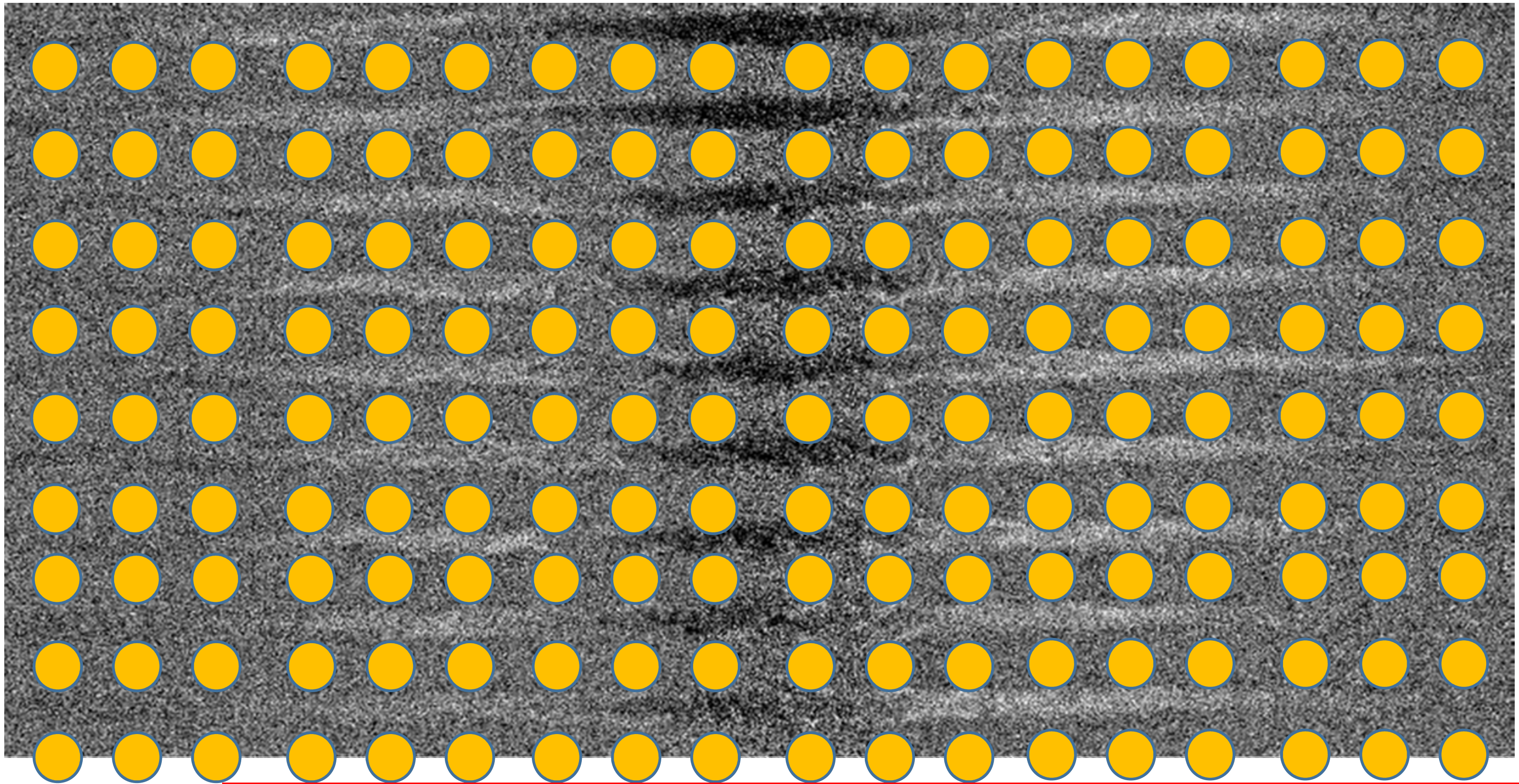

- **Unpublished so far**
- **Possible application: high quality tunable microwave filtering device**

Injection and control of Skyrmions

- **Visible Light**

- From the Group of Axel Hofmann
    - in Ta/CoFeB
    - Ta provides Spin-Orbit-Torque :=)

polar MOKE microscope

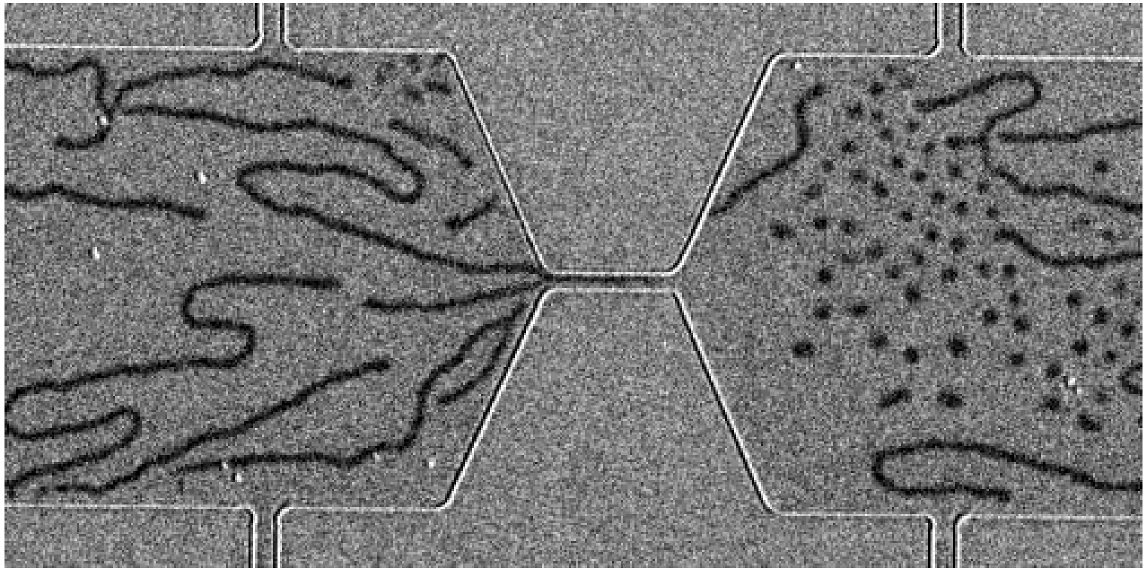

20µm

W. Jiang et al, Science, **349** (2015) 283-286

XMCD microscope

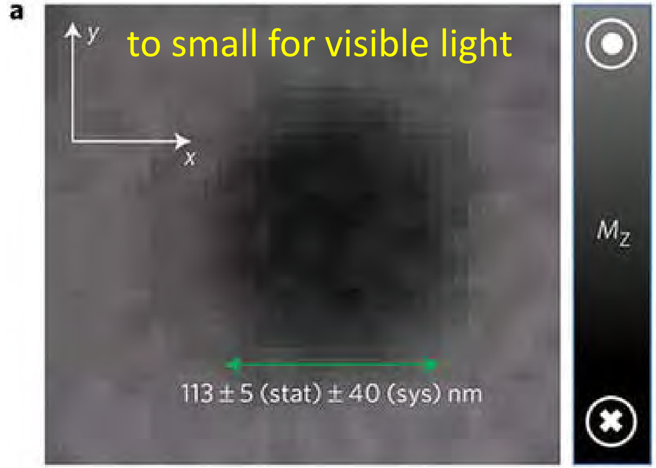

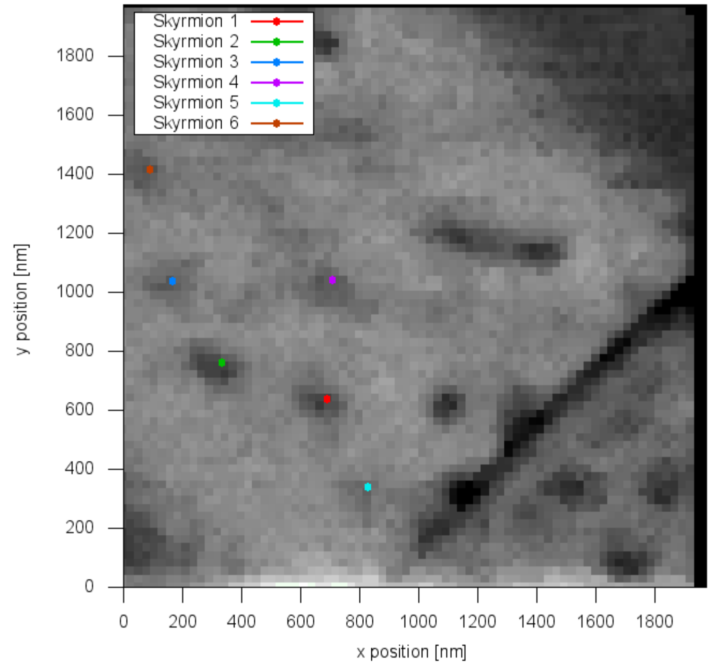

Kai Lizius et al., Nature Physics 13 (2017)

MAXYMUS MPI-IS

New ways: Ptychography

- Coherent Imaging + SXM ➔ Going beyond resolution limit
- Phase approximation problem:
  - Time consuming and complicated!

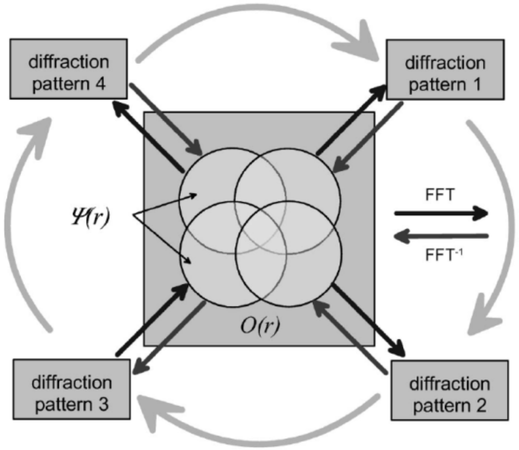

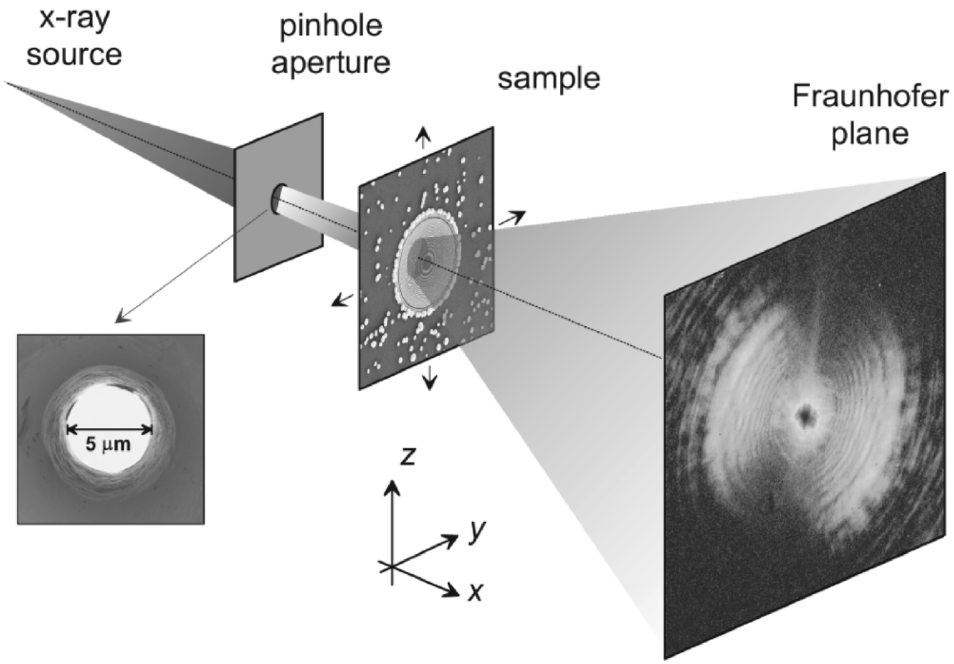

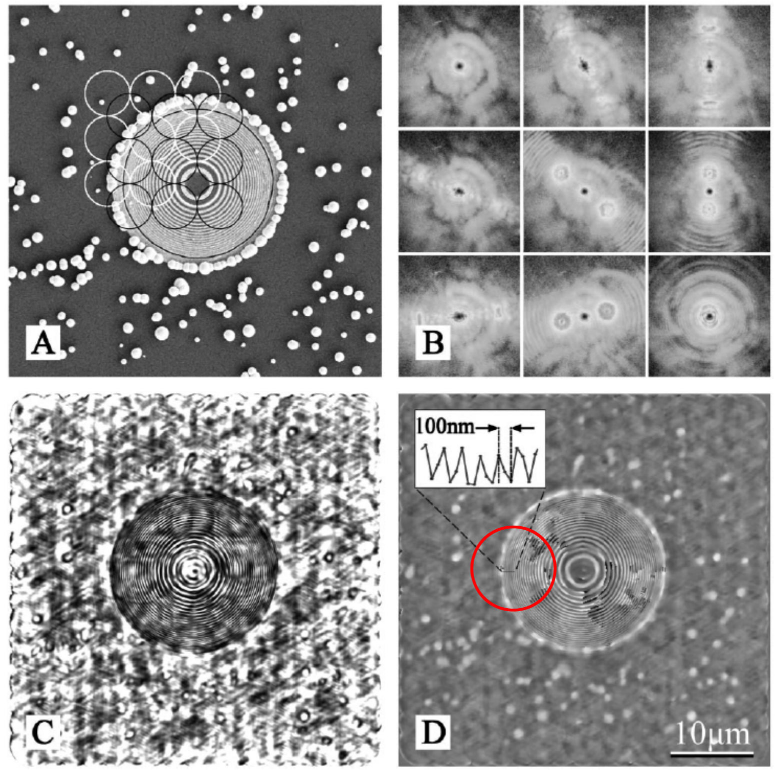

PRL 98 (2007) 03480 1. J. M. Rodenburg

Recording Sample Transmission

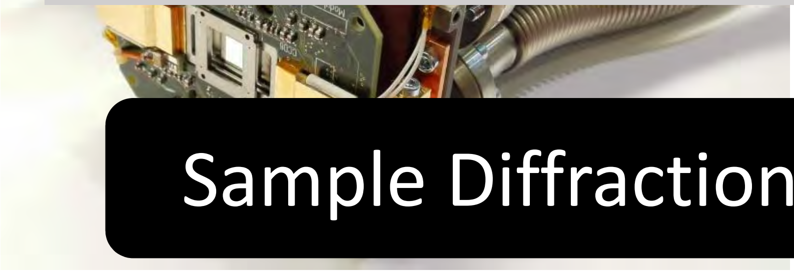

Keyword: Ptychography

10.1126/science.1158573

High-Resolution Scanning X-ray Diffraction Microscopy

Pierre Thibault,[1*] Martin Dierolf,[1] Andreas Menzel,[1] Oliver Bunk,[1] Christian David,[1] Franz Pfeiffer[1,2]

Coherent diffractive imaging (CDI) and scanning transmission x-ray microscopy (STXM) are two popular microscopy techniques that have evolved quite independently. CDI promises to reach

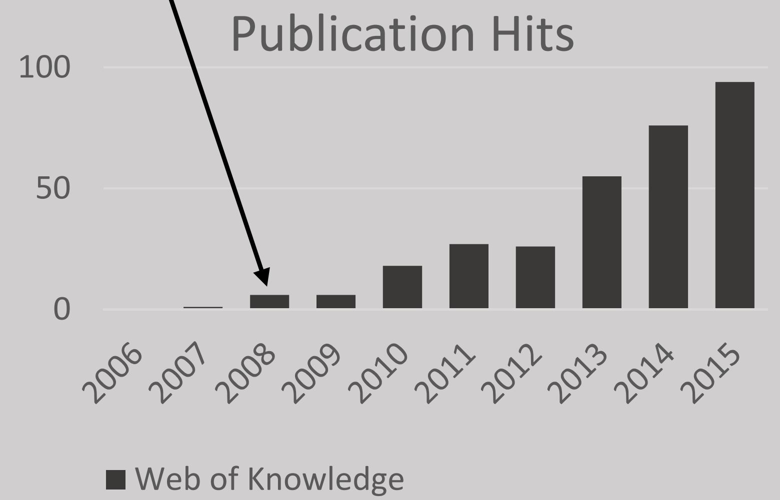

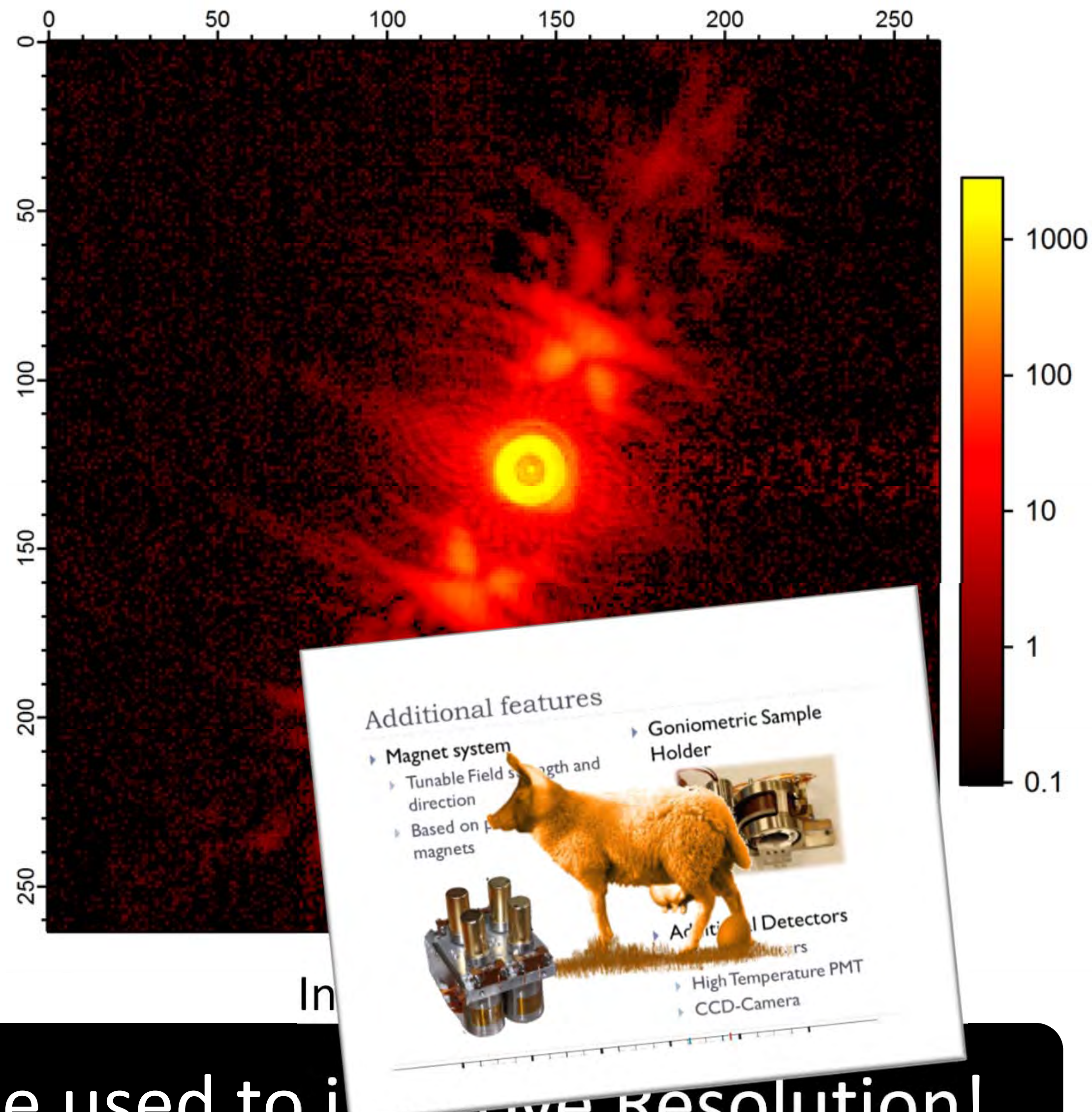

Sample Diffraction can be used to improve Resolution!

Ptychography @ MAXYMUS

- In principle its is very close to the procedure shown before
- The main constrictions are related to the phase match of adjacent pictures performed by “oversampling”
- The resulting dataset is completely redundant and error robust ➔ one is able to also extract the illumination function!

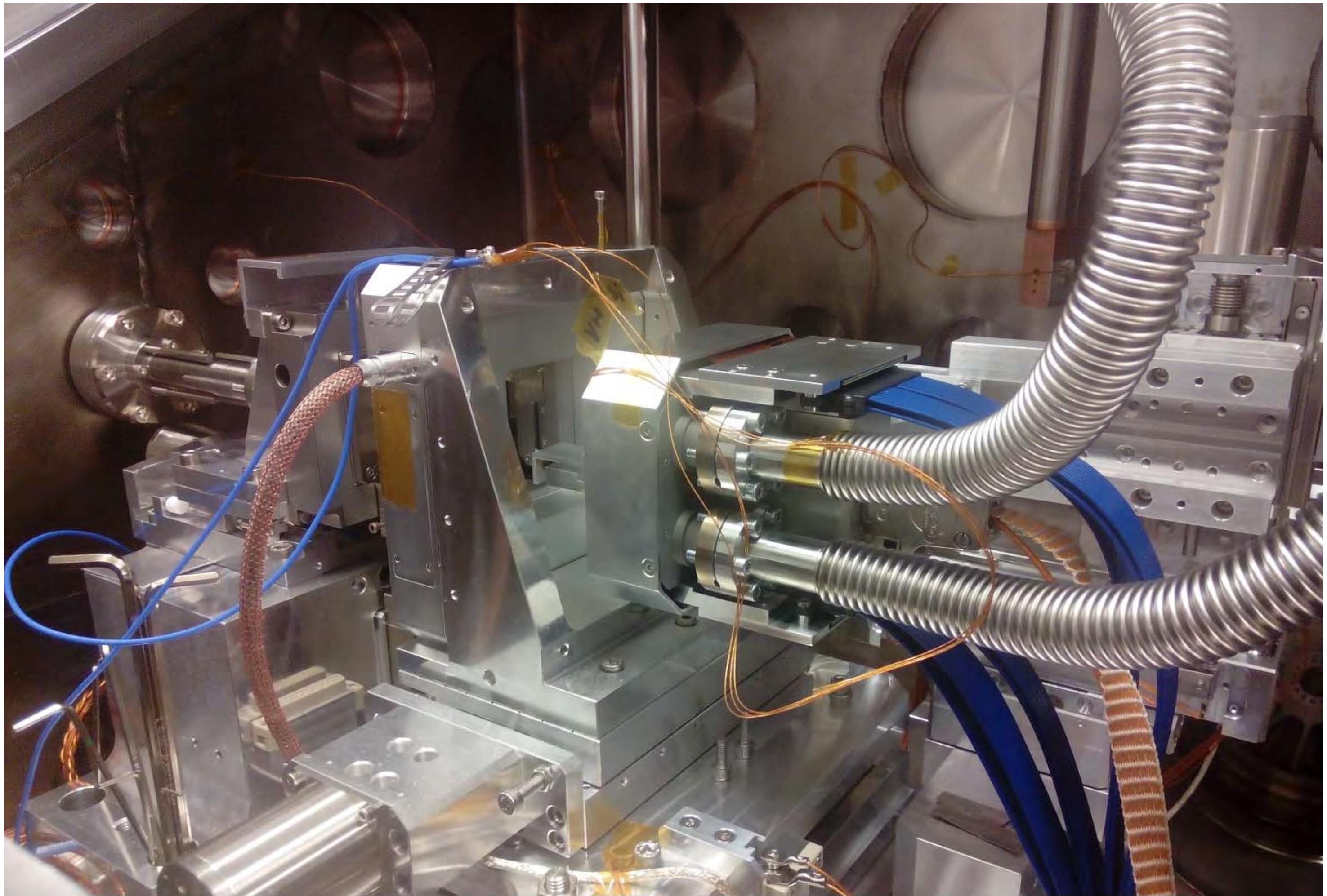

The Ptychographic Principle

(using „sharp camera“- D.A. Shapiro, et. al. Nature Photonics **8**, 765 (2014))

Classical STXM

Ptychography

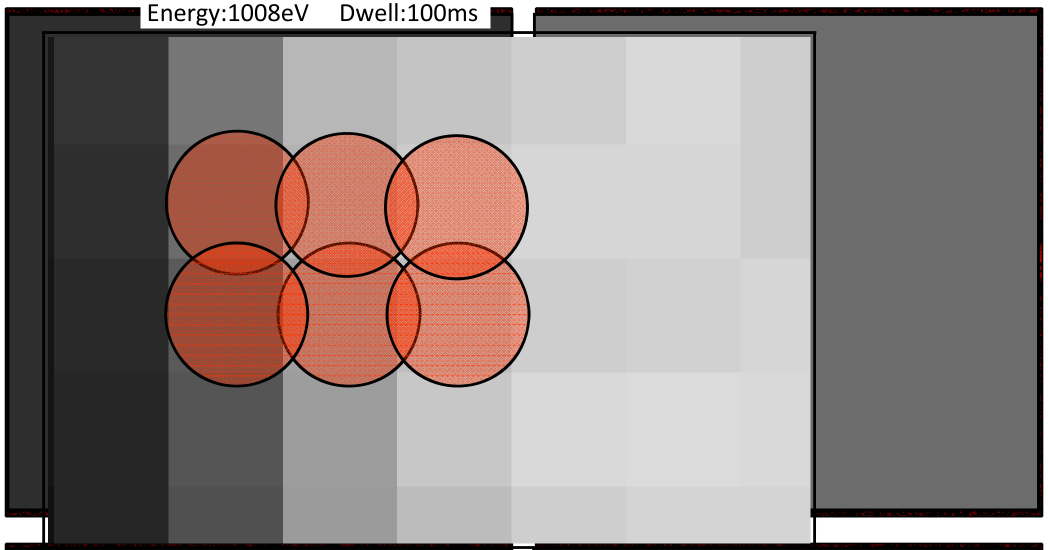

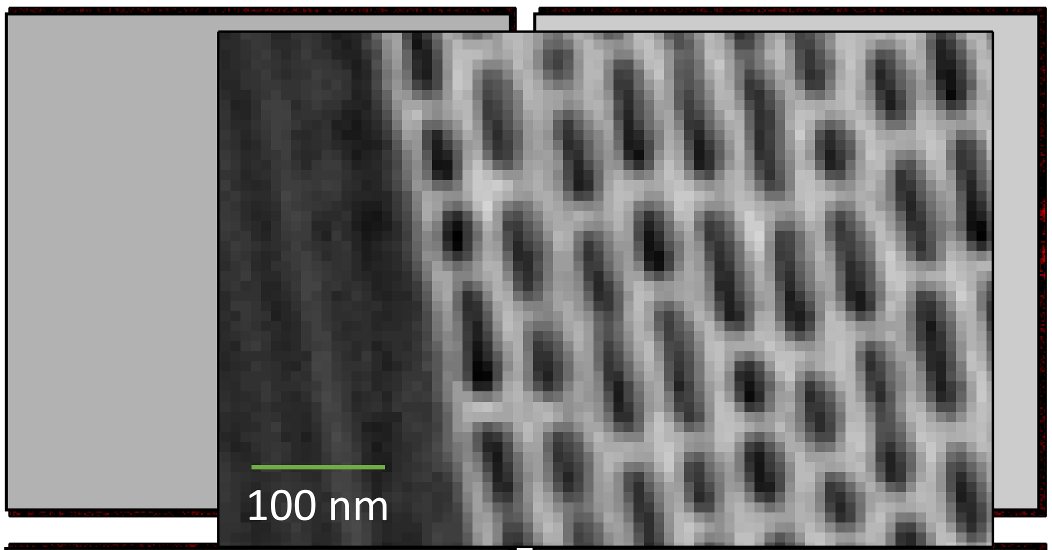

Improved Microcontrast

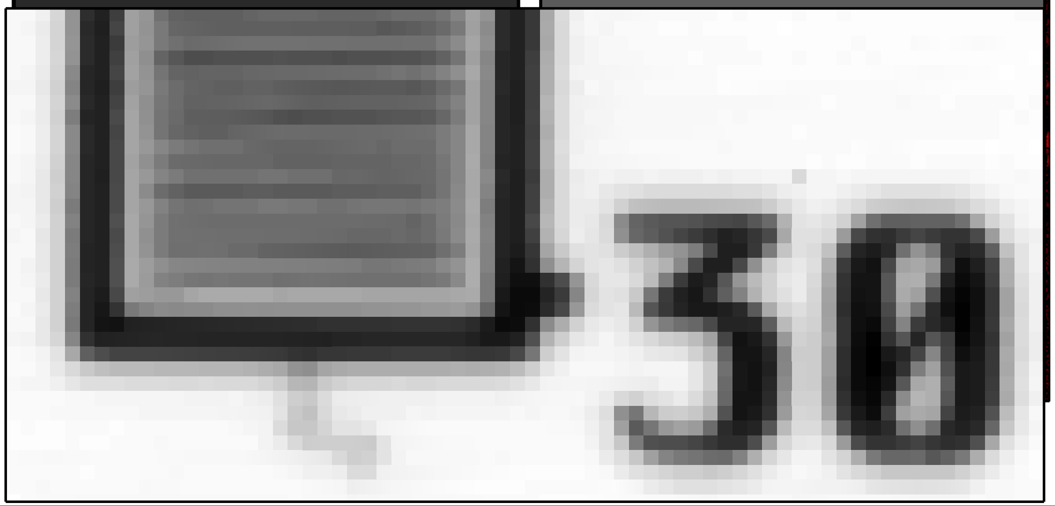

Why Ptychography now?

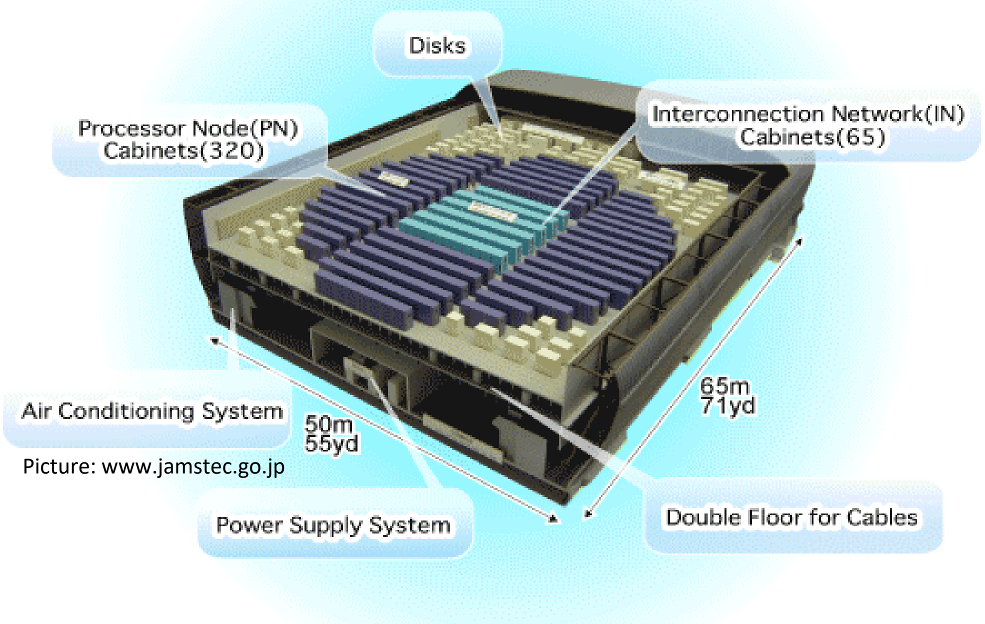

Picture: www.jamstec.go.jp

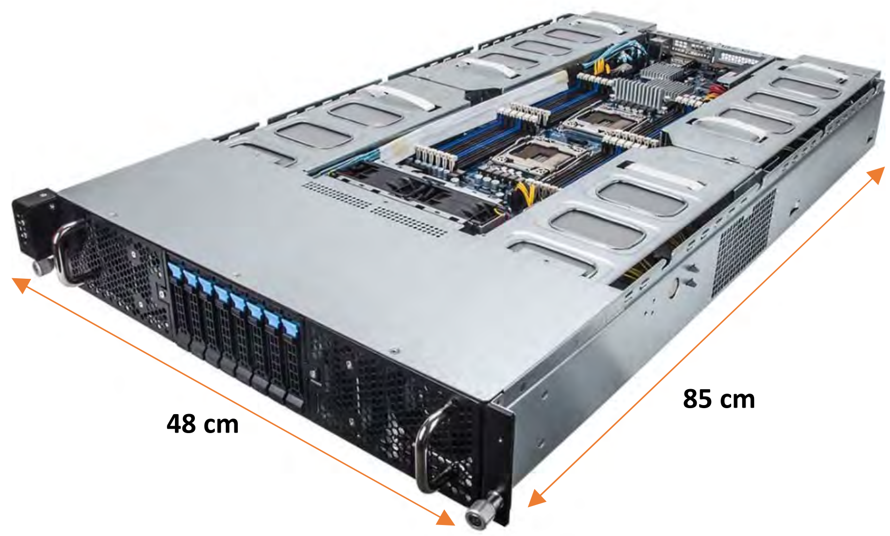

2004	2015
Earth Simulator	MAXYMUS Ptychography Server
Fastest Supercomputer in the world	Just a computer with 8 GPUs
60 billion yen	affordable
35.86 Tflops	48 Tflops peak

Ptychography Tests at MAXYMUS

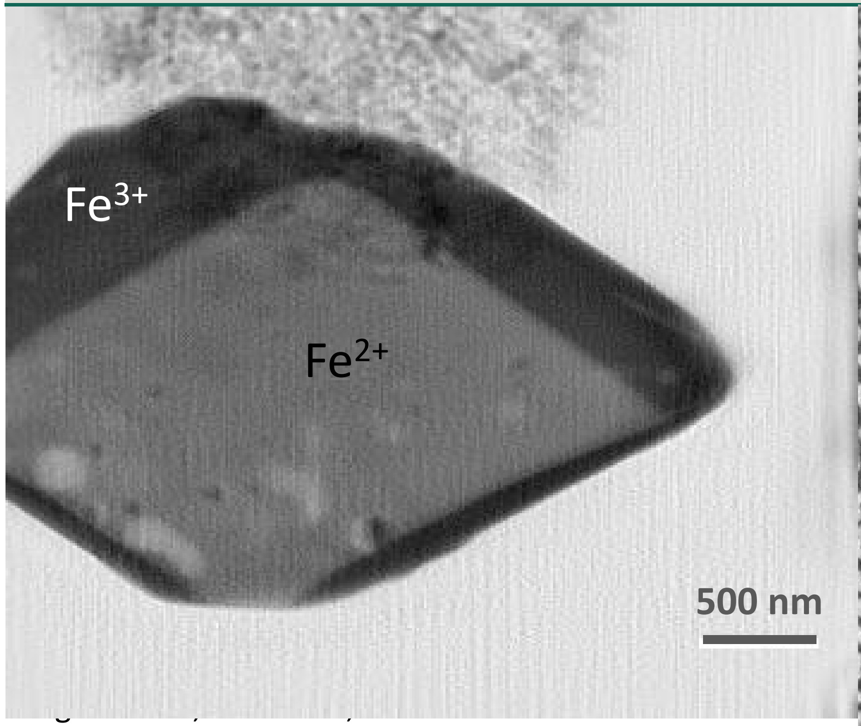

William Chueh Group
Materials Science and Engineering
Stanford University

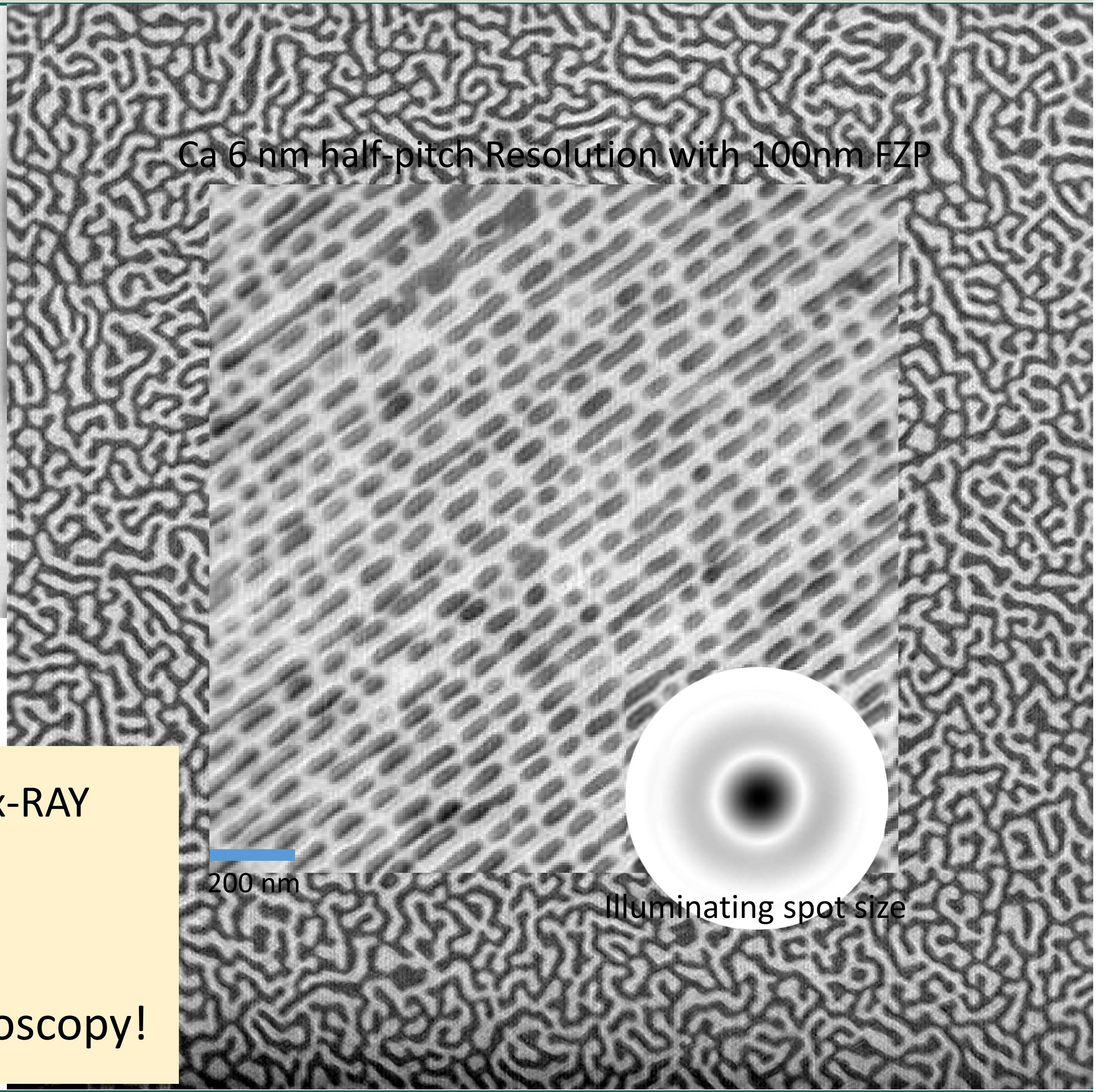

Benefits from rapid development of x-RAY cameras for FELs and upcoming high brilliance sources

Towards single nm chemical microscopy!

Ptychography @ MAXYMUS

- In principle its is very close to the procedure shown before
- We already have the reconstruction algorithm from David Schapiro
- The resulting dataset is completely redundant and error robust ➔ one is able to also extract the illumination function!

N. Chapman and K. Nugent, Nature Photonics, Focus review Nov. 2010

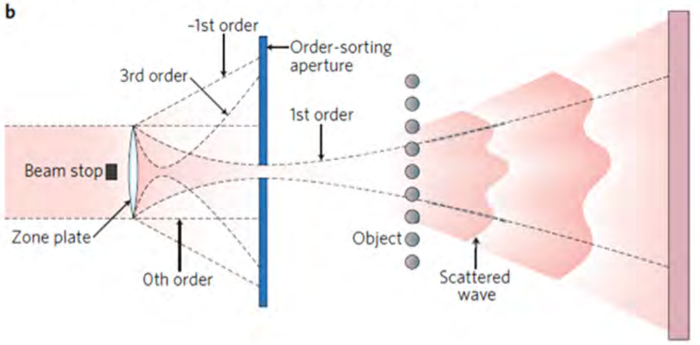

Key Parameter:

Active Area	1-3 cm^2
Pixel Size	36 x 36 μm^2 up to 150 x 150 μm^2
CCD Geometry	frame store and image area or image area only e.g. 256 x 256 pixels or 64 x 200 pixels
Operating Modes	full frame, frame-store, window modes, continuous readout
Read Out Speed	400 Hz f. 256 x 256 pixels (up to 1 MHz)
Elec. Noise	down to 2.5e- per pixel @190K, t_{int} = 50ms
Energy Resolution	130 eV FWHM @MnK, 190K, , tint = 50ms
Sensitivity	> 90% f.200eV -15KeV > 90% in the optical range supported by antireflective coatings (ARC) on the detector surface

Detector: pnSensor CCD
256x256 Pixel 32bit/pixel
➔ about 260.000 Byte/frame

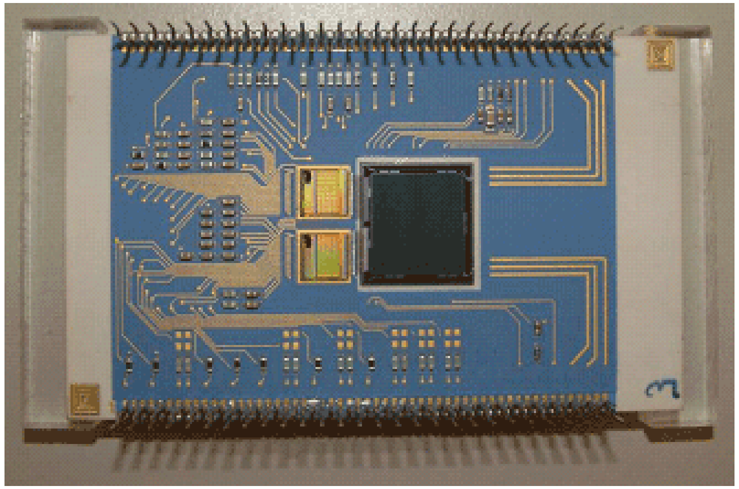

Maxymus Image has 100x100 up to 500x500 pixel (typical 200x200)

➔ 2-30 Gbyte/Image

- Thats it!

- Thanks for your attention!